USING MULTITEMPORAL SATELLITE IMAGERY TO MONITOR THE RESPONSE OF VEGETATION TO DROUGHT IN THE GREAT LAKES REGION

BY SUSAN DUNHAM

THESIS

Presented to the Graduate Council of
Southwest Texas State University
in Partial Fulfillment of
the Requirements

For the Degree

Master of APPLIED GEOGRAPHY

By

Susan Dunham, B.A.

San Marcos, Texas
August 2003

ACKNOWLEDGEMENTS

I would like to thank Dr. Fonstad (committee chair) for being the backbone of this project. His constant stream of ideas and enthusiasm kept me motivated and always on my toes. I would also like to thank Dr. Anderson (co-advisor) for taking me on as her "first" student. Her upbeat attitude and constant devotion to the completion of this project gave me the support and ability to persevere. I would also like to thank Dr. Czajkowski for his kindness and constant support. Combined, this trio was an unbeatable team and the best committee anyone could ask for providing constant support, mentoring, and expanding my knowledge of the techniques and applications of remote sensing and the trials and tribulations of life. I would also like to thank team Ms. Pacman (and other fellow grad pitters) for all of their encouragement and assistance. The bond created over many hours at the joystick will never be broken. I would also like to thank my family for loving and supporting me through all of my hair-brained ideas. I would like to thank Thomas Heddinghaus from the National Oceanic and Atmospheric Administration for helping me to weed out the relevant nuggets from stacks of Palmer drought information. Finally, a special thank you goes to my undergraduate advising team Dr.Vasiliev and Dr.Nichols who still support me and keep tabs on me from afar.

This manuscript was submitted August 2003.

TABLE OF CONTENTS

LIST OF TABLES

LIST OF FIGURES

ABSTRACT

USING MULTITEMPORAL SATELLITE IMAGERY TO MONITOR THE RESPONSE OF VEGETATION TO DROUGHT IN THE GREAT LAKES REGION

by

Susan Dunham, B.A.

Southwest Texas State University

August 2003

SUPERVISING PROFESSOR: MARK A. FONSTAD

The use of satellite imagery to monitor vegetation has been important for decades. Previous studies focus on the use of AVHRR based vegetation indices to assess vegetation response to climatic conditions. This study focuses on the relationship between the Palmer Drought Severity Index (PDSI) and different vegetation types through the use of several vegetation indices derived from Landsat ETM+ data (NDVI, Tasseled Cap, and SAVI). The methodology for this study consisted of three major phases; (1) obtaining georeferenced PDSI values that correspond to available imagery, (2) statistical comparison between PDSI and average values from vegetation indices, and (3) utilizing the results to make temporal inferences about the condition of vegetation in a portion of the Cuyahoga River watershed in northeastern Ohio. The potential existence of a lag between the onset of climatic conditions and vegetation response was partially addressed using these correlation methods.

Keywords: Landsat ETM+, vegetation indices, Palmer Drought Severity Index, Ohio

CHAPTER 1

INTRODUCTION

Drought is one of the most adverse and powerful weather-related disasters. It produces negative impacts on mankind, and these impacts can be devastating on a large area (Kogan 1997). Droughts are among the world's most costly natural disasters and cause an average of $6-8 billion in global damages annually (Keyantash and Dracup 2002). Given the consequences of drought, it is important to assess the severity of droughts along with the resulting impacts in order to understand and monitor this global phenomenon.

The use of satellite imagery to monitor vegetation has been important for decades. Previous studies have focused on the use of AVHRR based vegetation indices to assess the response of vegetation to climatic conditions. This study examines the use of some of the more commonly known vegetation-monitoring techniques by assessing their ability to detect drought stress for different vegetation types over a four-year period from September 1999 to September 2002 using Landsat 7 Enhanced Thematic Mapper Plus (ETM+) imagery for a portion of the Cuyahoga River Watershed in northeastern Ohio.

Specifically, the major objectives of this study were 1) to test the use of NDVI and two other indices to see if NDVI is the best vegetation index to use for drought studies with satellite imagery, 2) to determine if the state of vegetation can predict the

existence of drought conditions, and 3) to see if a lag time can be detected for the response of various types of vegetation to changes in climatic conditions.

This study is important because there is a known relationship between climate and vegetation dynamics as monitored from space, however few studies investigate vegetation index variation on individual homogeneous land cover units as they relate to specific climate and environmental influences at local scale/watershed scale of analysis. Since drought is such a dynamic and powerful weather-related disaster and accurately monitoring drought has been shown to be a challenge, the need exists for studies that provide alternate ways of studying the response of specific vegetation types to changes in climatic conditions using higher resolution imagery. This study helps to refine the methodologies used in current studies and expands on the knowledge of the different capabilities of some of the most widely used tools available for vegetation monitoring.

As physical/environmental geographers we study the processes that happen on the Earth's surface over time and space and how these processes impact the environment and human activities. Collecting field data or extracting data by other means and then analyzing it through the use of remote sensing and geographic information system techniques is done in order to better understand these processes. This study focuses on the analysis of patterns exhibited by different vegetation types as a result of changing climatic conditions and therefore contributes to these sub-disciplines of the umbrella we call Geography.

CHAPTER 2

LITERATURE REVIEW

Drought Defined

The wide variety of sectors affected by drought and its diverse geographical and temporal distribution along with human water demand makes it difficult to develop one accepted definition of drought (Heim, Jr 2002). Therefore, the American Meteorological Society groups drought definitions into four categories: meteorological/climatological, agricultural, hydrological, and socioeconomic. Meteorological drought occurs when the atmospheric conditions result in the absence or reduction in the amount of precipitation present in a region. These conditions can last from months to years, or can disappear overnight (Heim, Jr 2002).

After a few weeks of meteorological drought, dryness in the surface layer of the soil (root zone), if it occurs during a crucial time during the growing season, can result in agricultural drought, which can severely reduce crop yields. The onset of agricultural drought often lags behind that of meteorological drought depending on the state of the surface layers of soil prior to the event (Heim, Jr 2002).

Hydrological droughts occur when precipitation deficits over a prolonged period affect surface or subsurface water supplies (i.e. reduce stream flow, groundwater,

reservoir, or lake levels). These conditions can continue long after the meteorological drought has ended (Heim, Jr 2002). Socioeconomic drought takes into account the supply and demand of some economic good that is impacted by the other types of drought (Heim, Jr 2002).

Due to the complicated nature of the relationships between different types of drought, the international meteorological community defines drought in general terms as a "prolonged absence or marked deficiency of precipitation," a "deficiency of precipitation that results in water shortage for some activity or for some group," or a "period of abnormally dry weather sufficiently prolonged for a lack of precipitation to cause a serious hydrological imbalance" (American Meteorological Society 1997; World Meteorological Organization 1992). The definition of drought adopted for this study was defined by Palmer and used in his method of determining the Palmer Drought Severity Index as "a prolonged and abnormal moisture deficiency" (Palmer 1965).

Vegetation Types

This study focuses on the response of different vegetation types to changes in climatic conditions. The four vegetation types are agricultural/crops, riparian vegetation, forest, and natural/other vegetation. For the purpose of this study, "forest" will be referred to as a dense growth of trees (Woolf et al 1977). "Riparian vegetation" will be defined as vegetation that is in or near a river channel and directly influenced by river-related processes (Malanson 1993). "Agriculture/crops" is defined as cultivated and managed vegetated areas

(FGDC 1996). Finally, "natural/other" vegetation is defined as roadside vegetation and vegetation not classified as other vegetation types through the image classification procedure.

Vegetation Indices and AVHRR

Generally, healthy green vegetation reflects about 40 to 50 percent of the incident energy from the near-infrared portion of the electromagnetic spectrum (0.7 to 1.1μm), and absorbs approximately 80 to 90 percent of the energy in the visible (blue, green, and red) part of the spectrum (0.4 to 0.7μm) due to the chlorophyll and other pigments that are present in the leaves (figure 1). Thus when studying varying characteristics of vegetation like leaf area index, greenness, or vegetation vitality algorithms are created to extract this information from multispectral sensors, which are collectively known as vegetation indices (Ray 1994; Jensen 1996).

Vegetation indices have been developed to quantify different environmental and ecological conditions using these bands of information. The Normalized Difference Vegetation Index (NDVI) has become the primary tool for the description of vegetation changes and is used to interpret of impacts of environmental phenomena in different scenarios related to vegetation condition (Kogan 1990). There are also several NDVI-based indices that have been created to make NDVI more adaptable to different situations.

Peters, Rundquist, and Wilhite (1991) evaluated the use of coarse resolution Advanced Very High Resolution Radiometer (AVHRR) data for drought detection and monitoring in Nebraska. They showed that the Palmer Drought Severity Index (PDSI) and

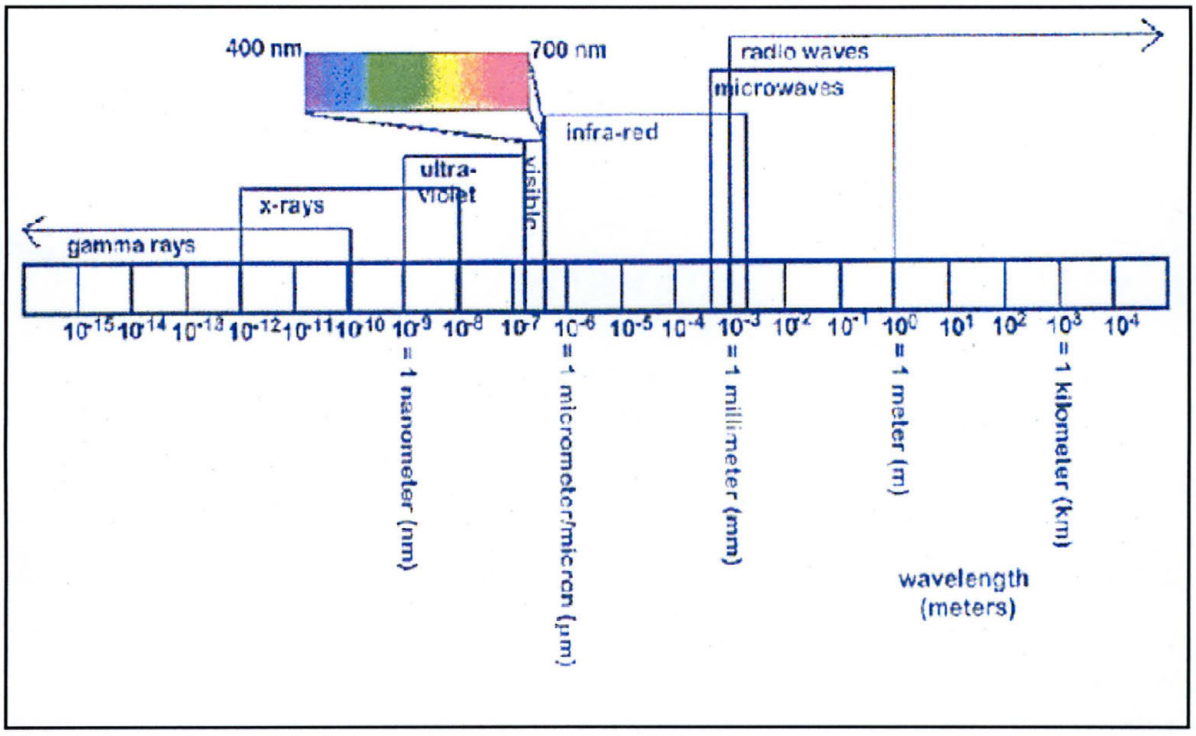

Figure 1: Electromagnetic Spectrum (Blair 1999)

the Crop Moisture Index (CMI) were not adequate for determining the onset, spatial extent, severity, and termination of agricultural drought when evaluated alone since the measurements taken to calculate these indices are calculated from a few point observations in each climate division.

They determined through spatial and temporal analysis of NDVI response to precipitation characteristics that drought characteristics can be detected using AVHRR data for example the geographic core of the 1988 drought was accurately identified in Nebraska. They also determined that the average NDVI value for a climate division might be a good substitute for the short-term variables that constitute agricultural drought.

Rundquist (1997) and Rundquist et al (2000) used NDVI from AVHRR data for the years 1988 to 1996 in conjunction with climate data (PDSI, temperature, precipitation, actual evapotranspiration, potential evapotranspiration, and climatic water balance (CWB)) to examine the strength of their relationship for the nine climate divisions in the state of Kansas. The scientists found that overall the relationship between NDVI, the climate, and the water budget variables existed. They also determined that when looking at each climate division separately there was a statistically significant relationship between the aforementioned variables.

Tao et al (1997) analyzed the relationship between AVHRR NDVI data from 1988, 1991, and 1993 along with rainfall patterns in agricultural areas of Ford County, Kansas. They found that an integrated NDVI response coincided with the crop phenological growing cycle. They also found that the level of positive correlation between rainfall and NDVI variation improves as a temporal scale increases. Therefore, monthly analysis of NDVI

responses was preferable to a biweekly analysis. They also found that there was an apparent lag time of fourteen days for NDVI to respond to rainfall.

Kogan (1990, 1995a, 1995b) proposes the use of a modified NDVI called the Vegetation Condition Index (VCI) for AVHRR data in the Global Vegetation Index (GVI) format. He tested the effectiveness of this index in Sudan and the United States and found through these studies that VCI showed an excellent ability to detect drought. He also found that this index was also able to measure the time of its onset, intensity, duration, dynamics, and the impacts on vegetation. He suggests that the index is also a good estimator of vegetation condition along with yield, and that it works especially well for non-homogeneous areas.

Kogan (1997) suggests that a good accompaniment to the VCI is another index called the Temperature Condition Index (TCI), which was derived from the thermal channels of AVHRR and has been used to increase the accuracy of drought monitoring and also provided useful information for monitoring vegetation stress due to soil saturation. In this study, Kogan proposes the use of the combination of these indices for global drought monitoring. He finds that these indices are useful for real-time assessments and diagnosis of vegetation condition as well as the impacts of weather on vegetation at a global scale.

Peters et al (2002) used twelve years of AVHRR data (1989-2000) and standardized it by time of the year, using NDVI values to supplement drought-monitoring techniques in the Great Plains. They used an NDVI derived index called the Standardized Vegetation Index (SVI) to describe the probability of vegetation deviation from normal conditions based on weekly calculations of NDVI values. They found that SVI is a good indicator of vegetation

response to short-term weather conditions and that it is a tool that is capable of providing a near real time indicator of the onset, extent, intensity, and duration of vegetation stress. They hypothesized that it would be especially useful when combined with some of the other drought monitoring indicators previously mentioned.

Peters et al (1993) tested the ability of low spatial resolution AVHRR-HRPT (High Resolution Picture Transmission) data to detect short term spatial and temporal drought effects on native plant communities in New Mexico using NDVI and climatic variables (PDSI, DMI, and precipitation departure from normal). They determined that the spectral response of individual plant communities was a useful measure of drought severity.

The studies above show the usefulness of AVHRR data in the analysis of vegetation response to drought conditions. However, other sensors have been shown to be useful for this purpose as well.

Vegetation Indices and Other Imagery

Investigations of drought have also been performed using other sensors in order to monitor the condition of vegetation during these climatic conditions. Chavez Jr. and MacKinnon (1994) used multitemporal Landsat Multi Spectral Scanner (MSS) data and compared that to Visible-Infrared Spin-Scan Radiometer (VISSR) data and in situ data for automatically mapping vegetation changes in the southwestern United States. They found that changes were detected in natural vegetation in the arid to semi-arid desert of the southwestern United States. In addition the use of selective principle components analysis (PCA) on uncalibrated images allowed the automatic detection of changes. They were also

able to detect vegetation changes in areas of low vegetation and found that by mapping the areas with relatively low vegetation density they were also indirectly mapping areas where soils would support vegetation if rainfall is sufficient. They also provided information that will help to identify soils vulnerable to wind erosion and desertification as well as information about possible grazing locations.

Washington-Allen et al (1998) attempted to characterize the typical seasonal response of vegetation cover and identify and describe changes in vegetation cover attributed to drought on the vegetation resources of subsistence agropastoral communities on the Bolivian Altiplano using MSS and Landsat Thematic Mapper (TM) derived TNDVI (transformed NDVI). They were able to determine that TNDVI is useful for determining that the vegetation cover is fairly stable under drought conditions.

Huete et al (1997) used Landsat TM images representing a wide range of vegetation conditions from the NASA Pathfinder global land cover test site initiative and processed them so that they would simulate Moderate Resolution Imaging Spectroradiometer (MODIS) global vegetation index imagery in order to do a comparison of the differences and similarities of sensitivity to vegetation conditions for several vegetation indices (NDVI, SAVI, ARCI, SARVI and SARVI2). All of the indices demonstrated a healthy range from arid regions to densely vegetated forests. They also determined that SARVI2, SARVI, and SAVI can help to refine global vegetation studies by extending the range of sensitivity of vegetation indices into densely vegetated forested regions and sparsely vegetated arid and semiarid regions.

Pinder III and McLeod (1999) used multitemporal TM data and tree ring analysis to study the impact of drought on longleaf pines in a U.S. Department of Energy's Savannah River Site in Georgia and South Carolina. They found that TM data was able to detect changes in reflectance that were correlated with drought stress effects on tree growth.

Nagler, Glenn, and Huete (2001) tested the relationship between three vegetation indices (NDVI, SAVI, and EVI), percent vegetation cover, and leaf area index over a riparian landscape in the Colorado River Delta, Mexico using a three band digital camera (Dycam) to collect data from an aircraft flying at 150 meters above the ground. They found that the vegetation indices were most related to the percent vegetation cover rather than the species differences in leaf area index or vegetation index values. They also found that there was almost a 1:1 correspondence between the Dycam and TM NDVI values.

Finally, Gosh (1997) studied drought in the Shahpur and Shorapur areas of Gulbarga district in Karnataka State, India through the use of multitemporal satellite data (IRS-1A LISS 2-Indian Remote Sensing Satellite-1A Series Linear Imaging Self-Scanning Sensors 2). He generated changes in albedo and vegetation (NDVI), used meteorological data for identifying changes in soil moisture, and used GIS to integrate satellite-based indicators with meteorological based indicators in order to define drought severity. He determined that a composite drought index derived from the combined analysis of GIS and remote sensing layers can provide a useful tool for investigation, monitoring, and prediction of drought.

It is apparent that studies have been completed that utilize satellite imagery and recognize the importance of a continuous data set for vegetation studies. However, this overview of trends in the literature indicates that there needs to be more studies done

involving higher resolution satellite imagery and assessing the impacts of drought on varying vegetation communities at the local level. Therefore this study looks at the impact of drought on vegetation in a watershed in northeastern Ohio. A two step process will be employed; (1) use three vegetation indices (NDVI, SAVI, Tasseled Cap) to see if there is a difference in the degree of vegetation stress detected by each index, and (2) do statistical analysis between the vegetation index values and the values obtained by calculating the Palmer Drought Severity Index (PDSI) to see if the state of vegetation can predict the existence of drought conditions.

CHAPTER 3

METHODOLOGY

Study Area

The Cuyahoga River begins in Geauga County and runs 100 miles southwest through Cuyahoga Falls, and northwest through the urban and industrial centers of Akron (southwest) and Cleveland (northwest) before emptying into Lake Erie (Figure 2). The Cuyahoga River Watershed drains 813 square miles in Cuyahoga, Summit, Portage, Geauga, and Medina counties in northeast Ohio (CWAP 2002).

The climate of Ohio varies with a wide range of air temperatures throughout the state. The majority of precipitation is received during the spring and summer months with less in the fall and winter, although portions of the watershed, the Lake Erie "snow belt", receive a significant amount of lake effect snow during the fall and early winter months. Most soils are saturated during March and early April. The growing season rainfall varies from approximately 19 to 21 inches for the watershed area. Soil moisture declines throughout June and July, and is usually reduced by about 80 percent or more by the end of August (Beuerlein et al 1995).

This five county region is quite agricultural with the number of farms ranging from 180 to 1,170 per county and the average acreage per farm ranging from three to 131 acres.

The major agricultural products produced in this region are vegetables, fruit, and dairy. The topography of the area is dominated by flat plains, rolling hills, glaciated rolling plateaus, and sharp slopes along the rivers (OPLIN 2003). Beech and oak forests are the dominant type of vegetation in the region both of which are deciduous meaning that they are broad leaved and tend to lose their leaves during the autumn months (Schultz 2003). This region also has several mineral resources including sand, gravel, shale, petroleum, and salt (OPLIN 2003).

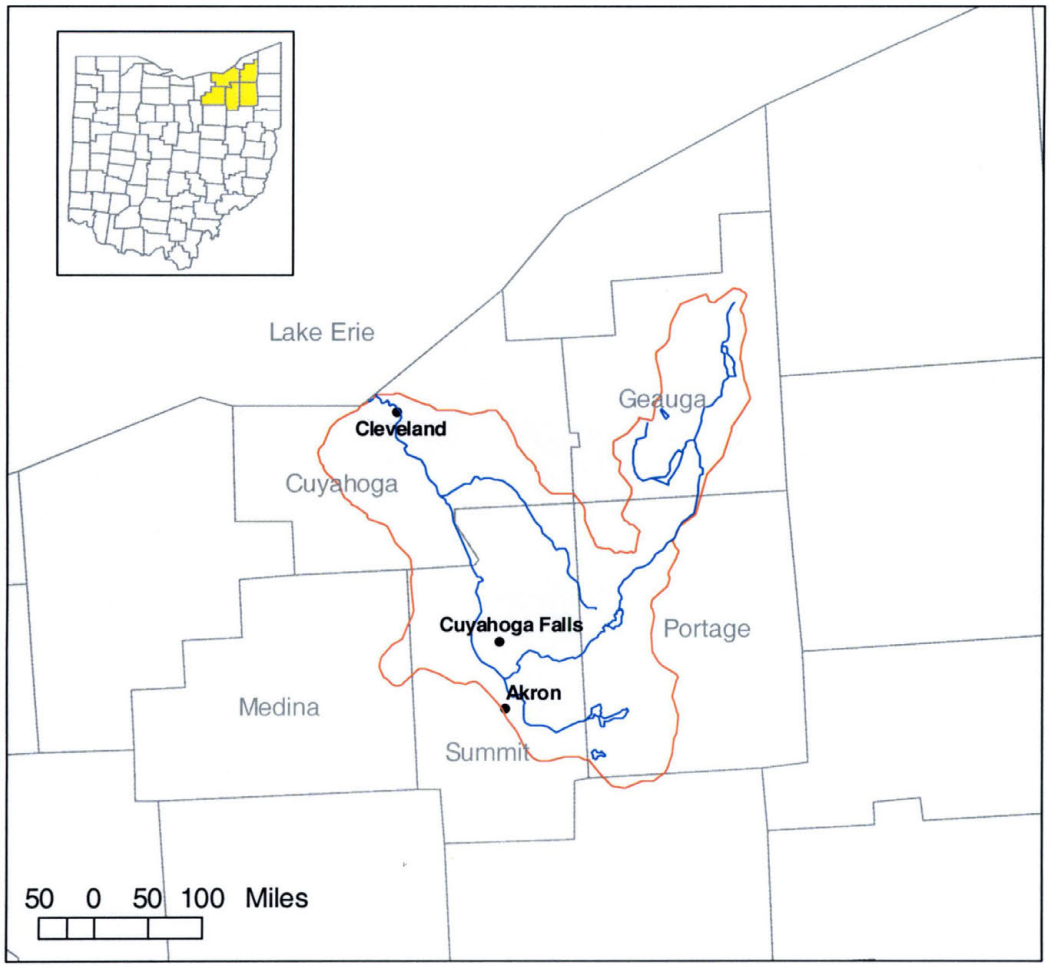

Figure 2: Cuyahoga River Watershed location map

Data

Satellite Imagery

Landsat 7 ETM+ images were selected from a list of images dating from 1999 to 2002 on the OhioView Imagery Collection Network. OhioView is a grassroots organization of Ohio universities and government/state organizations formed in 1996 to promote the low cost distribution of United States government satellite data to the public, educators, scientists, and community leaders (OhioView 2002). These images were georeferenced by EROS data center in Sioux Falls, South Dakota and then converted into GEOTIFF format. Each image was selected based upon the amount of clouds in the study area and whether the effects of clouds can be removed from the imagery using atmospheric correction techniques (Table 1). Images that contained clouds over more than half of the study area were not included in this analysis.

Path	Row	Imagery Date	Cloud Cover	Climate Condition
19	31	September 26, 1999	0%	normal
19	31	October 12, 1999	0%	normal
19	31	November 13, 1999	unavailable	normal
19	31	March 4, 2000	0%	normal
19	31	April 5, 2000	0%	normal
19	31	October 14, 2000	20%	wet
19	31	October 30, 2000	0%	normal
19	31	March 23, 2001	0%	normal
19	31	April 8, 2001	0%	normal
19	31	August 14, 2001	0%	severe drought
19	31	August 30, 2001	0%	moderate drought
19	31	July 16, 2002	0%	moderate drought
19	31	August 1, 2002	0%	moderate drought
19	31	September 2, 2002	30%	moderate drought

Table 1: Selected images

The Landsat 7 ETM+ satellite was launched in 1999 and has a repetitive, circular, sun synchronous, and near polar at a nominal altitude of 705 kilometers (438 miles) at the Equator. The spacecraft crosses the Equator from north to south on a descending orbital node between 10 am and 10:15 am local time on each pass. It circles the Earth at 7.5 kilometers/second and each orbit takes approximately 99 minutes. This satellite completes just over fourteen orbits per day and covers the entire Earth between 81 degrees north and south every sixteen days (swathing pattern). Each swath is a fixed 185 kilometers and the world reference system (WRS) indexes orbits (paths) and scene centers (rows) into a global grid system comprising of 233 paths by 248 rows. WRS path/row maps are available from the EROS Data Center (Figure 3)(Williams 2003).

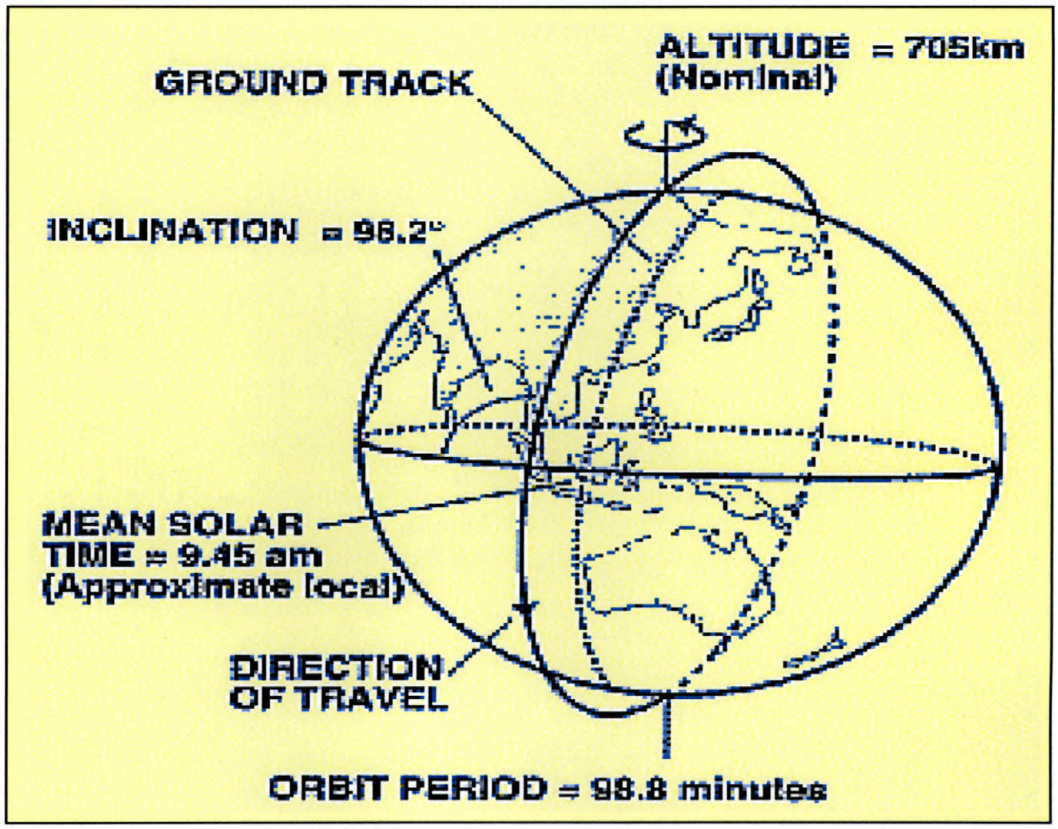

Figure 3: Landsat 7 orbital patterns (Williams 2003).

The Landsat 7 system is designed to collect seven bands or channels of reflected energy and one channel of emitted energy. Each particular band corresponds to a particular portion of the electromagnetic spectrum and records data only in that specific wavelength. The eight bands of ETM+ data are used to discriminate between Earth surface materials through the development of spectral signatures. For any material, the amount of emitted and reflected radiation varies by wavelength and these variations are used to establish the signature reflectance fingerprint for each material. ETM+ data is sampled at three different resolutions, 30 meters for bands 1-5 and 7, 60 meters for band 6, and 15 meters for band 8 and each scene is approximately 185 kilometers by 180 kilometers in area (Table 2).

Landsat 7 ETM+ Satellite Characteristics

Band Number	Band Type	Band Width (μm)	Resolution (meters)
1	Blue	0.450-0.515	30
2	Green	0.525-0.605	30
3	Red	0.630-0.690	30
4	Near-Infrared	0.750-0.900	30
5	Mid-Infrared	1.55-1.75	30
6	Thermal	10.40-12.50	60
7	Mid-Infrared	2.08-2.35	30
8	Panchromatic	0.50-0.90	15

Table 2: Landsat 7 characteristics (Jensen 2000)

PDSI

The Palmer Drought Severity Index (Palmer 1965) is a popular drought determination method in the United States and has been used for a variety of applications (Hayes 2002). Palmer based his index on the supply and demand concept of the water balance equation and used the average monthly values of precipitation and temperature for the foundation of his drought calculations (Wilhite et al 1987; Peters et al 1991). The calculation of a PDSI value is a complicated and multi-step process. The first step is to input temperature, precipitation, normal temperatures, latitude, and available water holding capacity (AWC) of the soil. The temperature values are the average daily temperature for each time period. Precipitation is the total amount of precipitation received over each time period. The normal temperatures are the long-term average temperatures for each period. The latitude is used as part of Thornthwaite's calculation of potential evapotranspiration or the amount of water that could be lost by the soil and plants provided the supply was unlimited (Palmer 1965; Wells 2002). Next, the values for potential evapotranspiration, potential recharge, potential runoff, potential loss, evapotranspiration, recharge, runoff, and loss are calculated for each period using the water balance equation. The next step is to calculate the moisture departure for each time period and then calculate the moisture anomaly. Then the values are calibrated using a duration factor and the climate characteristic is determined using the moisture anomaly and climate characteristic value that is weighted according to where the value falls in the expected –6 to +6 range. Finally the PDSI value is determined using the three resulting values of X1 (severity of an incipient wet spell), X2 (severity of an incipient dry spell),

and X3 (severity of the current spell) along with the probability that the current spell will end (Wells 2002). For a more detailed explanation of the entire procedure and the particular equation used refer to publications by Palmer (1965), Wells (2002), and Hayes (1999).

The United States is broken up into climate divisions (maximum of ten in each state) and an index value is calculated for every division (Figure 4). Calculations are based upon multiple years of data, which have been analyzed to determine "normal" conditions in each climate division. Any deviation from that "normal" is represented by the index of some form of dry or wet condition (Table 3). Each index value is assigned to a condition class ranging from extreme drought (-6) to extremely wet (+6) (Peters et al 1993; Hayes 1999).

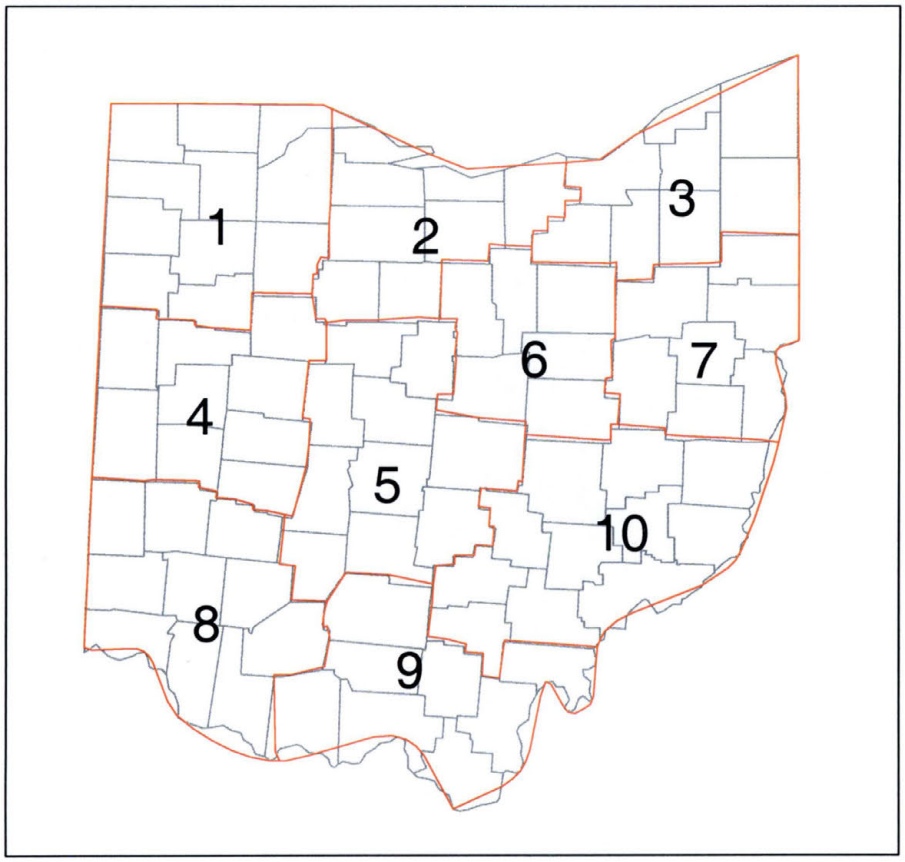

Figure 4: Climate divisions for Ohio

-4.0 or less	Extreme Drought
-3.0 to –3.9	Severe Drought
-2.0 to –2.9	Moderate Drought
-1.9 to 1.9	Near Normal
2.0 to 2.9	Unusual Moist Spell
3.0 to 3.9	Very Moist Spell
4.0 and greater	Extremely Moist

Table 3: Palmer Drought Severity Index classifications (Climate Prediction Center 2002)

PDSI values are also standardized so that they can be directly compared both spatially and temporally in order to help monitor meteorological drought and assess growing season conditions. PDSI values are calculated weekly across the nation and are published by the Joint Agricultural Weather Facility and are available through the National Climatic Data Center and the Climate Prediction Center (NOAA) (Peters et al 1991; Hayes 1999). This study focuses on the analysis of vegetation and climatic conditions in a portion of climate division 3 in Ohio.

According to Kogan (1995), this weather-based index has not found much application outside of North America due to the lack of weather stations in many countries. He goes on to say that possible explanations for this are that PDSI does not predict conditions well in regions where there are extremes in variability of rainfall or runoff (i.e. Australia or South Africa). PDSI does not accurately represent the hydrological impacts resulting from longer droughts or in areas where there is varying topography. However, because no better agricultural indices really exist, the PDSI is used by federal officials as the major criterion for declaring drought disaster areas (Wilhite 1983). Table 4 shows why the Palmer Drought Severity index should or should not be used.

Pro	Con
Provides decision makers with a measurement of the abnormality of the recent weather for a region	The two soil layer model used may be too simplistic to accurately represent a location
	Snowfall, snow cover, and frozen ground are not included in the index (all treated as rain)
Provides an opportunity to place current weather observations into a historical context	Runoff is underestimated-lag between falling precipitation and runoff is not considered
	Potential evapotranspiration (PET) is estimated using the Thornthwaite method (only an approximation)
Provides spatial and temporal representations of historical droughts	Index is not sensitive to the available water content of different soil types-using one index value for an entire climate division results in overgeneralization
	Man-made changes in local water supply (irrigation and reservoirs) are not considered
	Intensity of drought and signaling the beginning and end of a dry or wet spell have little scientific meaning-selected based on Palmer's study of central Iowa and western Kansas

Table 4: Drawbacks and advantages to using PDSI (Hayes 1999)

Weekly Palmer Drought Severity Index data was obtained from the National Climate Data Center. Values were entered into a geographic information system (GIS) database using ArcView 3.2 software in order to create Ohio state maps of drought conditions corresponding to the imagery dates (Figure 5).

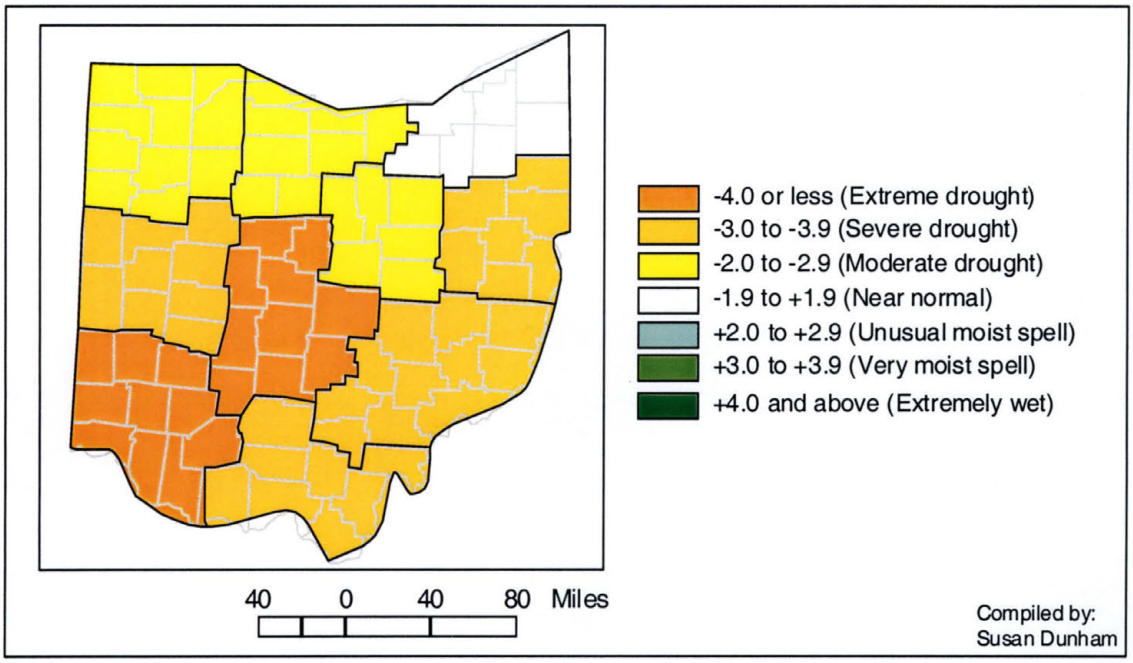

Figure 5: Example of Palmer Drought Severity Index map (refer to appendix II)

Image Processing

Atmospheric Correction

The atmosphere affects images by scattering, absorbing, and refracting light. Thus it is important to minimize the effects of the atmosphere in order to accurately assess what is happening on the ground. Generally, atmospheric correction identifies the pixels that are impacted by the atmosphere the most and adjusts the histogram so that they are not included in the new image (Figure 6). Atmospheric correction was done using the ATCOR module for ERDAS imagine. ATCOR is generally used for atmospheric correction, topographic correction, haze removal for multispectral and hyperspectral satellite images. It also converts the digital numbers of each pixel into scaled reflectance at sensor values ranging from 0 to 255. The benefit to using ATCOR over traditional atmospheric correction techniques is that the resulting images can be analyzed multi-temporally because the influence of different atmospheric conditions on the actual reflectance values of the pixels in each image is virtually removed. In order to do the calibration, ATCOR takes into account the radiance scattered by different layers of the atmosphere, reflected radiation from each pixel, and adjacency effects (radiation reflected into the view by the pixels around it) (GEOSystems 2000).

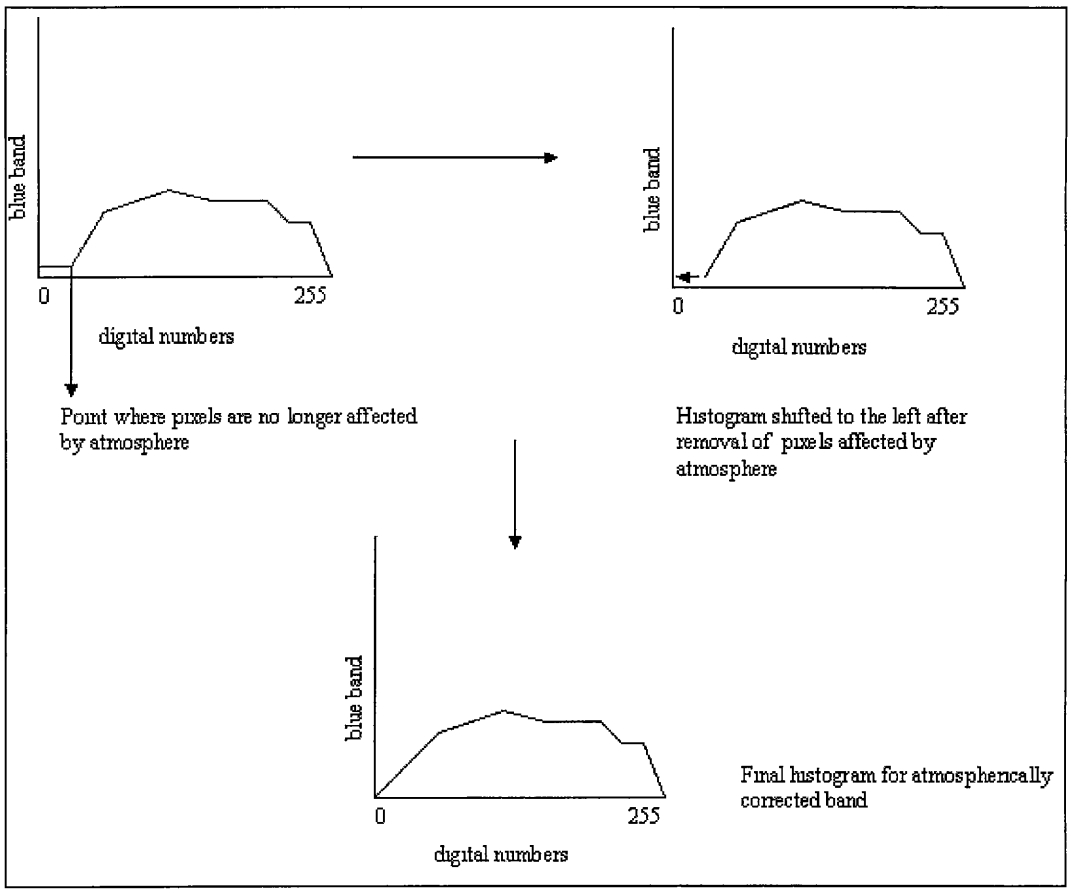

Figure 6: General atmospheric correction model

Atmospheric correction was performed on each image using the same specified atmospheric parameters for each one. Atmospheric correction was also used as a normalization technique for the images in this study in order to make the multitemporal images comparable (Figure 7).

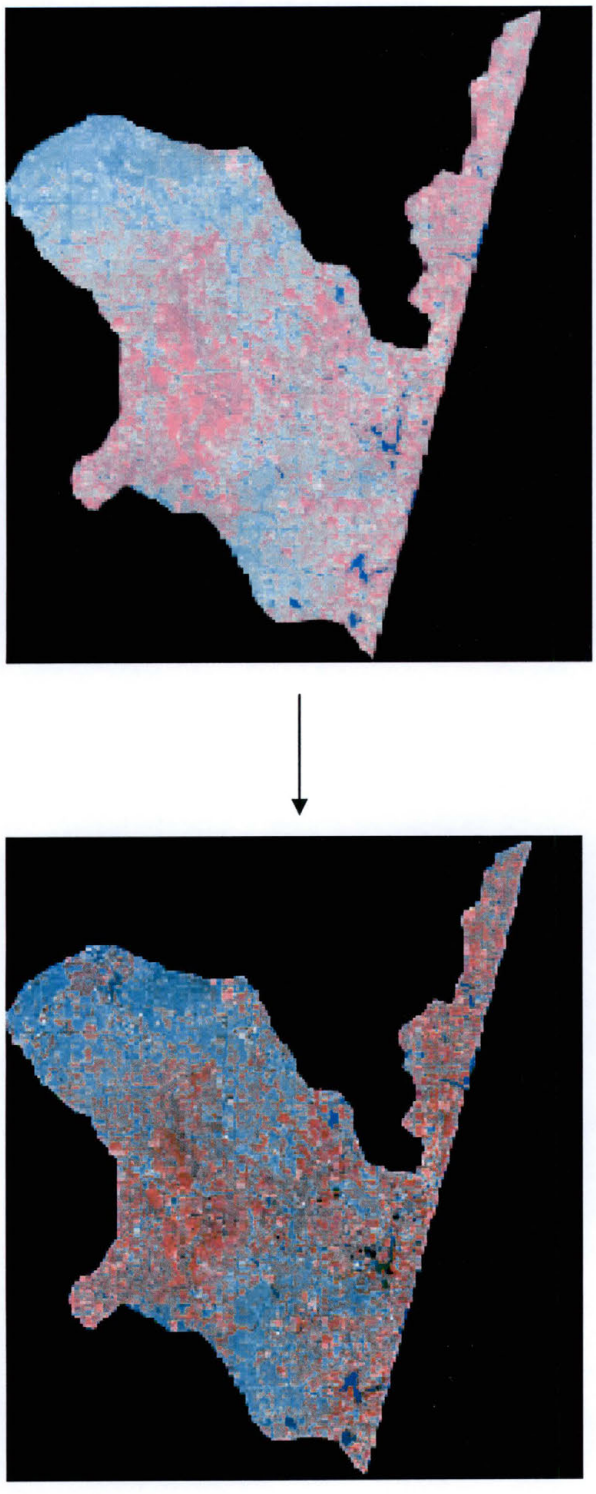

Figure 7: Example of result of atmospheric correction (refer to appendix II)

Classification

Image classification was performed in order to identify vegetated areas. Six land cover classes were chosen; developed (urban areas and roads), forest, water, active agriculture, non-active agriculture, and other vegetation. In addition, on the images that included clouds two more classes were added in order to identify the clouds and their shadows. A supervised classification was performed on each of the fourteen images using the same training sites for developed, water, forest, and other vegetation classes. Training sites for the active agriculture and non-active agriculture classes were changed due to the nature of the vegetation and their changing spectral characteristics (Figure 8).

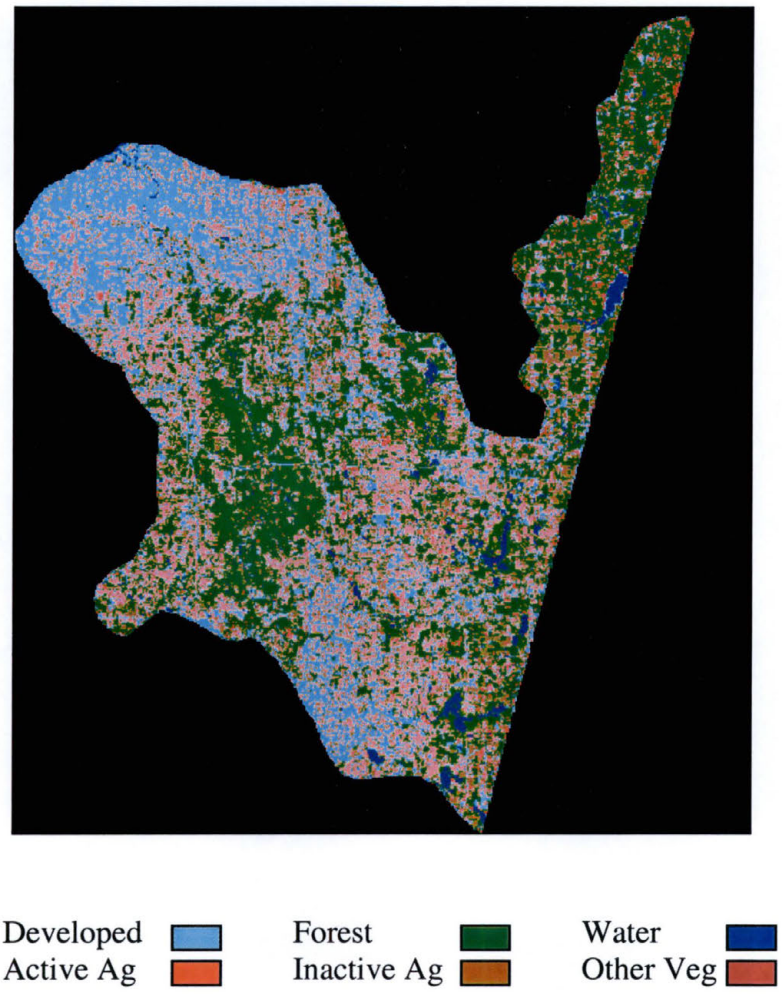

Figure 8: Example of a classified image (refer to appendix II)

A transform divergence separability test was used on the signatures for each class in order to determine the ability of the computer to differentiate each class. Separability test values range from 0 to 2000 with a value of 2000 indicating complete separability, values greater than 1900 provide good separability, and values below 1700 provide poor separability of class signatures (Table 5) (Jensen 1996).

	Forest	ActAG	Dev	NonAct	Water	OtherVeg
Forest		2000	2000	2000	2000	2000
ActAg	2000		2000	2000	2000	2000
Dev	2000	2000		2000	2000	2000
NonAct	2000	2000	2000		2000	2000
Water	2000	2000	2000	2000		2000
OtherVeg	1999	2000	2000	1999	2000	

Table 5:Example of best average separability results (refer to appendix I)

After all fourteen classifications were complete, a test was conducted in order to search for discrepancies in the classifications. Tables were created that included all of the pixel amounts for each of the classes included in each image and graphs were created to look for peaks where inconsistencies in the classification would appear (Figure 9).

9/26/99 image		
	# pixels	% total
Unclassified	3140349	61.67
Nat Veg	469758	9.22
Ag Act	46874	0.92
Ag Nonact	165981	3.26
Forest	683994	13.43
Developed	541739	10.64
Water	43873	0.86
Clouds	0.00	0.00
Shadow	0.00	0.00

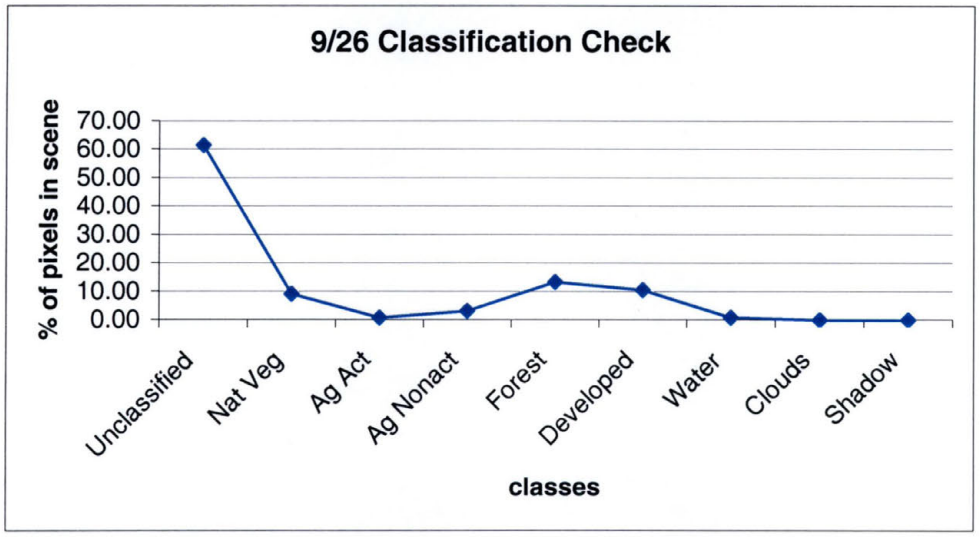

Figure 9: Example of classification check table and graph (refer to appendix I)

After looking at all of the results from this exercise, it was determined that although there were slight differences in the amounts of pixels classified as each class, there were no large discrepancies that warranted a reproduction of the entire classification procedure.

Riparian vegetation was identified by delineating a buffer around the river channel using on-screen digitizing over Digital Orthophoto Quarter Quads (DOQQs) of the study area. Then a knowledgebase was created based upon a few simple rules:

1) If riparian and water then use water class
2) If riparian and developed then use developed class
3) If riparian and forest then use new riparian class
4) If riparian and natural vegetation then use new riparian class
5) If riparian and active agriculture then use new riparian class
6) If riparian and inactive agriculture then use new riparian class
7) If riparian and clouds then use clouds class
8) If riparian and shadow then use shadow class

The riparian area was used along with the other pre-existing classes in order to create a riparian class in the classified images. Then an expert classification was performed using the knowledgebase and the previously classified images yielding an end result of a new riparian class on each classified image (Figure 10).

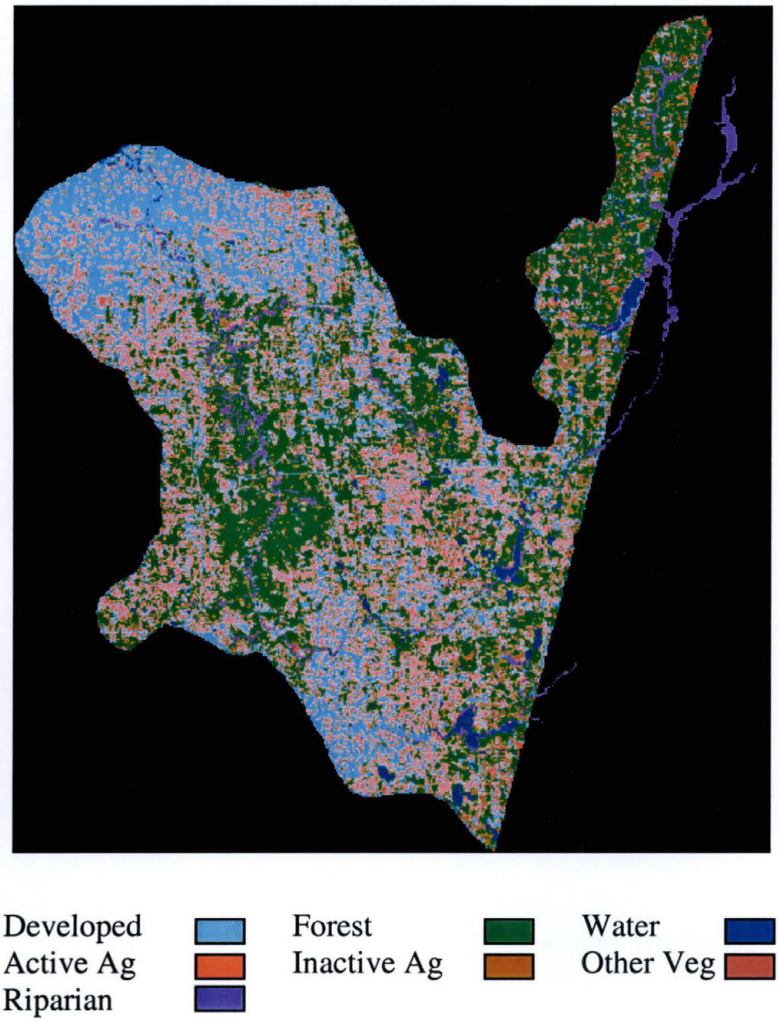

Figure 10: Example of classification using knowledgebase and expert classification procedure (refer to appendix II)

An accuracy assessment was also performed in order to ensure the quality of the classified images using a random stratified sample of 127 points with a minimum of 20 points in each class. The random points were overlain on top of Digital Orthophoto Quarter Quadrangles (DOQQs) of the area. Digital Orthophoto Quarter Quadrangles are either gray-scale, natural color, or color-infrared images with one-meter ground resolution. They cover an area measuring either 3.75 minutes longitude by 3.75 minutes latitude or 7.5 minutes longitude by 7.5 minutes latitude. These images are aerial photographs that have been corrected to remove distortions from camera orientation and terrain and are therefore useful for various geographic information system applications (USGS 2003). The September 26, 1999 image was used for assessment since the date was closest to that of the DOQQs. An error matrix was created using the classes that were assigned by the computer for the image and the classes that were determined visually using the DOQQs (Figure 11).

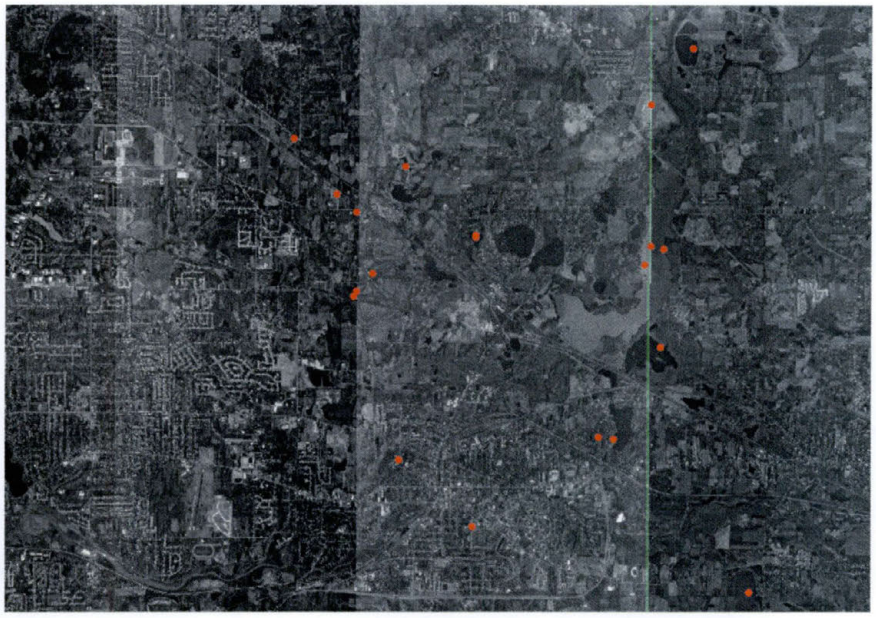

(a)

	Undef	Riparian	Ag_Nonact	Ag_Act	Forest	Water	Developed	Other_Veg	Total
Undef	0	0	0	0	0	0	0	0	0
Riparian	0	4	0	0	0	0	0	0	4
Ag_Nonact	0	0	4	0	2	0	2	0	8
Ag_Act	0	0	0	11	6	0	0	0	17
Forest	0	0	1	1	23	0	0	0	25
Water	0	1	1	1	0	16	1	0	20
Developed	0	0	0	6	3	0	22	0	31
Other_Veg	0	0	0	3	5	0	5	9	22
Total	0	5	6	22	39	16	30	9	127

(b)

Figure 11: (a) Example of random points overlaid on DOQQs; (b) Accuracy assessment error matrix (refer to appendix I)

Vegetation Indices

NDVI

The Normalized Difference Vegetation Index (NDVI) (Rouse et al 1974) is a ratio based vegetation index that has been widely used and related to percent vegetative cover, leaf area index, and the amount of green biomass present (Peters et al 1991; Jensen 2000). It is among the simplest indices and uses the infrared band (band 4 for the ETM+) and the red band (band 3 for the ETM+) because of the response of green vegetation in these two wavelengths and what is revealed about the characteristics of vegetation.

$$NDVI = \frac{NIR - red}{NIR + red}$$

This equation produces values that lie between −1 and +1 with higher index values indicating higher levels of healthy vegetation cover and lower values indicating non-vegetated surfaces or areas of less vegetation cover (University of Arizona 2002). The resulting images are black and white with lighter areas indicating areas of bright green vegetation.

SAVI

The Soil Adjusted Vegetation Index (SAVI) (Huete 1988) is an index that is used to help decipher spectral changes between vegetation and soil.

$$SAVI = (1+L) * [(NIR - red) / (NIR + red + L)]$$

Where L is a constant or adjustment factor that is dependent on the amount of vegetation present at a location ranging from 0 to 1. For most types of vegetation cover, it has been shown that an adjustment factor of 0.5 produces a vegetation index value that is superior to NDVI (Huete 1988). This index produces values that range from –1 to +1. These black and white images look similar to those produced using the NDVI equation where brighter areas indicate areas of green vegetation.

Tasseled Cap

The Tasseled Cap transformation (Kauth and Thomas 1976), originally for Multispectral Scanner data, is intended to define a new rotated coordinate system in order to better represent the properties of vegetation and soil (Mather 1999). A Tasseled Cap transformation was adapted to Thematic Mapper data using bands 1-5 and 7 in which three axes were determined; brightness, greenness, and wetness. Brightness is a partial sum of all bands, greenness describes the contrast between the near infrared and the visible bands, and wetness contrasts middle-infrared reflectance with visible and near infrared reflectance. It has been shown that this method is useful for enhancing image interpretability (Crist and Cicone 1984b). Brightness is responsive to changes in total reflectance and to those processes that affect total reflectance. Thus differences in soil characteristics like particle size distribution are clearly expressed in brightness. Greenness responds to the combination of high absorption in the visible bands due to plant pigments and high reflectance in the near-infrared due to internal leaf structures. This second feature has been shown to be correlated with percent canopy cover, leaf area

index, and fresh biomass and when combined with TM Brightness they define the "Plane of Vegetation". Since the longer-infrared TM bands have been suggested to be most sensitive to both soil and plant moisture, changes in moisture status affect these longer-infrared bands more substantially than the visible or shorter-infrared bands. Thus the contrast between these two sets of bands highlights moisture related scene characteristics (primarily soil moisture status) and together combined with brightness they define the "Plane of soils" (Crist and Cicone 1984a). Since this study was primarily focused on vegetation characteristics the greenness and wetness components of the Tasseled Cap transformation are used in this study. The interpretation of these images is similar to that of the NDVI and SAVI images previously mentioned. In tasseled cap greenness images, the brighter areas indicate areas of green vegetation. In the tasseled cap wetness images, bright areas indicate areas that contain a lot of water and could be associated with healthy green vegetation. Table 6 shows the coefficients for Landsat 7 ETM+ data.

Once all of the vegetation index images were created for the selected image dates, a zonal function model was created to get the average index value for each class specified in the classification procedure. Zonal functions are used to evaluate the values of grid cells that are contained within a specified zone or region (DeMers 2002).

Index	Band 1	Band 2	Band 3	Band 4	Band 5	Band 7
Greenness	-0 3344	-0 3544	-0 4556	0 6966	-0 0242	-0 263
Wetness	0.2626	0 2141	0.0926	0.0656	-0.7629	-0 5388

Table 6: Landsat 7 ETM+ tasseled cap transformation coefficients (Huang et al 2002)

CHAPTER 4

DATA ANALYSIS

Linear regression analysis is a fairly simple and robust technique that is not only used to determine whether a relationship exists between two variables, but the nature of this relationship, and the predictive quality of the resulting regression equation (Kachigan 1991). There are several assumptions that need to be recognized when using linear regression analysis:

1. variable y (dependent variable) is measured at the interval or ratio scale
2. variable x (independent variable) is measured without error, any measurement error in variable y is random
3. the relationship between y and x is linear
4. the error variable has a mean of zero
5. the error variable has a constant variance
6. all pairs of errors are independent
7. the error variable is normally distributed (Griffith and Amrhein 1991)

Regression analysis was chosen as the statistical analysis technique for this study because vegetation condition was being used as an indicator for the existence of drought conditions. Analysis was conducted in three separate phases in order to extract as much information as possible about the vegetation in the watershed from the satellite imagery.

Phase 1

The first phase of data analysis was conducted in the form of a pilot study to look at the general trends in the data and to make sure that the classification scheme and procedure was adequate. Regression analysis was performed using the average vegetation index values for all of the vegetation in the watershed as the independent variable to predict whether drought conditions existed using the weekly PDSI values as the dependent variable. This test was conducted to see if it was necessary to separate the index values by vegetation type in order to extract more information about their condition and the existence of drought or non-drought conditions.

Phase 2

The second phase of data analysis involved the use of regression analysis in order to see if the condition of different vegetation types could predict whether or not drought existed for the imagery dates studied. Therefore, independent regressions were run for each vegetation type specified in the classification procedure to see if the different vegetation types showed results that were not only different from each other, but also different from the data analysis done on all of the vegetation in the watershed as one unit in phase 1.

Phase 3

Another way to try to extract more information about the relationship between the state of the vegetation and PDSI values was to consider that there might be a lag or a

lapse in time between the onset of changing climatic conditions and vegetation response. For this phase of data analysis, regression was used along with PDSI values from two weeks prior and four weeks prior to the satellite images for a two or four week time lag. This was done in order to see if there would be an increase in r-squared values for the different vegetation types indicating that there was a detectable lag in the response of particular vegetation types to changing climatic conditions (Rundquist 1997; Tao et al 1997).

Results

Classification Procedure-Separability

After running a transformed divergence separability test on all of the signatures for each image, tables were created to compare the average separabilities. In only two cases was the best average separability below 1800. This means that, overall, there was a good selection of training site signatures on which to base the classification of all of the images. For the two cases that did fall below 1800 for their best average separability the classification tables and graphs that were created to double check the classifications were consulted. The percent pixels in each class for the two dates looked to be in the same range as the other images, and the graphic representation of the classification by class showed the same general trends as the others. Thus it was determined that no further investigation of the classification procedure was necessary.

Classification Procedure-Assessment

An accuracy assessment was performed in order to ensure the quality of the classified images. The September 26, 1999 image was used along with 127 points collected using a random stratified sample and DOQQs of the study are from 1995. The September 1999 image was chosen because this date was closest to that of the available DOQQs. The random points were generated and then overlain on top of the DOQQs to identify their class identity. Then the class reference values from the DOQQs were compared to the classes that the computer had assigned yielding an overall accuracy of 70.08 percent and an overall kappa coefficient of 0.6362.

Phase 1

In order to determine the overall trends in the data, the average index values were plotted against the image dates (Figure 12). The first set of regression analyses were run using the average index values for all of the vegetation in general in the watershed and resulted in the creation of four r-squared values indicating the relationship between vegetation and PDSI values for the watershed. This analysis yielded r-squared values of 0.266 for the normalized difference vegetation index (NDVI), 0.351 for the soil adjusted vegetation index (SAVI), 0.231 for tasseled cap greenness (TCG), and 0.101 for tasseled wetness (TCW).

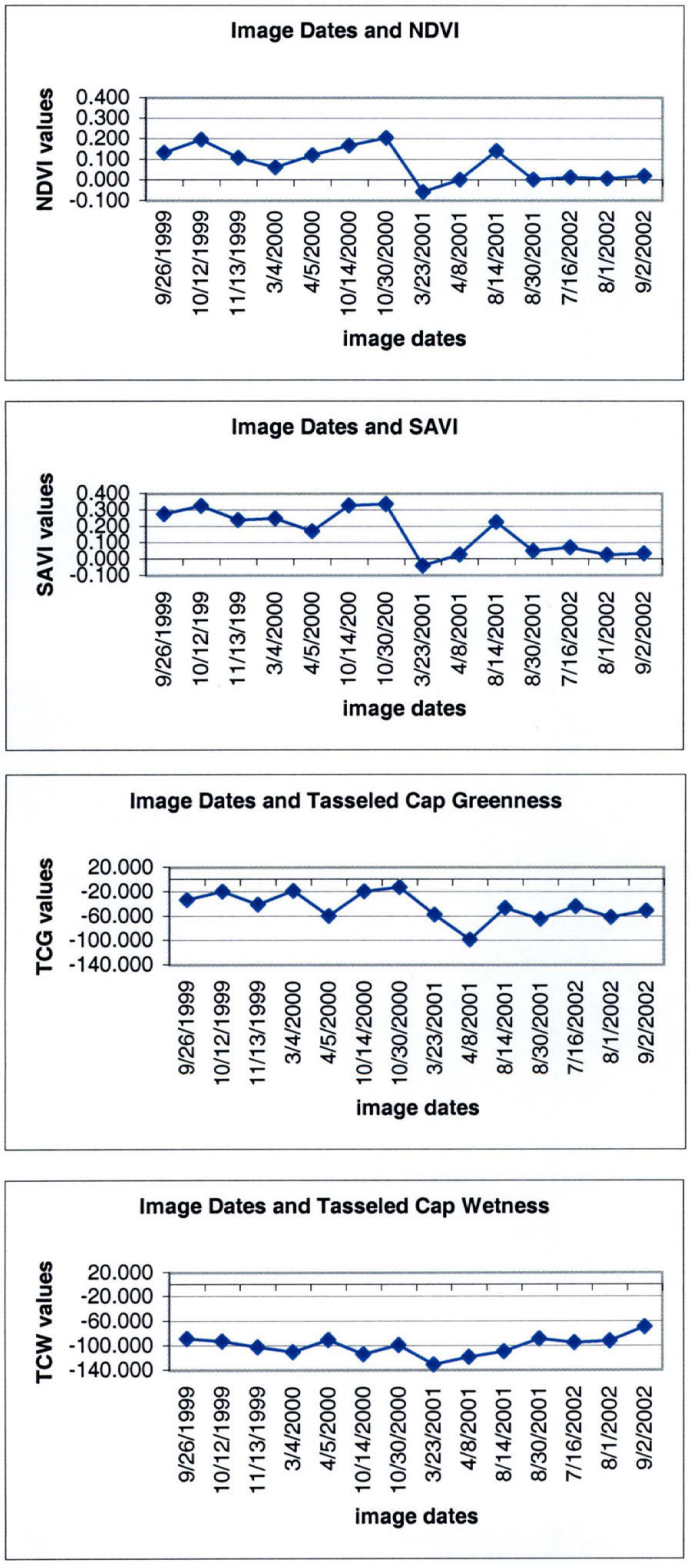

Figure 12: Image dates versus average index values for overall data trends

Phase 2

The next set of regression analyses were run using the average index values for each individual type of vegetation (riparian, active agriculture, inactive agriculture, and other vegetation). The r-squared values for NDVI ranged from 0.003 for the riparian vegetation class to 0.530 for the active agriculture class. The r-squared values for SAVI ranged from 0.017 for the riparian vegetation class to 0.625 for the other vegetation class. R-squared values from the regression analysis between tasseled cap greenness for all of the vegetation types and the palmer drought severity index (PDSI) values ranged from 0.000 for the inactive agriculture class to 0.732 for the other vegetation class. For the tasseled cap wetness index r-squared values ranged from 0.004 for the active agriculture class to 0.274 for the riparian vegetation class.

Phase 3

To test to see if there was a detectable time lag, the regression analysis for the two-week lag resulted in r-squared values that ranged from 0.240 for NDVI to 0.276 for tasseled cap greenness for all of the vegetation in the watershed. For the four week lag r-squared values ranged from 0.014 for SAVI to 0.284 for tasseled cap wetness for all of the vegetation in the watershed.

Testing for a detectable two-week time lag for each vegetation type yielded r-squared values ranging from 0.003 for the forest class to 0.241 for the active agriculture class for NDVI. For SAVI, r-squared values ranged from 0.029 for the inactive agriculture class to 0.293 for the active agriculture class. For tasseled cap greenness, r-squared values ranged from 0.068 for the forest class to 0.375 for the active agriculture

class. For tasseled cap wetness, r-squared values ranged from 0.064 for the inactive agriculture class to 0.235 for the other vegetation class.

Testing for a four-week time lag for each vegetation type yielded r-squared values ranging from 0.007 for the active agriculture class to 0.117 for the inactive agriculture class for NDVI. R-squared values resulting form the SAVI regression ranged from 0.002 for the other vegetation class to 0.156 for the inactive agriculture class. Tasseled cap greenness analysis resulted in r-squared values ranging from 0.000 for the other vegetation class to 0.099 for the active agriculture class. Finally, tasseled cap wetness yielded r-squared values ranging from 0.046 for inactive agriculture to 0.366 for active agriculture. Table 7 shows all of the results from the regression analyses performed in each phase.

Regression-for whole watershed

Index	r-squared	2 wk lag	4 wk lag
NDVI	0 266	0 240	0 015
SAVI	0 351	0 268	0 014
TCG	0 231	0 276	0 017
TCW	0.101	0 241	0 284

(a)

Regression-each vegetation type				
Vegetation Type	NDVI	SAVI	Tasseled Cap-Greenness	Tasseled Cap-Wetness
riparian	0 003	0 017	0 010	0 274
inactive agriculture	0 055	0 028	0 000	0.179
active agriculture	0 530	0 223	0 238	0.004
forest	0.083	0 082	0.037	0.145
other vegetation	0 528	0.625	0 732	0.047

(b)

2 week lag				
Vegetation Type	NDVI	SAVI	Tasseled Cap-Greenness	Tasseled Cap-Wetness
riparian	0.023	0 082	0.096	0 110
inactive agriculture	0.022	0 029	0 097	0 064
active agriculture	0 241	0.293	0 375	0.192
forest	0 003	0 039	0.068	0 084
other vegetation	0 193	0 175	0 161	0.235

(c)

4 week lag				
Vegetation Type	NDVI	SAVI	Tasseled Cap-Greenness	Tasseled Cap-Wetness
riparian	0 008	0 025	0 041	0 150
inactive agriculture	0 117	0 156	0 008	0 046
active agriculture	0 007	0 058	0 099	0 366
forest	0 014	0 047	0.038	0.125
other vegetation	0 012	0 002	0 000	0 180

(d)

Table 7: (a) Regression results for entire watershed; (b) Regression results for individual vegetation types; (c) and (d) Regression results for individual vegetation types for the two and four-week time lags

CHAPTER 5

DISCUSSION

Watershed Scale of Analysis

Once all of the index values were obtained, plots were created using the average index values versus the image dates to identify the overall trends in the data. It was observed that the average index values were generally lower during times of drought and higher during normal or wetter periods. This followed the trends in other studies where drought conditions and the impacts on vegetation were studied (Peters 1993; Kogan 1997). However, several anomalies did emerge in looking at the overall trends in the data. For example, there is an overall decrease in average index values on the March 23, 2001 image even though there are normal conditions and normal conditions existed prior to this image and afterwards as well. There also seems to be fairly high index values on the August 14, 2001 image even though there are supposed to be severe drought conditions. This indicates that maybe one type of vegetation could be skewing the index values due to its resilience to drought conditions and that it could be possible to find out more information about what is going on in this watershed if particular vegetation types are considered for analysis instead of just looking at one value to represent all of the vegetation in an area.

In looking at the r-squared values from the regression analysis between the average index values and their corresponding PDSI values, which are generally low (ranging from 0.101 to 0.351), it seems evident that there is a slight but weak relationship in terms of the condition of vegetation being able to predict the existence of drought conditions (refer to Table 7). This is consistent with the results of another study in which precipitation records and the linear relationships between AVHRR and NDVI were studied (Harrington Jr and Greegor Jr 1988). However, when looking at the two and four week time lags more information can be extracted. In examining the two-week time lag, the r-squared value for tasseled cap greenness increases indicating that a time lag is detected and that there is a two-week time lag for vegetation to show changes in greenness or vitality for the watershed. When the four week time lag is considered, a higher r-squared value is observed for tasseled cap wetness indicating that it takes approximately four weeks for the vegetation in the watershed to exhibit signs of stress due to changes in the amount of water stored in the soil as well as in the plants themselves.

These results from the pilot study indicate that although little can be determined about the relationship between the condition of vegetation and the existence of drought conditions by trying to compare the average vegetation index values of vegetation for an entire area, some information is revealed by using several indices for the same area instead of just one. It is also apparent that perhaps a better approach would be to look at individual types of vegetation or vegetation communities to find out more about how they

are impacted by drought conditions. The next portion of this discussion addresses this issue in more detail.

Individual Vegetation Types

In plotting the average index values and the image dates several patterns emerged. Looking at the individual vegetation types helped to reveal more about the characteristics of each type of vegetation and explain why the index values obtained did not always coincide with what was expected.

NDVI Plots

In looking at a plot of all of the NDVI values for each index over time, it is apparent that there are more factors at play than climatic conditions alone that determine the index value response of these different vegetation types (Figure 13). Inactive agriculture stays fairly constant over the course of the imagery dates, this was to be expected based upon the nature of this vegetation type and the understanding that these locations were either fallow fields or mostly soil. Active agriculture appeared to have the overall trends that were anticipated with higher values during normal and wetter periods and lower values during times of drought. This could also be attributed to the phenological cycle of the plants and the dates of the individual imagery. Several dates were during the growing season of the agricultural areas and exhibited lower index values during the time when the plants would be expected to reach maturity and therefore exhibit green lush vegetation, which could be attributed to climatic conditions.

The riparian vegetation exhibited an interesting pattern. In several imagery dates of normal conditions the riparian values are fairly high and then during other times during which there were normal conditions they are fairly low. This appears to have a

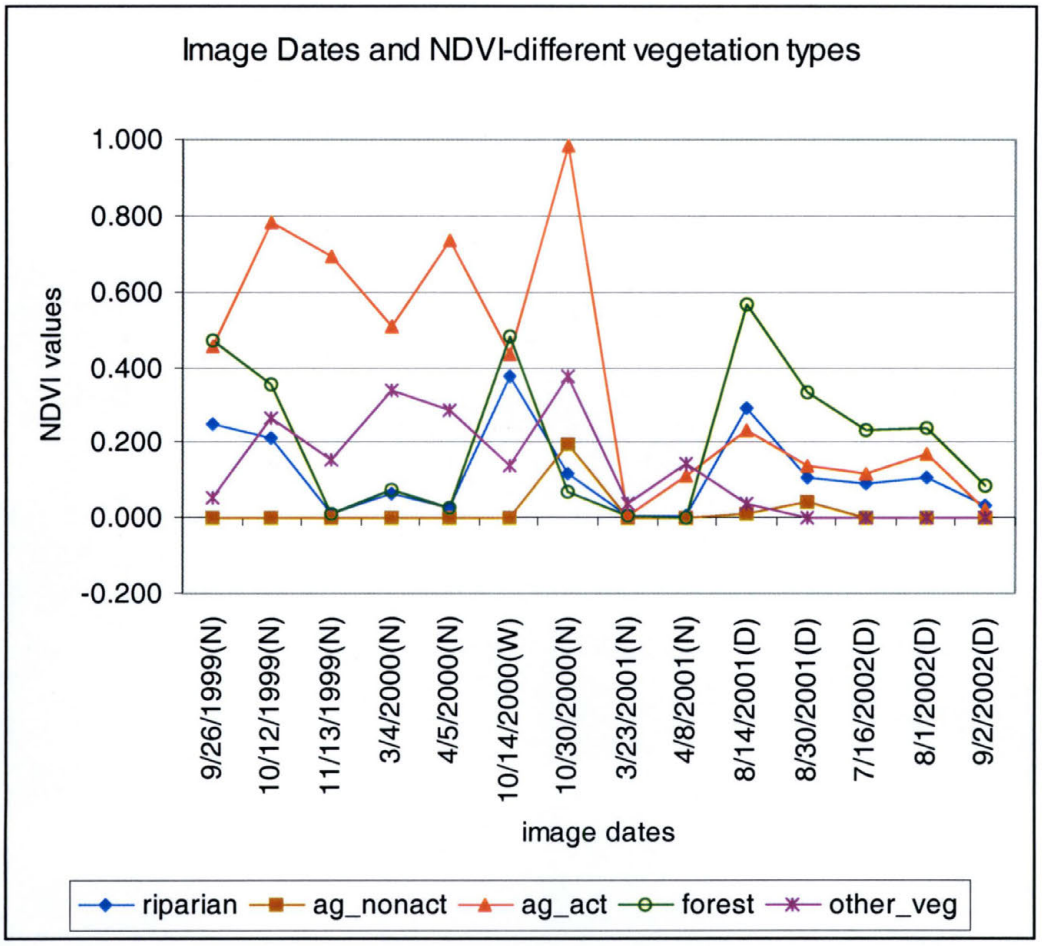

Figure 13: Normalized Difference Vegetation Index values over time for all vegetation types (N = normal conditions; W = wet conditions; D = drought conditions)

connection to the overall streamflow characteristics of the river and may not necessarily be attributed to climatic conditions alone. There is also a spike during wet conditions and then another during drought conditions, which also indicates that streamflow, might be more of a determining characteristic of riparian vegetation health.

Forested areas also exhibited an interesting pattern as well. Although low index values were found during some times of normal conditions, the time of year has an impact on the amount of green vegetation present on these trees due to the fact that most of the trees in this region are deciduous and lose their leaves during the winter and have regrowth in the spring. There are also higher index values during periods of drought conditions, but these times also corresponded to when there would be maximum growth on the trees and therefore there would be a lot of green biomass and higher index values than expected. There are some low index values during the dormant times of year for this vegetation type and some higher values during when there would be maximum growth for the dates that the satellite imagery was used indicating that the normal cycle of this vegetation type might have more of an effect on the index response of this vegetation type than the climate conditions existing at the time.

Other vegetation in this case was defined to be grasses and low shrubs which seem to exhibit the similar pattern as was expected where there were higher values during times of normalcy and wetness and lower values obtained during periods of drought.

SAVI Plots

In looking at the SAVI plots for all of the vegetation types there seem to be fairly similar trends as with the NDVI plots (Figure 14). All of the values are generally higher than those of NDVI, but this is a function of the adjustment factor in the SAVI equation. This adjustment factor is used to try to reduce the amount of reflectance by soil and tries to focus the index value on the reflectance of the vegetation. The line for inactive agriculture, riparian vegetation, and other vegetation appeared to have a similar general shape as that of the NDVI line, which was to be expected since SAVI is a variation on the NDVI equation. However, the active agriculture exhibited a different pattern indicating that the use of the SAVI might be better in cases where there is a lot of soil exposed like in cultivated agricultural fields. The line for the forested areas also exhibited a different pattern than what was observed for the NDVI values, however there was still the same general trend of lower index values during expected dormant periods of this vegetation type and higher values during expected peak times. This indicates that the phenological cycle does have an impact on the index value observed at different times of the year regardless of climatic conditions.

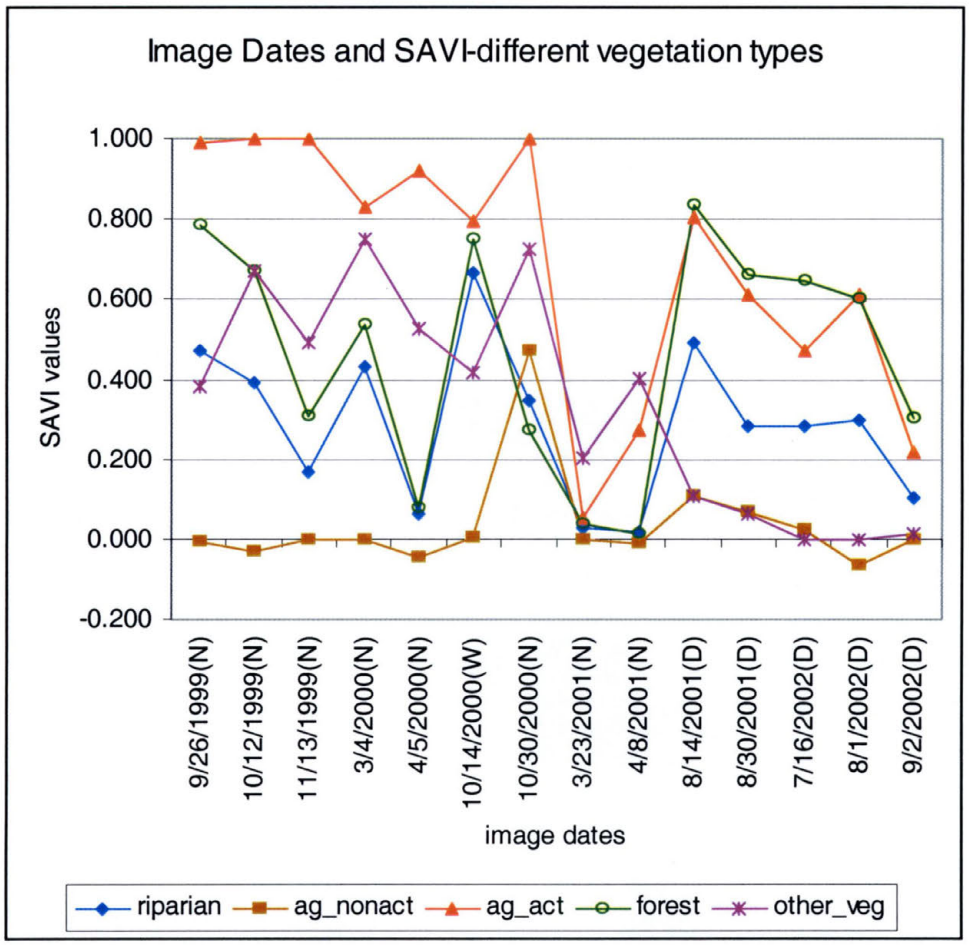

Figure 14: Soil Adjusted Vegetation Index values over time for all vegetation types (N = normal conditions; W = wet conditions; D = drought conditions)

Tasseled Cap Greenness and Wetness Plots

The plot for the tasseled cap greenness index appeared to have smoother lines than the other two and showed the general expected trends where lower values (more negative) were obtained during times of drought and higher values were obtained during times of normal or wet conditions (Figure 15). It also seemed to exhibit some of the similar patterns of the individual vegetation characteristics discussed above including influences on vegetation due to streamflow characteristics and the phenological cycle of the individual plant type.

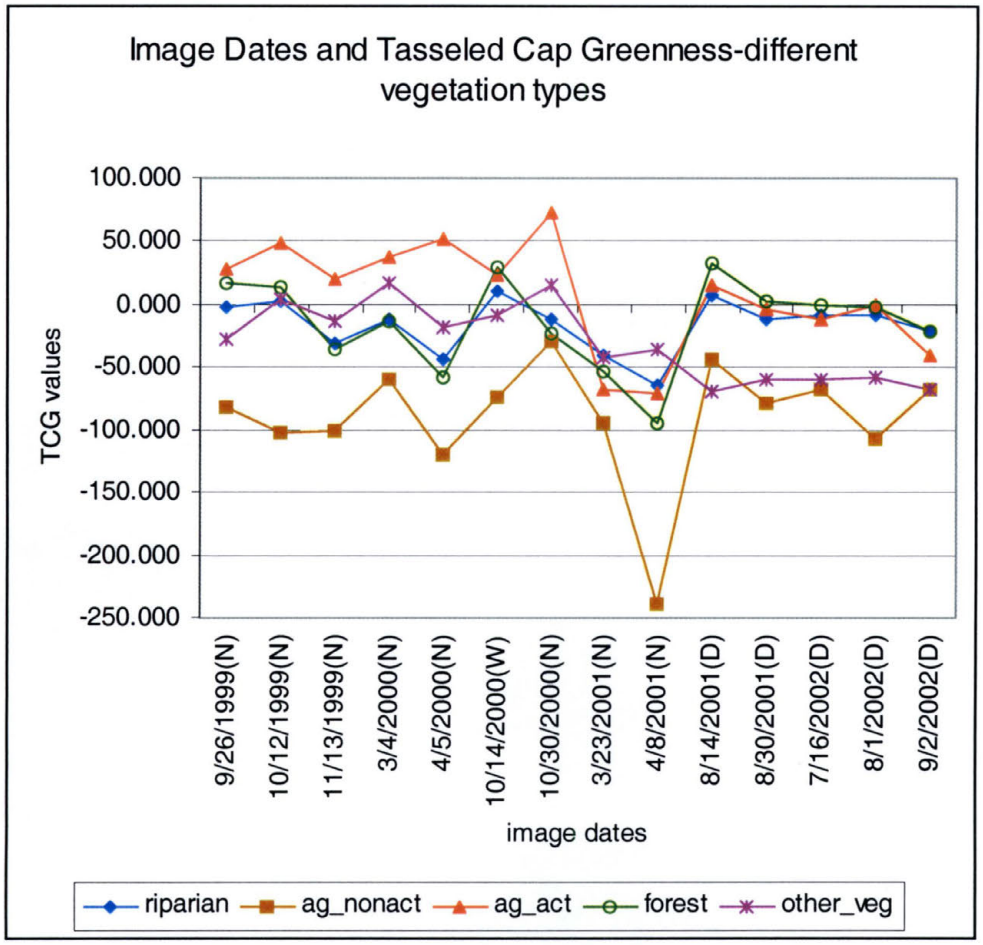

Figure 15: Tasseled Cap Greenness values over time for all vegetation types (N = normal conditions; W = wet conditions; D = drought conditions)

For the tasseled cap wetness plots, the riparian vegetation and forest had similar trends in which higher index values were observed during times of normalcy and times of drought indicating that not only streamflow characteristics but also the phenological cycle of these vegetation types were key factors as observed in the other three plots. The other three vegetation types exhibited similar trends in portions of the lines at particular times of the year, indicating that there was something related to all three of these vegetation types that caused spikes to occur. Times of high moisture (less negative) index values can also be indicative of healthy vegetation, which could not only be the result of changes in climatic conditions, but could also be attributed to soil characteristics, as well as the phenological cycle and planting cycle of these different types of vegetation (Figure 16).

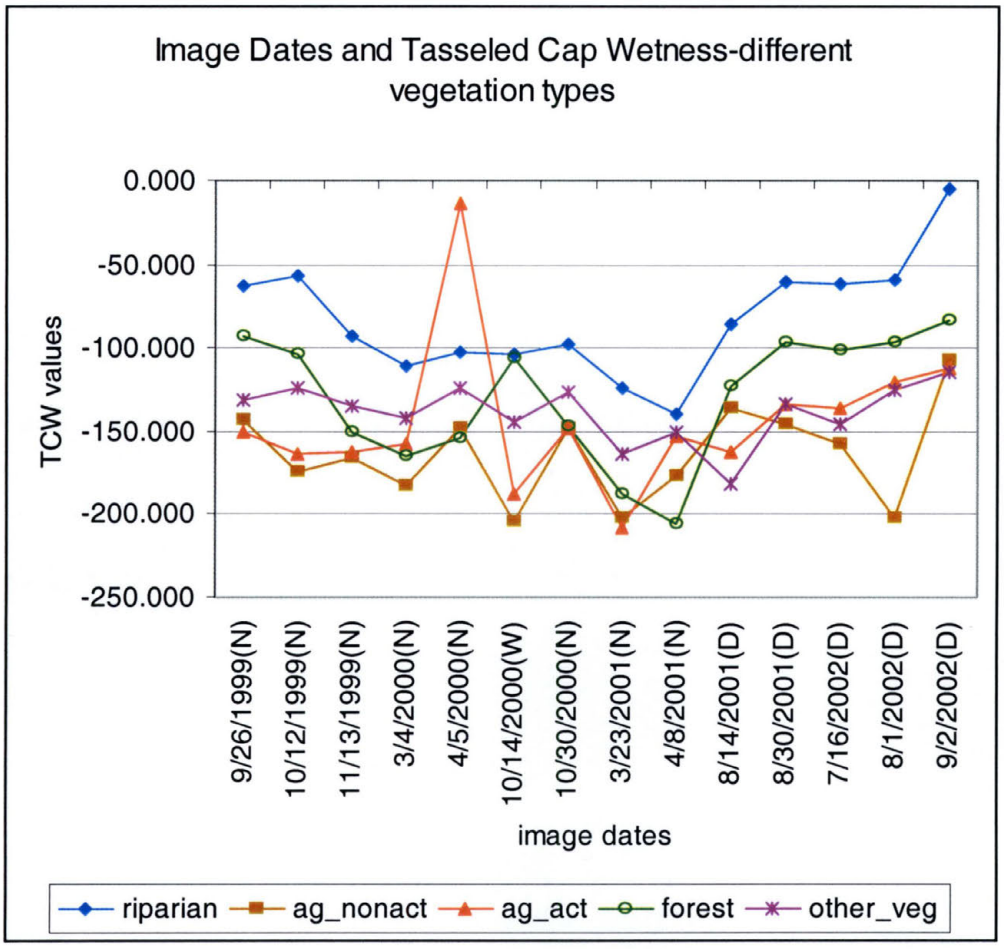

Figure 16: Tasseled Cap Wetness index values over time for all vegetation (N = normal conditions; W = wet conditions; D = drought conditions)

R-squared Values

Once r-squared values were obtained for the relationship between the average index value for each vegetation type and the PDSI the r-squared values were ranked by vegetation type to see how the types of vegetation were ranked based on each index used. The r-squared values for NDVI ranged from 0.003 for the riparian vegetation class to 0.530 for the active agriculture class. There was a moderately strong relationship between the condition of vegetation and the prediction of drought conditions for the active agriculture and other vegetation classes with values of 0.530 and 0.528 respectively.

For SAVI r-squared values ranged from 0.017 for the riparian vegetation class to 0.625 for the other vegetation class. There was a fairly strong relationship between the state of vegetation and the prediction of drought conditions for the other vegetation class with a value of 0.625 and a fairly weak but existent relationship for the active agriculture class with a value of 0.223.

Tasseled cap greenness and wetness values ranged from 0.000 for the inactive agriculture class to 0.732 for the other vegetation class and 0.004 for active agriculture class to 0.274 for the riparian vegetation class respectively. A moderately strong relationship was obtained for the other vegetation class with an r-squared value of 0.732 for tasseled cap greenness and a relatively weak but existent relationship for the riparian vegetation class with an r-squared value of 0.274 for tasseled cap wetness (Table 8).

Regression-each vegetation type				
Vegetation Type	**NDVI**	**SAVI**	**Tasseled Cap-Greenness**	**Tasseled Cap-Wetness**
riparian	0.003	0 017	0 010	0 274
inactive agriculture	0.055	0.028	0.000	0.179
active agriculture	0.530	0 223	0 238	0.004
forest	0 083	0.082	0.037	0.145
other vegetation	0.528	0 625	0.732	0.047

(a)

Vegetation Type	**NDVI**	**SAVI**	**TCG**	**TCW**
riparian	5	5	4	1
inactive agriculture	4	4	5	2
active agriculture	1	2	2	5
forest	3	3	3	3
other vegetation	2	1	1	4

(b)

Table 8: (a) R-squared values obtained for regression analysis between different vegetation types and PDSI values; (b) Ranking of r-squared values by vegetation type.

Once these values were ranked by vegetation type it became evident that forest was consistently ranked third by all four indices, active agriculture was ranked first by one out of the four indices, other vegetation was ranked first by two of the four indices used, inactive agriculture was ranked fourth by two of the four indices, and finally riparian was ranked last by two of the four indices. It was interesting that the same vegetation class was not consistently ranked first by the different greenness indicators (NDVI, SAVI, and Tasseled Cap Greenness) seeing as how the indices were all using the greenness of the vegetation present in an attempt to characterize its vitality and overall condition.

The r-squared values resulting from the two and four week time lag regression analyses revealed other information about the individual vegetation types. For NDVI, it appears that there is a two week time lag for the riparian vegetation to react to changes in climatic conditions based on the r-squared value of 0.023, which is higher than that of the original r-squared valued of 0.003. This trend also appears to be true for SAVI and tasseled cap greenness as well where there are consistently larger r-squared values when a two-week time lag is considered. This indicates that overall, it takes approximately two weeks for there to be a visible change in greenness for this vegetation type.

For the inactive agriculture vegetation class there appears to be a two-week time lag when using the tasseled cap greenness index and a detectable four-week time lag when using both NDVI and SAVI. This means that depending on the vegetation type on the field it can take up to four weeks for there to be a visible reduction in the amount of greenness, which could be an indicator of stress due to changes in climatic conditions.

For the active agriculture vegetation class there appears to be a detectable two-week time lag when using SAVI and tasseled cap greenness indices and a four-week time lag when using the tasseled cap wetness index. This means that it can take approximately two weeks to show differences in greenness that can be associated with changes in climatic conditions for actively cultivated vegetation, and up to four weeks for these plants to exhibit water stress from the same changing environmental factors.

When looking at the forest vegetation class there appears to be a two week time lag when using the tasseled cap greenness index indicating that it can take up to two weeks to observe changes in greenness and thus vitality for forested areas.

For the other vegetation class, there is a two-week time lag when using the tasseled cap wetness vegetation index indicating that this vegetation type exhibits moisture stress after approximately two weeks.

The ranking of these r-squared values revealed that for the two week time lag active agriculture was ranked first by three of the four indices, other vegetation was ranked second by three of the four indices, riparian and inactive agriculture were both ranked third by two of the four indices, and the forest vegetation type was ranked last by three of the four indices. Ranking of the r-squared values for the four week time lag also showed that active agriculture and inactive agriculture were both ranked first by two of the four indices used, forest was ranked third by two of the four indices, riparian vegetation class was ranked fourth by two of the four indices, and the other vegetation class was ranked last by two of the four indices used. Table 9 shows

all of the r-squared values for each vegetation type along with the ranking of the two and four week time lag r-squared values.

2 week lag				
Vegetation Type	**NDVI**	**SAVI**	**Tasseled Cap-Greenness**	**Tasseled Cap-Wetness**
riparian	0 023	0.082	0.096	0 110
inactive agriculture	0 022	0.029	0 097	0 064
active agriculture	0 241	0.293	0.375	0 192
forest	0 003	0 039	0 068	0.084
other vegetation	0 193	0 175	0.161	0 235

(a)

4 week lag				
Vegetation Type	**NDVI**	**SAVI**	**Tasseled Cap-Greenness**	**Tasseled Cap-Wetness**
riparian	0 008	0 025	0 041	0.150
inactive agriculture	0 117	0.156	0 008	0.046
active agriculture	0 007	0 058	0 099	0.366
forest	0 014	0 047	0 038	0.125
other vegetation	0 012	0 002	0.000	0.180

(b)

2 week lag				
Vegetation Type	**NDVI**	**SAVI**	**TCG**	**TCW**
riparian	3	4	4	3
inactive agriculture	4	3	3	5
active agriculture	1	1	1	2
forest	5	5	5	4
other vegetation	2	2	2	1

(c)

4 week lag				
Vegetation Type	**NDVI**	**SAVI**	**TCG**	**TCW**
riparian	4	4	2	3
inactive agriculture	1	1	4	5
active agriculture	5	2	1	1
forest	2	3	3	4
other vegetation	3	5	5	2

(d)

Table 9: (a) and (b) R-squared values for time lag analysis; (c) and (d) Rankings of index values based on vegetation types

CHAPTER 6

SUMMARY AND CONCLUSIONS

Summary

The use of satellite imagery to monitor vegetation has been important for decades. The majority of previous studies have focused on the use of AVHRR based vegetation indices, primarily NDVI, to assess the response of vegetation to changes in climatic conditions. This study focused on the use of Landsat 7 ETM+ derived vegetation indices to study the relationship between vegetation condition and the existence of drought conditions over a four-year period for the Cuyahoga River Watershed in northeastern Ohio. Three vegetation indices were selected (NDVI, SAVI, Tasseled Cap) to test their utility when studying the response of different types of vegetation to drought. Specifically, the major objectives of this study were 1) to test the use of NDVI and two other indices to see if NDVI is the best vegetation index to use for drought studies with satellite imagery, 2) to determine if the state of vegetation can predict the existence of drought conditions, and 3) to see if a lag time can be detected for the response of vegetation to changes in climatic conditions.

This study is important because there is a known relationship between climate and vegetation dynamics as monitored from space, however few studies investigate

vegetation index variation on individual homogeneous land cover units as they relate to specific climate and environmental influences at a local scale. Since drought is such a dynamic and powerful weather-related disaster and accurately monitoring drought has been shown to be a challenge, studies that provide alternate ways of studying the response of specific vegetation types to changes in climatic conditions using higher resolution imagery help to refine the methodologies used in these studies and expand the knowledge of the different capabilities of some of the most widely used tools available for vegetation monitoring. Studies like this one also help to test the different applications of remote sensing and provide a means by which information can be extracted from this extremely useful data source.

Future Considerations

There are many directions that this research could take in the future. However, there are two main points that should be addressed when continuing this research. The first is that the Palmer Drought Severity Index, although it is widely used for drought monitoring is not well suited for local scale analysis. There are many reasons why this is be true, however the ones most relevant to this research are the significance of a single value used to cover a rather large area and the use of only a single soil type to calculate the index value for an entire climate division (climate division 3). It seems hard to believe that only one value can accurately represent the climatic conditions in such a large area (approximately 3,735 square miles), especially when there are varying soil types within the region (Figure 17).

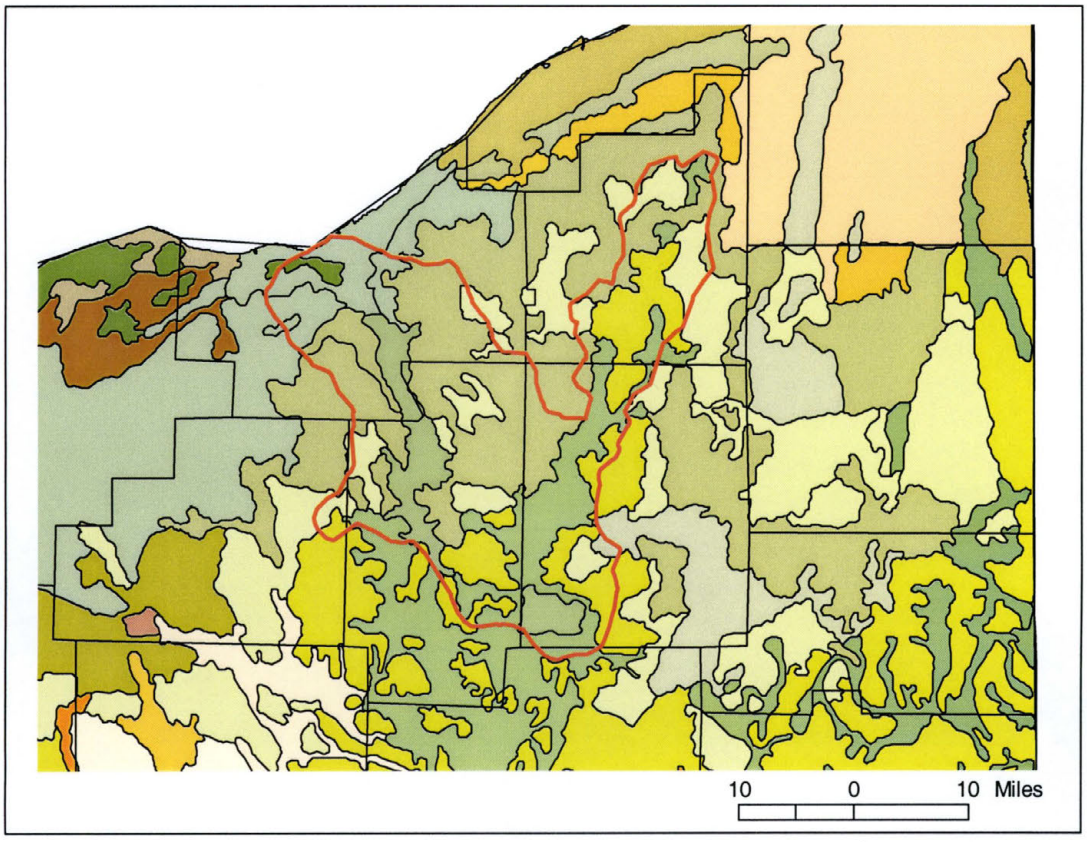

Figure 17: Soils map of Cuyahoga River Watershed

It seems evident from looking at this map that using one soil type for this study is just not going to yield an accurate value for calculating a climatological index for this region. For information on other criticisms of the use of the Palmer Drought Severity Index see publications by Alley (1984) and Heddinghaus and Sabol (1991). It seems that the best-case scenario for using this index would have to be a study where an entire state or climate division was used for analysis instead of a small portion, thus limiting its potential for use in drought studies at a local scale.

Another is that past studies have seemed to rely heavily on linear regression analysis for determining the relationship between vegetation characteristics and climatic variables. However, future research needs to examine the possibility that this relationship may not be linear. Perhaps if more than fourteen images were available for use in this study more of a pattern could be revealed. This is definitely be something that could be expanded on in the future since the data as they are now do not seem to display that particular pattern (Figure 18).

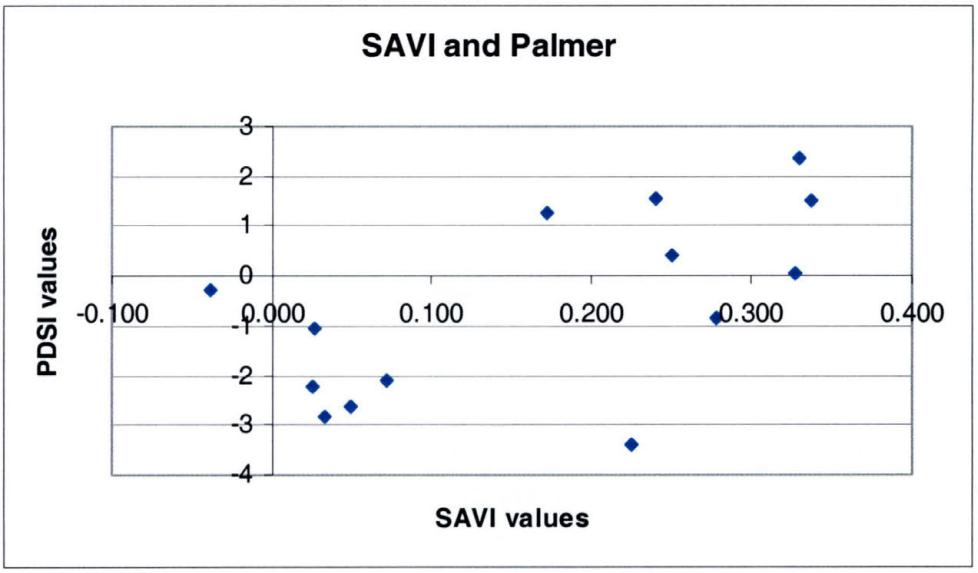

Figure 18: Example of distribution of points for the fourteen images chosen.

Conclusions

Results of the watershed scale analysis revealed that overall trends in the data seemed to follow those of other drought and vegetation studies in times of drought were accompanied by low vegetation index values and times of normal or wet conditions were accompanied by generally higher index values. The fact that there was a detectable two-week time lag for tasseled cap greenness and a four-week time lag for tasseled cap wetness meant that there was a lag in the response of vegetation to the changing climate conditions. This could be a reason for the lack of variance explained by using the regression analysis of the images and their corresponding PDSI values. The low r-squared values resulting from the regression analysis indicate that the response of vegetation to drought conditions cannot be explained well by using an average vegetation index value for an entire area and that perhaps a better approach to studying the impact of drought conditions on vegetation requires the study of the response of individual plant communities or specific vegetation types in order to better understand their response to drought.

In looking at the results for the individual vegetation types considered in this study, it becomes apparent that more information can be extracted about what is going on in the watershed in terms of the response of vegetation to drought conditions. It was evident after looking at the plots of the index values over time that more factors contribute to changes in vegetation condition and characteristics (time of year, phonological cycle, water availability) than simply climatic conditions. It was also

apparent after looking at the r-squared values that the condition of vegetation could predict the existence of drought conditions, depending on the type of vegetation studied. For example the highest r-squared values obtained were for the other vegetation class and active agriculture. It was also determined that the best index to use for riparian vegetation, forest, and inactive agriculture was tasseled cap wetness. For active agriculture the best index was NDVI and for the other vegetation class tasseled cap greenness provided the best results. Overall, it was apparent that the riparian vegetation class and the forest vegetation class were both more resilient to changes in climatic conditions than any of the other vegetation types. Inactive agriculture also appeared to be unaffected by changes in climate as well due to the nature of this variable. For the active agriculture class a two-week time lag was observed using the tasseled cap greenness index meaning that it takes approximately two weeks for cultivated agriculture areas approximately two weeks to show signs of stress in terms of vegetation greenness and vitality. There was also a four-week time lag for this vegetation class using the tasseled cap wetness index indicating that it can take up to approximately four weeks for the vegetation to exhibit signs of water stress associated with climatic changes. The other vegetation class showed a two-week time lag using the tasseled cap wetness index indicating that it takes approximately two weeks for this vegetation type to exhibit signs of moisture stress.

The results obtained in this study help to reinforce the importance of studies that explore the use of various techniques to observe and monitor changes in vegetation as a result of changing climatic conditions. This study also shows that NDVI is not

necessarily the best vegetation index to use depending on the specific issue being examined and the size of the study area.

APPENDIX I

ATCOR REPORTS

9/26/1999

```
Number of rows    : 2392
Number of columns: 2129

Subset definition:
ulx=0       uly=0
lrx=2128    lry=2391
Ignore zero in output statistics: Yes

Sensor = Landsat-7 TM
Filelayer - Sensorband correspondence:
    0   -   1
    1   -   2
    2   -   3
    3   -   4
    4   -   5
    5   -   6
    6   -   7
Pixelsize: 30.000000 meters
Acquisition date (day/month) = 26/9
Mean ground elevation of site = 0.300000 km
Solar zenith angle = 47.200000 degrees

Adjacency window size (pixels) = 33 * 33
Multiplication factor for reflective bands: 4.000000
Multiplication factor for TM-Band 6: 4.000000
Offset value for TM-Band 6: 0.000000 degrees Celcius

Model: Constant spatial atmospheric Conditions
Visibility: 15.000000 km

Calibration coefficients(mW / cm^2 sr micrometer)
band        c0            c1           gain setting
-------------------------------------------------
1       -0.258000       0.125800       1.000000
2       -0.265000       0.126500       1.000000
3       -0.073000       0.097300       1.000000
4       -0.077000       0.097700       1.000000
5       -0.020200       0.020200       1.000000
7       -0.069100       0.006910       1.000000

 TM thermal band calibration coefficients
at-sensor radiance              L = c0 + c1 * DN
at-sensor brightn. temperature  T = K2 / ( K1 - ln (c0+c1*DN))
 c0 = 0.124000        c1 = 0.005630 (mW/cm^2 sr micron)
 K1 = 4.175400        K2 = 1274.670000

Haze Removal Policy: Haze Removal, omit VIS. INDEX file
Haze Removal Algorithm: none (fastest)

Coefficients for Tasseled Cap Haze Band: Blue: 0.846000     Red: -
0.464000
```

```
Haze threshold T3: 0.700000
Haze threshold T4: 2.000000
Cloud threshold T5: 4.000000
```

10/12/1999

```
Number of rows    : 2392
Number of columns: 2129

Subset definition:
ulx=0       uly=0
lrx=2128    lry=2391
Ignore zero in output statistics: No

Sensor = Landsat-7 TM
Filelayer - Sensorband correspondence:
    0   -   1
    1   -   2
    2   -   3
    3   -   4
    4   -   5
    5   -   6
    6   -   7
Pixelsize: 30.000000 meters
Acquisition date (day/month) = 12/10
Mean ground elevation of site = 0.300000 km
Solar zenith angle = 52.600000 degrees

Adjacency window size (pixels) = 33 * 33
Multiplication factor for reflective bands: 4.000000
Multiplication factor for TM-Band 6: 4.000000
Offset value for TM-Band 6: 0.000000 degrees Celcius

Model: Constant spatial atmospheric Conditions
Visibility: 15.000000 km

Calibration coefficients(mW / cm^2 sr micrometer)
band        c0            c1           gain setting
-----------------------------------------------------
1      -0.258000      0.125800      1.000000
2      -0.265000      0.126500      1.000000
3      -0.073000      0.097300      1.000000
4      -0.077000      0.097700      1.000000
5      -0.020200      0.020200      1.000000
7      -0.069100      0.006910      1.000000

 TM thermal band calibration coefficients
at-sensor radiance              L = c0 + c1 * DN
at-sensor brightn. temperature  T = K2 / ( K1 - ln (c0+c1*DN))
 c0 = 0.124000        c1 = 0.005630 (mW/cm^2 sr micron)
 K1 = 4.175400        K2 = 1274.670000

Haze Removal Policy: Haze Removal, omit VIS. INDEX file
Haze Removal Algorithm: none (fastest)
```

```
Coefficients for Tasseled Cap Haze Band: Blue: 0.846000     Red: -
0.464000
Haze threshold T3: 0.700000
Haze threshold T4: 2.000000
Cloud threshold T5: 4.000000
```

11/13/1999

```
Number of rows    : 2392
Number of columns: 2129

Subset definition:
ulx=0       uly=0
lrx=2128    lry=2391
Ignore zero in output statistics: No

Sensor = Landsat-7 TM
Filelayer - Sensorband correspondence:
    0   -   1
    1   -   2
    2   -   3
    3   -   4
    4   -   5
    5   -   6
    6   -   7
Pixelsize: 30.000000 meters
Acquisition date (day/month) = 13/11
Mean ground elevation of site = 0.300000 km
Solar zenith angle = 62.600000 degrees

Adjacency window size (pixels) = 33 * 33
Multiplication factor for reflective bands: 4.000000
Multiplication factor for TM-Band 6: 4.000000
Offset value for TM-Band 6: 0.000000 degrees Celcius

Model: Constant spatial atmospheric Conditions
Visibility: 15.000000 km

Calibration coefficients(mW / cm^2 sr micrometer)
band        c0            c1           gain setting
-----------------------------------------------------
1      -0.258000      0.125800      1.000000
2      -0.265000      0.126500      1.000000
3      -0.073000      0.097300      1.000000
4      -0.077000      0.097700      1.000000
5      -0.020200      0.020200      1.000000
7      -0.069100      0.006910      1.000000

 TM thermal band calibration coefficients
at-sensor radiance              L = c0 + c1 * DN
at-sensor brightn. temperature  T = K2 / ( K1 - ln (c0+c1*DN))
 c0 = 0.124000        c1 = 0.005630 (mW/cm^2 sr micron)
 K1 = 4.175400        K2 = 1274.670000
```

```
Haze Removal Policy: Haze Removal, omit VIS. INDEX file
Haze Removal Algorithm: none (fastest)
Coefficients for Tasseled Cap Haze Band: Blue: 0.846000     Red: -
0.464000
Haze threshold T3: 0.700000
Haze threshold T4: 2.000000
Cloud threshold T5: 4.000000
```

3/4/2000

```
Number of rows    : 2392
Number of columns: 2129

Subset definition:
ulx=0       uly=0
lrx=2128    lry=2391
Ignore zero in output statistics: No

Sensor = Landsat-7 TM
Filelayer - Sensorband correspondence:
    0   -   1
    1   -   2
    2   -   3
    3   -   4
    4   -   5
    5   -   6
    6   -   7
Pixelsize: 30.000000 meters
Acquisition date (day/month) = 4/3
Mean ground elevation of site = 0.300000 km
Solar zenith angle = 53.600000 degrees

Adjacency window size (pixels) = 33 * 33
Multiplication factor for reflective bands: 4.000000
Multiplication factor for TM-Band 6: 4.000000
Offset value for TM-Band 6: 0.000000 degrees Celcius

Model: Constant spatial atmospheric Conditions
Visibility: 15.000000 km

Calibration coefficients(mW / cm^2 sr micrometer)
band        c0            c1           gain setting
-----------------------------------------------------
1      -0.258000      0.125800      1.000000
2      -0.265000      0.126500      1.000000
3      -0.073000      0.097300      1.000000
4      -0.077000      0.097700      1.000000
5      -0.020200      0.020200      1.000000
7      -0.069100      0.006910      1.000000

 TM thermal band calibration coefficients
at-sensor radiance              L = c0 + c1 * DN
at-sensor brightn. temperature  T = K2 / ( K1 - ln (c0+c1*DN))
 c0 = 0.124000        c1 = 0.005630 (mW/cm^2 sr micron)
 K1 = 4.175400        K2 = 1274.670000
```

```
Haze Removal Policy: Haze Removal, omit VIS. INDEX file
Haze Removal Algorithm: none (fastest)
Coefficients for Tasseled Cap Haze Band: Blue: 0.846000     Red: -
0.464000
Haze threshold T3: 0.700000
Haze threshold T4: 2.000000
Cloud threshold T5: 4.000000
```

4/5/2000

```
Number of rows    : 2392
Number of columns: 2129

Subset definition:
ulx=0       uly=0
lrx=2128    lry=2391
Ignore zero in output statistics: No

Sensor = Landsat-7 TM
Filelayer - Sensorband correspondence:
    0   -   1
    1   -   2
    2   -   3
    3   -   4
    4   -   5
    5   -   6
    6   -   7
Pixelsize: 30.000000 meters
Acquisition date (day/month) = 5/4
Mean ground elevation of site = 0.300000 km
Solar zenith angle = 41.400000 degrees

Adjacency window size (pixels) = 33 * 33
Multiplication factor for reflective bands: 4.000000
Multiplication factor for TM-Band 6: 4.000000
Offset value for TM-Band 6: 0.000000 degrees Celcius

Model: Constant spatial atmospheric Conditions
Visibility: 15.000000 km

Calibration coefficients(mW / cm^2 sr micrometer)
band        c0            c1           gain setting
-----------------------------------------------------
1      -0.258000      0.125800      1.000000
2      -0.265000      0.126500      1.000000
3      -0.073000      0.097300      1.000000
4      -0.077000      0.097700      1.000000
5      -0.020200      0.020200      1.000000
7      -0.069100      0.006910      1.000000

 TM thermal band calibration coefficients
at-sensor radiance              L = c0 + c1 * DN
at-sensor brightn. temperature  T = K2 / ( K1 - ln (c0+c1*DN))
 c0 = 0.124000        c1 = 0.005630 (mW/cm^2 sr micron)
```

```
 K1 = 4.175400        K2 = 1274.670000

Haze Removal Policy: Haze Removal, omit VIS. INDEX file
Haze Removal Algorithm: none (fastest)

Coefficients for Tasseled Cap Haze Band: Blue: 0.846000     Red: -
0.464000
Haze threshold T3: 0.700000
Haze threshold T4: 2.000000
Cloud threshold T5: 4.000000
```

10/14/2000

```
Number of rows    : 2392
Number of columns: 2129

Subset definition:
ulx=0       uly=0
lrx=2128    lry=2391
Ignore zero in output statistics: No

Sensor = Landsat-7 TM
Filelayer - Sensorband correspondence:
    0   -   1
    1   -   2
    2   -   3
    3   -   4
    4   -   5
    5   -   6
    6   -   7
Pixelsize: 30.000000 meters
Acquisition date (day/month) = 14/10
Mean ground elevation of site = 0.300000 km
Solar zenith angle = 53.300000 degrees

Adjacency window size (pixels) = 33 * 33
Multiplication factor for reflective bands: 4.000000
Multiplication factor for TM-Band 6: 4.000000
Offset value for TM-Band 6: 0.000000 degrees Celcius

Model: Constant spatial atmospheric Conditions
Visibility: 15.000000 km

Calibration coefficients(mW / cm^2 sr micrometer)
band        c0            c1           gain setting
-----------------------------------------------------
1      -0.258000      0.125800      1.000000
2      -0.265000      0.126500      1.000000
3      -0.073000      0.097300      1.000000
4      -0.077000      0.097700      1.000000
5      -0.020200      0.020200      1.000000
7      -0.069100      0.006910      1.000000

 TM thermal band calibration coefficients
at-sensor radiance              L = c0 + c1 * DN
```

```
at-sensor brightn. temperature  T = K2 / ( K1 - ln (c0+c1*DN))
 c0 = 0.124000        c1 = 0.005630 (mW/cm^2 sr micron)
 K1 = 4.175400        K2 = 1274.670000

Haze Removal Policy: Haze Removal, omit VIS. INDEX file
Haze Removal Algorithm: none (fastest)

Coefficients for Tasseled Cap Haze Band: Blue: 0.846000     Red: -
0.464000
Haze threshold T3: 0.700000
Haze threshold T4: 2.000000
Cloud threshold T5: 4.000000
```

10/30/2000

```
Number of rows    : 2392
Number of columns: 2129

Subset definition:
ulx=0       uly=0
lrx=2128          lry=2391
Ignore zero in output statistics: No

Sensor = Landsat-7 TM
Filelayer - Sensorband correspondence:
    0   -   1
    1   -   2
    2   -   3
    3   -   4
    4   -   5
    5   -   6
    6   -   7
Pixelsize: 30.000000 meters
Acquisition date (day/month) = 30/10
Mean ground elevation of site = 0.300000 km
Solar zenith angle = 58.500000 degrees

Adjacency window size (pixels) = 33 * 33
Multiplication factor for reflective bands: 4.000000
Multiplication factor for TM-Band 6: 4.000000
Offset value for TM-Band 6: 0.000000 degrees Celcius

Model: Constant spatial atmospheric Conditions
Visibility: 15.000000 km

Calibration coefficients(mW / cm^2 sr micrometer)
band        c0            c1           gain setting
-------------------------------------------------
1      -0.258000      0.125800      1.000000
2      -0.265000      0.126500      1.000000
3      -0.073000      0.097300      1.000000
4      -0.077000      0.097700      1.000000
5      -0.020200      0.020200      1.000000
7      -0.069100      0.006910      1.000000
```

```
 TM thermal band calibration coefficients
at-sensor radiance              L = c0 + c1 * DN
at-sensor brightn. temperature  T = K2 / ( K1 - ln (c0+c1*DN))
 c0 = 0.124000        c1 = 0.005630 (mW/cm^2 sr micron)
 K1 = 4.175400        K2 = 1274.670000
Haze Removal Policy: Haze Removal, omit VIS. INDEX file
Haze Removal Algorithm: none (fastest)

Coefficients for Tasseled Cap Haze Band: Blue: 0.846000     Red: -
0.464000
Haze threshold T3: 0.700000
Haze threshold T4: 2.000000
Cloud threshold T5: 4.000000
```

3/23/2001

```
Number of rows    : 2392
Number of columns: 2129

Subset definition:
ulx=0       uly=0
lrx=2128    lry=2391
Ignore zero in output statistics: No

Sensor = Landsat-7 TM
Filelayer - Sensorband correspondence:
    0   -   1
    1   -   2
    2   -   3
    3   -   4
    4   -   5
    5   -   6
    6   -   7
Pixelsize: 30.000000 meters
Acquisition date (day/month) = 23/3
Mean ground elevation of site = 0.300000 km
Solar zenith angle = 45.900000 degrees

Adjacency window size (pixels) = 33 * 33
Multiplication factor for reflective bands: 4.000000
Multiplication factor for TM-Band 6: 4.000000
Offset value for TM-Band 6: 0.000000 degrees Celcius

Model: Constant spatial atmospheric Conditions
Visibility: 15.000000 km

Calibration coefficients(mW / cm^2 sr micrometer)
band        c0            c1           gain setting
-------------------------------------------------
1      -0.258000      0.125800      1.000000
2      -0.265000      0.126500      1.000000
3      -0.073000      0.097300      1.000000
4      -0.077000      0.097700      1.000000
5      -0.020200      0.020200      1.000000
7      -0.069100      0.006910      1.000000
```

```
 TM thermal band calibration coefficients
at-sensor radiance              L = c0 + c1 * DN
at-sensor brightn. temperature  T = K2 / ( K1 - ln (c0+c1*DN))
 c0 = 0.124000        c1 = 0.005630 (mW/cm^2 sr micron)
 K1 = 4.175400        K2 = 1274.670000

Haze Removal Policy: Haze Removal, omit VIS. INDEX file
Haze Removal Algorithm: none (fastest)

Coefficients for Tasseled Cap Haze Band: Blue: 0.846000     Red: -
0.464000
Haze threshold T3: 0.700000
Haze threshold T4: 2.000000
Cloud threshold T5: 4.000000
```

4/8/2001

```
Number of rows    : 2392
Number of columns: 2129

Subset definition:
ulx=0       uly=0
lrx=2128    lry=2391
Ignore zero in output statistics: No

Sensor = Landsat-7 TM
Filelayer - Sensorband correspondence:
    0   -   1
    1   -   2
    2   -   3
    3   -   4
    4   -   5
    5   -   6
    6   -   7
Pixelsize: 30.000000 meters
Acquisition date (day/month) = 8/4
Mean ground elevation of site = 0.300000 km
Solar zenith angle = 40.600000 degrees

Adjacency window size (pixels) = 33 * 33
Multiplication factor for reflective bands: 4.000000
Multiplication factor for TM-Band 6: 4.000000
Offset value for TM-Band 6: 0.000000 degrees Celcius

Model: Constant spatial atmospheric Conditions
Visibility: 15.000000 km

Calibration coefficients(mW / cm^2 sr micrometer)
band        c0            c1           gain setting
-----------------------------------------------------
1      -0.258000      0.125800      1.000000
2      -0.265000      0.126500      1.000000
3      -0.073000      0.097300      1.000000
4      -0.077000      0.097700      1.000000
```

```
5       -0.020200       0.020200       1.000000
7       -0.069100       0.006910       1.000000

 TM thermal band calibration coefficients
at-sensor radiance              L = c0 + c1 * DN
at-sensor brightn. temperature  T = K2 / ( K1 - ln (c0+c1*DN))
 c0 = 0.124000         c1 = 0.005630 (mW/cm^2 sr micron)
 K1 = 4.175400         K2 = 1274.670000

Haze Removal Policy: Haze Removal, omit VIS. INDEX file
Haze Removal Algorithm: none (fastest)

Coefficients for Tasseled Cap Haze Band: Blue: 0.846000     Red: -
0.464000
Haze threshold T3: 0.700000
Haze threshold T4: 2.000000
Cloud threshold T5: 4.000000
```

8/14/2001

```
Number of rows    : 2392
Number of columns: 2129

Subset definition:
ulx=0       uly=0
lrx=2128    lry=2391
Ignore zero in output statistics: No

Sensor = Landsat-7 TM
Filelayer - Sensorband correspondence:
    0   -   1
    1   -   2
    2   -   3
    3   -   4
    4   -   5
    5   -   6
    6   -   7
Pixelsize: 30.000000 meters
Acquisition date (day/month) = 14/8
Mean ground elevation of site = 0.300000 km
Solar zenith angle = 34.900000 degrees

Adjacency window size (pixels) = 33 * 33
Multiplication factor for reflective bands: 4.000000
Multiplication factor for TM-Band 6: 4.000000
Offset value for TM-Band 6: 0.000000 degrees Celcius

Model: Constant spatial atmospheric Conditions
Visibility: 15.000000 km

Calibration coefficients(mW / cm^2 sr micrometer)
band        c0            c1           gain setting
-------------------------------------------------
1       -0.258000       0.125800       1.000000
2       -0.265000       0.126500       1.000000
```

```
3       -0.073000       0.097300       1.000000
4       -0.077000       0.097700       1.000000
5       -0.020200       0.020200       1.000000
7       -0.069100       0.006910       1.000000

 TM thermal band calibration coefficients
at-sensor radiance              L = c0 + c1 * DN
at-sensor brightn. temperature  T = K2 / ( K1 - ln (c0+c1*DN))
 c0 = 0.124000        c1 = 0.005630 (mW/cm^2 sr micron)
 K1 = 4.175400        K2 = 1274.670000

Haze Removal Policy: Haze Removal, omit VIS. INDEX file
Haze Removal Algorithm: none (fastest)

Coefficients for Tasseled Cap Haze Band: Blue: 0.846000     Red: -
0.464000
Haze threshold T3: 0.700000
Haze threshold T4: 2.000000
Cloud threshold T5: 4.000000
```

8/30/2001

```
Number of rows    : 2392
Number of columns: 2129

Subset definition:
ulx=0       uly=0
lrx=2128    lry=2391
Ignore zero in output statistics: No

Sensor = Landsat-7 TM
Filelayer - Sensorband correspondence:
    0   -   1
    1   -   2
    2   -   3
    3   -   4
    4   -   5
    5   -   6
    6   -   7
Pixelsize: 30.000000 meters
Acquisition date (day/month) = 30/8
Mean ground elevation of site = 0.300000 km
Solar zenith angle = 39.000000 degrees

Adjacency window size (pixels) = 33 * 33
Multiplication factor for reflective bands: 4.000000
Multiplication factor for TM-Band 6: 4.000000
Offset value for TM-Band 6: 0.000000 degrees Celcius

Model: Constant spatial atmospheric Conditions
Visibility: 15.000000 km

Calibration coefficients(mW / cm^2 sr micrometer)
band        c0            c1           gain setting
-----------------------------------------------------
```

```
1       -0.258000       0.125800       1.000000
2       -0.265000       0.126500       1.000000
3       -0.073000       0.097300       1.000000
4       -0.077000       0.097700       1.000000
5       -0.020200       0.020200       1.000000
7       -0.069100       0.006910       1.000000

 TM thermal band calibration coefficients
at-sensor radiance              L = c0 + c1 * DN
at-sensor brightn. temperature  T = K2 / ( K1 - ln (c0+c1*DN))
 c0 = 0.124000          c1 = 0.005630 (mW/cm^2 sr micron)
 K1 = 4.175400          K2 = 1274.670000

Haze Removal Policy: Haze Removal, omit VIS. INDEX file
Haze Removal Algorithm: none (fastest)

Coefficients for Tasseled Cap Haze Band: Blue: 0.846000     Red: -
0.464000
Haze threshold T3: 0.700000
Haze threshold T4: 2.000000
Cloud threshold T5: 4.000000
```

7/16/2002

```
Number of rows    : 2392
Number of columns: 2129

Subset definition:
ulx=0       uly=0
lrx=2128    lry=2391
Ignore zero in output statistics: No

Sensor = Landsat-7 TM
Filelayer - Sensorband correspondence:
    0   -   1
    1   -   2
    2   -   3
    3   -   4
    4   -   5
    5   -   6
    6   -   7
Pixelsize: 30.000000 meters
Acquisition date (day/month) = 16/7
Mean ground elevation of site = 0.300000 km
Solar zenith angle = 29.400000 degrees

Adjacency window size (pixels) = 33 * 33
Multiplication factor for reflective bands: 4.000000
Multiplication factor for TM-Band 6: 4.000000
Offset value for TM-Band 6: 0.000000 degrees Celcius

Model: Constant spatial atmospheric Conditions
Visibility: 15.000000 km

Calibration coefficients(mW / cm^2 sr micrometer)
```

```
band        c0            c1           gain setting
-------------------------------------------------
1       -0.258000      0.125800      1.000000
2       -0.265000      0.126500      1.000000
3       -0.073000      0.097300      1.000000
4       -0.077000      0.097700      1.000000
5       -0.020200      0.020200      1.000000
7       -0.069100      0.006910      1.000000

 TM thermal band calibration coefficients
at-sensor radiance              L = c0 + c1 * DN
at-sensor brightn. temperature  T = K2 / ( K1 - ln (c0+c1*DN))
 c0 = 0.124000        c1 = 0.005630 (mW/cm^2 sr micron)
 K1 = 4.175400        K2 = 1274.670000

Haze Removal Policy: Haze Removal, omit VIS. INDEX file
Haze Removal Algorithm: none (fastest)

Coefficients for Tasseled Cap Haze Band: Blue: 0.846000     Red: -
0.464000
Haze threshold T3: 0.700000
Haze threshold T4: 2.000000
Cloud threshold T5: 4.000000
```

8/1/2002

```
Number of rows    : 2392
Number of columns: 2129

Subset definition:
ulx=0       uly=0
lrx=2128    lry=2391
Ignore zero in output statistics: No

Sensor = Landsat-7 TM
Filelayer - Sensorband correspondence:
    0   -   1
    1   -   2
    2   -   3
    3   -   4
    4   -   5
    5   -   6
    6   -   7
Pixelsize: 30.000000 meters
Acquisition date (day/month) = 1/8
Mean ground elevation of site = 0.300000 km
Solar zenith angle = 32.100000 degrees

Adjacency window size (pixels) = 33 * 33
Multiplication factor for reflective bands: 4.000000
Multiplication factor for TM-Band 6: 4.000000
Offset value for TM-Band 6: 0.000000 degrees Celcius

Model: Constant spatial atmospheric Conditions
Visibility: 15.000000 km
```

```
Calibration coefficients (mW / cm^2 sr micrometer)
band        c0            c1           gain setting
-------------------------------------------------
1      -0.258000      0.125800      1.000000
2      -0.265000      0.126500      1.000000
3      -0.073000      0.097300      1.000000
4      -0.077000      0.097700      1.000000
5      -0.020200      0.020200      1.000000
7      -0.069100      0.006910      1.000000

 TM thermal band calibration coefficients
at-sensor radiance              L = c0 + c1 * DN
at-sensor brightn. temperature  T = K2 / ( K1 - ln (c0+c1*DN))
 c0 = 0.124000        c1 = 0.005630 (mW/cm^2 sr micron)
 K1 = 4.175400        K2 = 1274.670000

Haze Removal Policy: Haze Removal, omit VIS. INDEX file
Haze Removal Algorithm: none (fastest)

Coefficients for Tasseled Cap Haze Band: Blue: 0.846000     Red: -
0.464000
Haze threshold T3: 0.700000
Haze threshold T4: 2.000000
Cloud threshold T5: 4.000000
```

9/2/2002

```
Number of rows    : 2392
Number of columns: 2129

Subset definition:
ulx=0       uly=0
lrx=2128    lry=2391
Ignore zero in output statistics: Yes

Sensor = Landsat-7 TM
Filelayer - Sensorband correspondence:
    0   -   1
    1   -   2
    2   -   3
    3   -   4
    4   -   5
    5   -   6
    6   -   7
Pixelsize: 30.000000 meters
Acquisition date (day/month) = 2/9
Mean ground elevation of site = 0.300000 km
Solar zenith angle = 39.800000 degrees

Adjacency window size (pixels) = 33 * 33
Multiplication factor for reflective bands: 4.000000
Multiplication factor for TM-Band 6: 4.000000
Offset value for TM-Band 6: 0.000000 degrees Celcius
```

Model: Constant spatial atmospheric Conditions
Visibility: 15.000000 km

Calibration coefficients(mW / cm^2 sr micrometer)

band	c0	c1	gain setting
1	-0.258000	0.125800	1.000000
2	-0.265000	0.126500	1.000000
3	-0.073000	0.097300	1.000000
4	-0.077000	0.097700	1.000000
5	-0.020200	0.020200	1.000000
7	-0.069100	0.006910	1.000000

TM thermal band calibration coefficients
at-sensor radiance L = c0 + c1 * DN
at-sensor brightn. temperature T = K2 / (K1 - ln (c0+c1*DN))
c0 = 0.124000 c1 = 0.005630 (mW/cm^2 sr micron)
K1 = 4.175400 K2 = 1274.670000

Haze Removal Policy: Haze Removal, omit VIS. INDEX file
Haze Removal Algorithm: none (fastest)

Coefficients for Tasseled Cap Haze Band: Blue: 0.846000 Red: -0.464000
Haze threshold T3: 0.700000
Haze threshold T4: 2.000000
Cloud threshold T5: 4.000000

BEST AVERAGE SEPARABILITY

9/26/1999	Forest	Water	Developed	Ag_Nonact	Ag_Act	Other_Veg
Forest		2000	2000	2000	2000	1999
Water	2000		2000	2000	2000	2000
Developed	2000	2000		2000	2000	2000
Ag_Nonact	2000	2000	2000		2000	1999
Ag_Act	2000	2000	2000	2000		2000
Other_Veg	2000	2000	2000	2000	2000	

10/12/1999	Water	Forest	Other_Veg	Developed	Ag_Act	Ag_Nonact
Water		2000	2000	2000	2000	2000
Forest	2000		1824	2000	2000	2000
Other_Veg	2000	2000		2000	2000	2000
Developed	2000	2000	2000		2000	2000
Ag_Act	2000	2000	2000	2000		
Ag_Nonact	2000	2000	2000	2000	2000	

11/13/1999	Forest	Water	Developed	Ag_Act	Ag_Nonact	Other_Veg
Forest		2000	2000	2000	1974	2000
Water	2000		2000	2000	2000	2000
Developed	2000	2000		2000	1998	2000
Ag_Act	2000	2000	2000		2000	1883
Ag_Nonact	2000	2000	2000	2000		2000
Other_Veg	2000	2000	2000	2000	2000	

3/4/2000	Forest	Water	Developed	Ag_Act	Ag_Nonact	Other_Veg
Forest		2000	2000	2000	1951	1998
Water	2000		2000	2000	2000	2000
Developed	2000	2000		2000	2000	2000
Ag_Act	2000	2000	2000		2000	1978
Ag_Nonact	2000	2000	2000	2000		2000
Other_Veg	2000	2000	2000	2000	2000	

4/5/2000	Forest	Water	Clouds	Shadow	Developed	Ag_Act	Ag_Nonact	Other_Veg
Forest		2000	2000	2000	1999	2000	1975	2000
Water	2000		2000	1988	2000	2000	2000	2000
Clouds	2000	2000		2000	2000	2000	2000	2000
Shadow	2000	2000	2000		2000	2000	2000	2000
Developed	2000	2000	2000	2000		2000	1980	2000
Ag_Act	2000	2000	2000	2000	2000		2000	2000
Ag_Nonact	2000	2000	2000	2000	2000	2000		2000
Other_Veg	2000	2000	2000	2000	2000	2000	2000	

10/14/2000	Ag_Act	Ag_Nonact	Forest	Developed	Water	Clouds	Other_Veg
Ag_Act		2000	2000	2000	2000	2000	1993
Ag_Nonact	2000		2000	2000	2000	2000	2000
Forest	2000	2000		2000	2000	2000	1687
Developed	2000	2000	2000		2000	2000	2000
Water	2000	2000	2000	2000		2000	2000
Clouds	2000	2000	2000	2000	2000		2000
Other_Veg	2000	2000	2000	2000	2000	2000	

10/30/2000	Water	Forest	Other_Veg	Developed	Ag_Act	Ag_Nonact
Water		2000	2000	2000	2000	2000
Forest	2000		1990	2000	2000	1723
Other_Veg	2000	2000		2000	2000	1999
Developed	2000	2000	2000		2000	2000
Ag_Act	2000	2000	2000	2000		2000
Ag_Nonact	2000	2000	2000	2000	2000	

3/23/2001	Forest	Water	Other_Veg	Developed	Ag_Act	Ag_Nonact
Forest		2000	2000	2000	2000	1997
Water	2000		2000	2000	2000	2000
Other_Veg	2000	2000		2000	1976	2000
Developed	2000	2000	2000		2000	2000
Ag_Act	2000	2000	2000	2000		2000
Ag_Nonact	2000	2000	2000	2000	2000	

4/8/2001	Forest	Water	Clouds	Shadow	Developed	Ag_Act	Ag_Nonact	Other_Veg
Forest		2000	2000	2000	1999	2000	2000	2000
Water	2000		2000	2000	2000	2000	2000	2000
Clouds	2000	2000		2000	2000	2000	2000	2000
Shadow	2000	2000	2000		2000	2000	2000	2000
Developed	2000	2000	2000	2000		2000	2000	2000
Ag_Act	2000	2000	2000	2000	2000		2000	1971
Ag_Nonact	2000	2000	2000	2000	2000	2000		2000
Other_Veg	2000	2000	2000	2000	2000	2000	2000	

8/14/2001	Forest	Water	Clouds	Shadow	Developed	Ag_Act	Ag_Nonact	Other_Veg
Forest		2000	2000	2000	2000	1998	1998	2000
Water	2000		2000	2000	2000	2000	1999	2000
Clouds	2000	2000		2000	2000	2000	2000	2000
Shadow	2000	2000	2000		2000	2000	2000	2000
Developed	2000	2000	2000	2000		2000	2000	1998
Ag_Act	2000	2000	2000	2000	2000		2000	1998
Ag_Nonact	2000	2000	2000	2000	2000	2000		1999
Other_Veg	2000	2000	2000	2000	2000	2000	2000	

8/30/2001	Clouds	Shadow	Water	Forest	Developed	Ag_Act	Ag_Nonact	Other_Veg
Clouds		2000	2000	2000	2000	2000	2000	2000
Shadow	2000		1932	2000	2000	2000	2000	2000
Water	2000	2000		2000	2000	2000	2000	2000
Forest	2000	2000	2000		2000	1922	1999	2000
Developed	2000	2000	2000	2000		2000	2000	2000
Ag_Act	2000	2000	2000	2000	2000		2000	1995
Ag_Nonact	2000	2000	2000	2000	2000	2000		1937
Other_Veg	2000	2000	2000	2000	2000	2000	2000	

7/16/2002	Forest	Water	Developed	Ag_Act	Ag_Nonact	Other_Veg
Forest		2000	2000	1995	1999	2000
Water	2000		2000	2000	2000	2000
Developed	2000	2000		2000	2000	2000
Ag_Act	2000	2000	2000		2000	2000
Ag_Nonact	2000	2000	2000	2000		1933
Other_Veg	2000	2000	2000	2000	2000	

8/1/2002	Forest	Water	Clouds	Shadow	Developed	Ag_Act	Ag_Nonact	Other_Veg
Forest		2000	2000	2000	2000	1966	2000	2000
Water	2000		2000	2000	2000	2000	2000	2000
Clouds	2000	2000		2000	2000	2000	2000	2000
Shadow	2000	2000	2000		2000	2000	2000	2000
Developed	2000	2000	2000	2000		2000	2000	2000
Ag_Act	2000	2000	2000	2000	2000		2000	2000
Ag_Nonact	2000	2000	2000	2000	2000	2000		2000
Other_Veg	2000	2000	2000	2000	2000	2000	2000	

9/2/2002	Developed	Ag_Act	Ag_Nonact	Forest	Water	Other_Veg
Developed		2000	2000	2000	2000	2000
Ag_Act	2000		2000	1986	2000	1934
Ag_Nonact	2000	2000		1999	2000	1815
Forest	2000	2000	2000		2000	2000
Water	2000	2000	2000	2000		2000
Other_Veg	2000	2000	2000	2000	2000	

CLASSIFICATION CHECK TABLES

9/26/99 image		
	# pixels	% total
Unclassified	3140349	61 67
Nat Veg	469758	9 22
Ag Act	46874	0.92
Ag Nonact	165981	3 26
Forest	683994	13 43
Developed	541739	10 64
Water	43873	0 86
Clouds	0	0.00
Shadow	0	0 00
Total	5092568	100 00

10/12 image		
	# pixels	% total
Unclassified	3232129	63 47
Nat Veg	387284	7.60
Ag Act	35409	0.70
Ag Nonact	26542	0 52
Forest	619769	12 17
Developed	760423	14 93
Water	31012	0 61
Clouds	0	0.00
Shadow	0	0 00
Total	5092568	100.00

11/13 image		
	# pixels	% total
Unclassified	3104707	60 97
Nat Veg	422741	8 30
Ag Act	65762	1 29
Ag Nonact	115321	2 26
Forest	745093	14.63
Developed	608802	11.95
Water	30142	0.59
Clouds	0	0.00
Shadow	0	0 00
Total	5092568	99.99

3/4 image		
	# pixels	% total
Unclassified	3000036	58 91
Nat Veg	441689	8.67
Ag Act	63455	1.25
Ag Nonact	96939	1.90
Forest	791385	15 54
Developed	660661	12 97
Water	38403	0.75
Clouds	0	0.00
Shadow	0	0 00
Total	5092568	100.00

4/5 image		
	# pixels	% total
Unclassified	3070584	60.30
Nat Veg	410197	8 05
Ag Act	50113	0 98
Ag Nonact	121613	2.39
Forest	668417	13.13
Developed	687376	13 49
Water	37445	0.74
Clouds	11368	0.22
Shadow	35455	0 70
Total	5092568	99.99

10/14 image		
	# pixels	% total
Unclassified	2848399	55 93
Nat Veg	205605	4.04
Ag Act	242719	4.77
Ag Nonact	86721	1.70
Forest	889827	17.47
Developed	747504	14.68
Water	35437	0.70
Clouds	36356	0 71
Shadow	0	0.00
Total	5092568	100 00

10/30 image		
	# pixels	% total
Unclassified	3053855	59.97
Nat Veg	524314	10.30
Ag Act	59068	1 16
Ag Nonact	162767	3.20
Forest	687269	13.50
Developed	564342	11.08
Water	40953	0 80
Clouds	0	0.00
Shadow	0	0.00
Total	5092568	100 00

3/23 image		
	# pixels	% total
Unclassified	3039872	59.69
Nat Veg	398933	7.83
Ag Act	143947	2 83
Ag Nonact	90168	1.77
Forest	695642	13 66
Developed	682768	13.41
Water	41238	0.81
Clouds	0	0 00
Shadow	0	0.00
Total	5092568	100.00

4/8 image		
	# pixels	% total
Unclassified	3035171	59 60
Nat Veg	221850	4.36
Ag Act	119110	2.34
Ag Nonact	108035	2.12
Forest	634114	12.45
Developed	796278	15 64
Water	27433	0.54
Clouds	37957	0.75
Shadow	112620	2.21
Total	5092568	100.01

8/14 image		
	# pixels	% total
Unclassified	3088049	60.64
Nat Veg	270820	5.32
Ag Act	136324	2 68
Ag Nonact	146564	2 88
Forest	518847	10 19
Developed	824567	16.19
Water	43115	0.85
Clouds	33026	0.65
Shadow	31256	0 61
Total	5092568	100.01

8/30 image		
	# pixels	% total
Unclassified	3195818	62.75
Nat Veg	371370	7.29
Ag Act	190190	3.73
Ag Nonact	162184	3.18
Forest	442139	8.68
Developed	643831	12.64
Water	28634	0.56
Clouds	13535	0.27
Shadow	44867	0 88
Total	5092568	99.98

7/16 image		
	# pixels	% total
Unclassified	3188412	62 61
Nat Veg	267130	5.25
Ag Act	96797	1.90
Ag Nonact	217530	4 27
Forest	427557	8 40
Developed	859575	16.88
Water	35567	0.70
Clouds	0	0.00
Shadow	0	0.00
Total	5092568	100.00

8/1 image		
	# pixels	% total
Unclassified	3169246	62.23
Nat Veg	302570	5 94
Ag Act	139341	2.74
Ag Nonact	92070	1 81
Forest	449732	8.83
Developed	879913	17.28
Water	29360	0.58
Clouds	5266	0.10
Shadow	25070	0 49
Total	5092568	100.00

9/2 image		
	# pixels	% total
Unclassified	3223804	63 30
Nat Veg	448680	8.81
Ag Act	120244	2.36
Ag Nonact	144680	2.84
Forest	465553	9.14
Developed	658376	12.93
Water	31231	0.61
Clouds	0	0.00
Shadow	0	0 00
Total	5092568	99.99

CLASSIFICATION CHECK GRAPHS

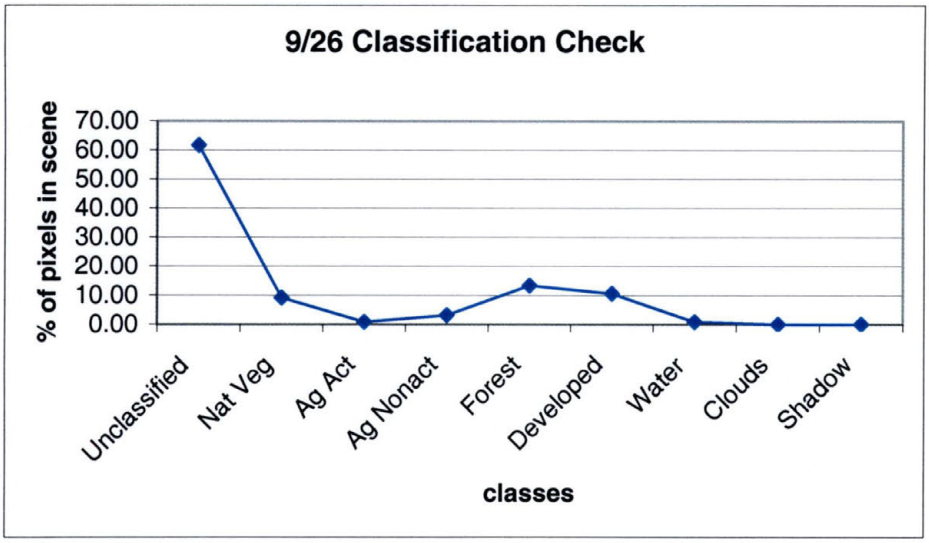

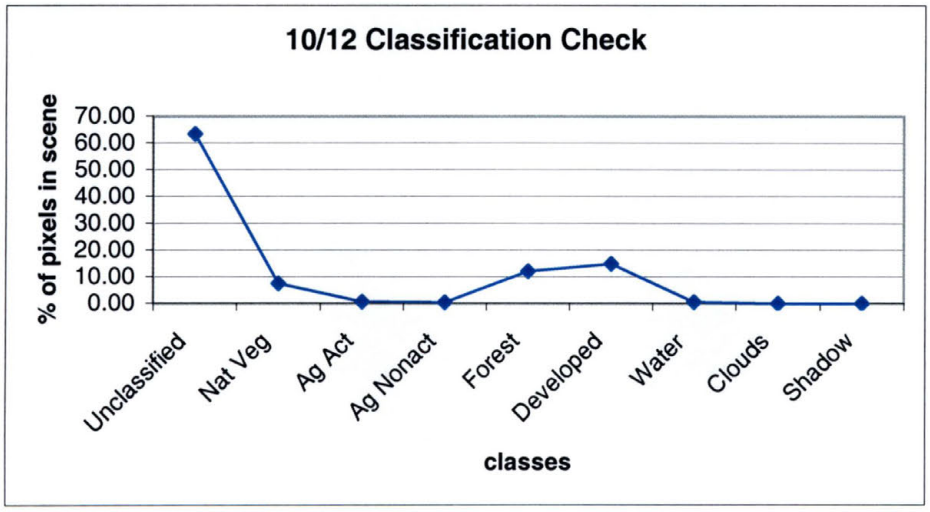

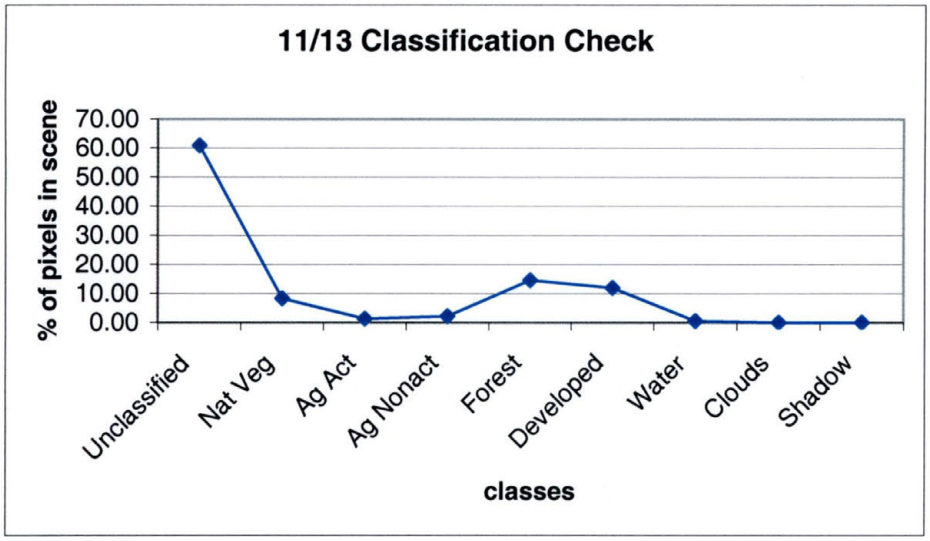
11/13 Classification Check
% of pixels in scene
70.00
60.00
50.00
40.00
30.00
20.00
10.00
0.00
Unclassified
Nat Veg
Ag Act
Ag Nonact
Forest
Developed
Water
Clouds
Shadow
classes

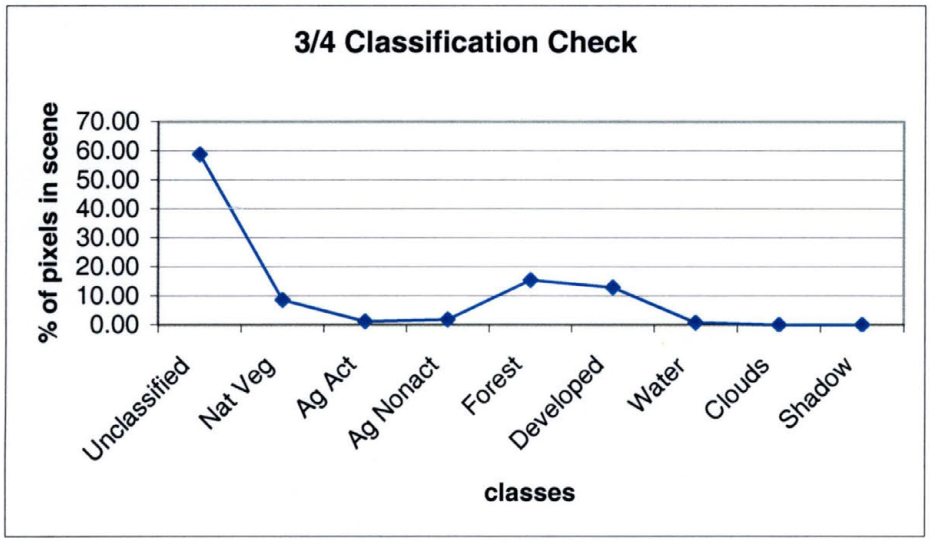
3/4 Classification Check
% of pixels in scene
70.00
60.00
50.00
40.00
30.00
20.00
10.00
0.00
Unclassified
Nat Veg
Ag Act
Ag Nonact
Forest
Developed
Water
Clouds
Shadow
classes

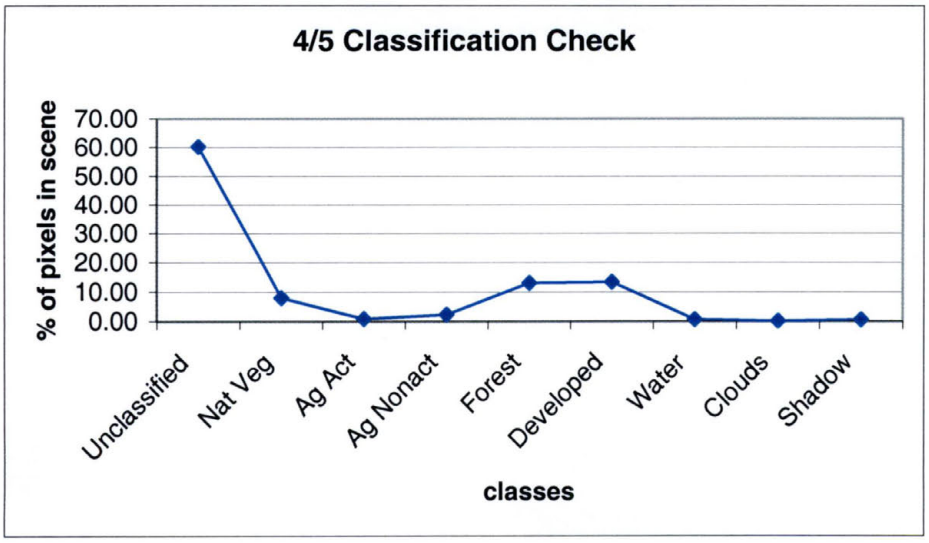
4/5 Classification Check
% of pixels in scene
70.00
60.00
50.00
40.00
30.00
20.00
10.00
0.00
Unclassified
Nat Veg
Ag Act
Ag Nonact
Forest
Developed
Water
Clouds
Shadow
classes

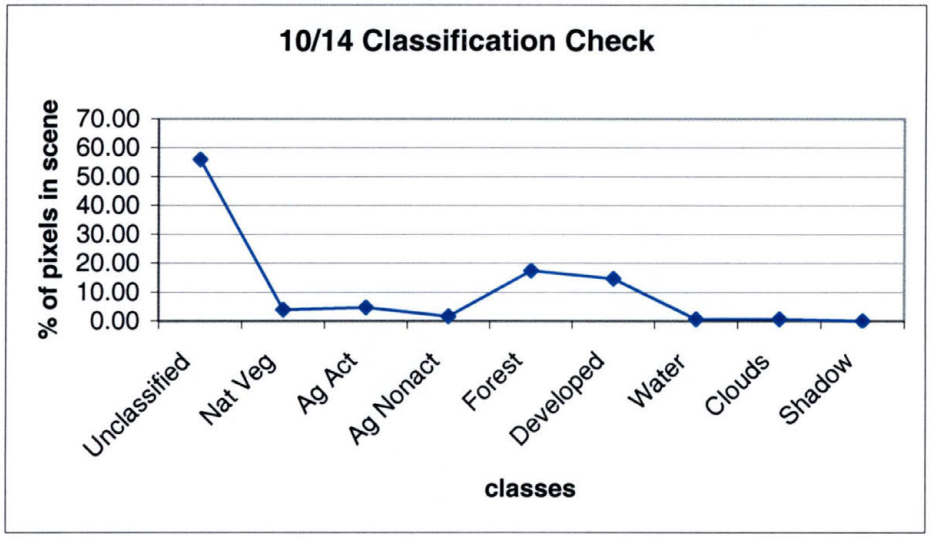
10/14 Classification Check
% of pixels in scene
70.00
60.00
50.00
40.00
30.00
20.00
10.00
0.00
Unclassified
Nat Veg
Ag Act
Ag Nonact
Forest
Developed
Water
Clouds
Shadow
classes

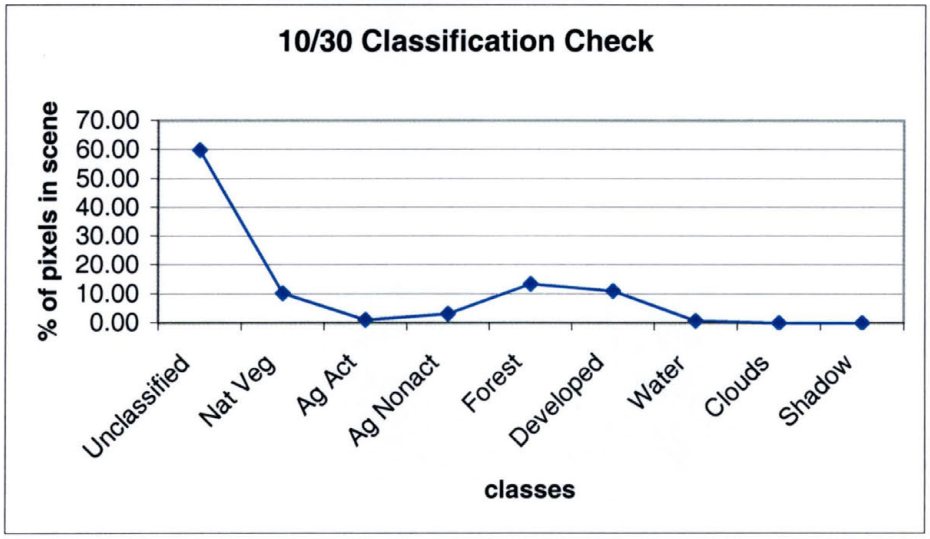
10/30 Classification Check
% of pixels in scene
70.00
60.00
50.00
40.00
30.00
20.00
10.00
0.00
Unclassified
Nat Veg
Ag Act
Ag Nonact
Forest
Developed
Water
Clouds
Shadow
classes

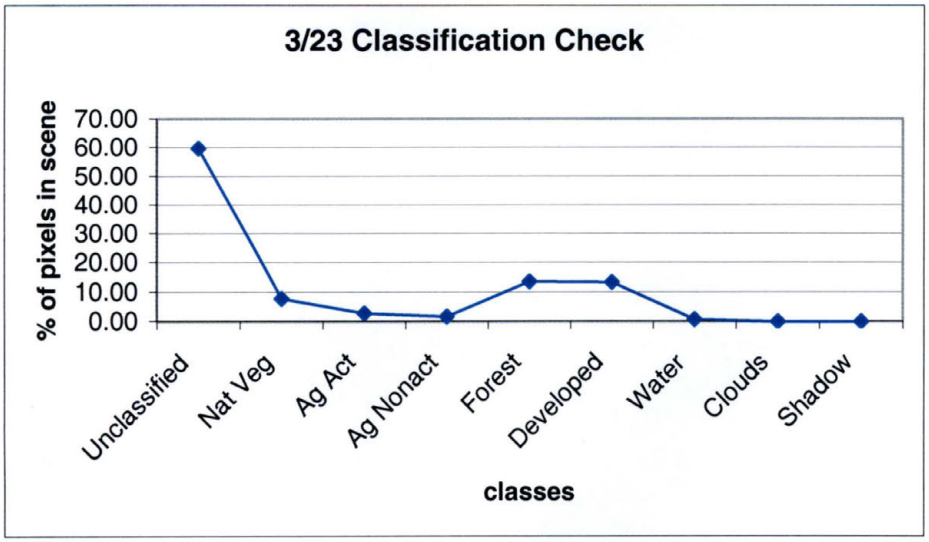
3/23 Classification Check
% of pixels in scene
70.00
60.00
50.00
40.00
30.00
20.00
10.00
0.00
Unclassified
Nat Veg
Ag Act
Ag Nonact
Forest
Developed
Water
Clouds
Shadow
classes

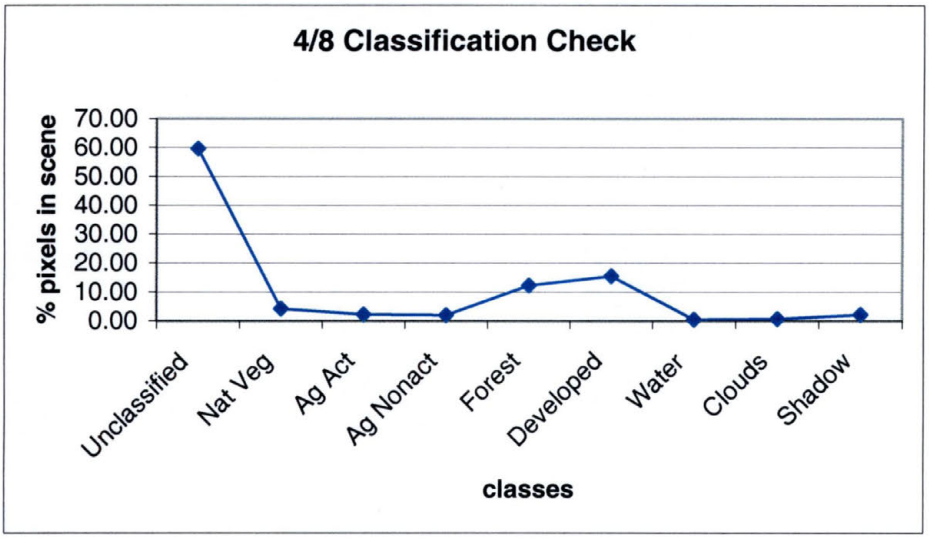
4/8 Classification Check
% pixels in scene
70.00
60.00
50.00
40.00
30.00
20.00
10.00
0.00
Unclassified
Nat Veg
Ag Act
Ag Nonact
Forest
Developed
Water
Clouds
Shadow
classes

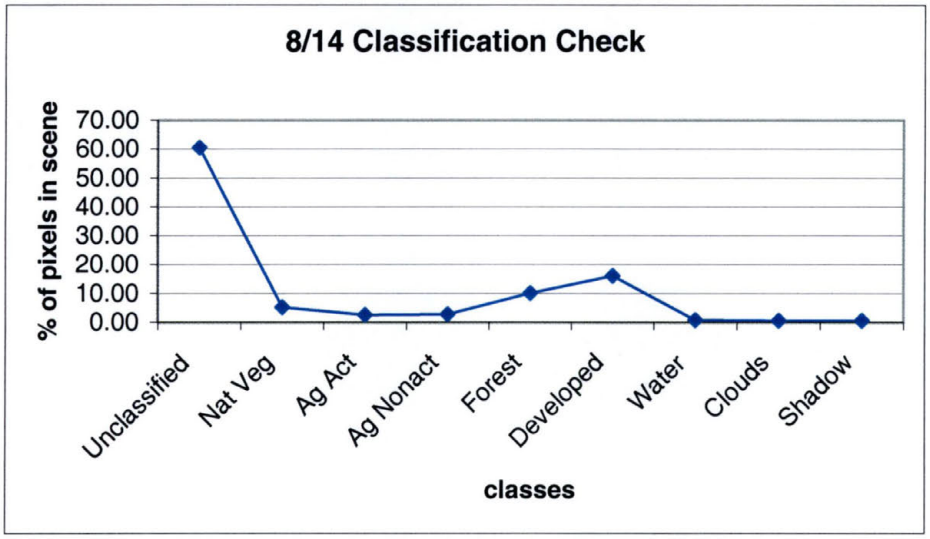
8/14 Classification Check
% of pixels in scene
70.00
60.00
50.00
40.00
30.00
20.00
10.00
0.00
Unclassified
Nat Veg
Ag Act
Ag Nonact
Forest
Developed
Water
Clouds
Shadow
classes

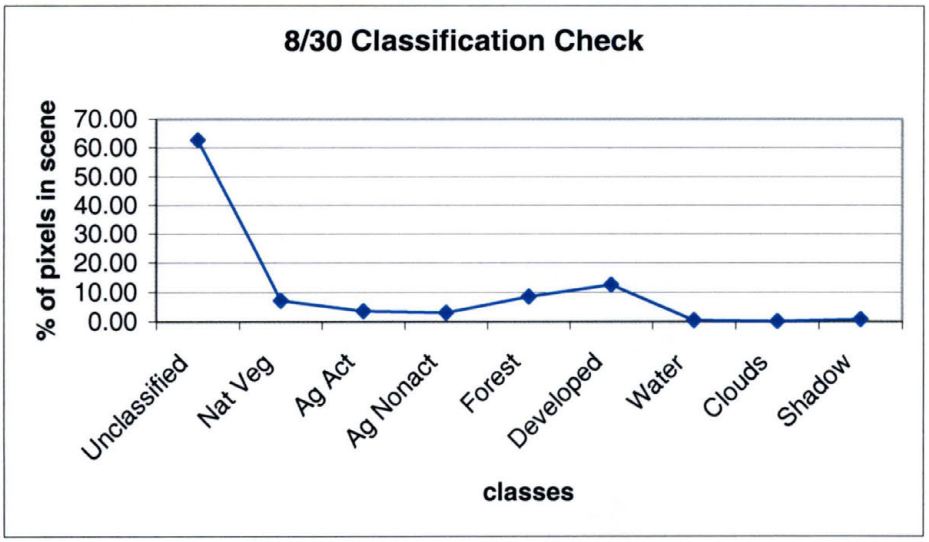
8/30 Classification Check
% of pixels in scene
70.00
60.00
50.00
40.00
30.00
20.00
10.00
0.00
Unclassified
Nat Veg
Ag Act
Ag Nonact
Forest
Developed
Water
Clouds
Shadow
classes

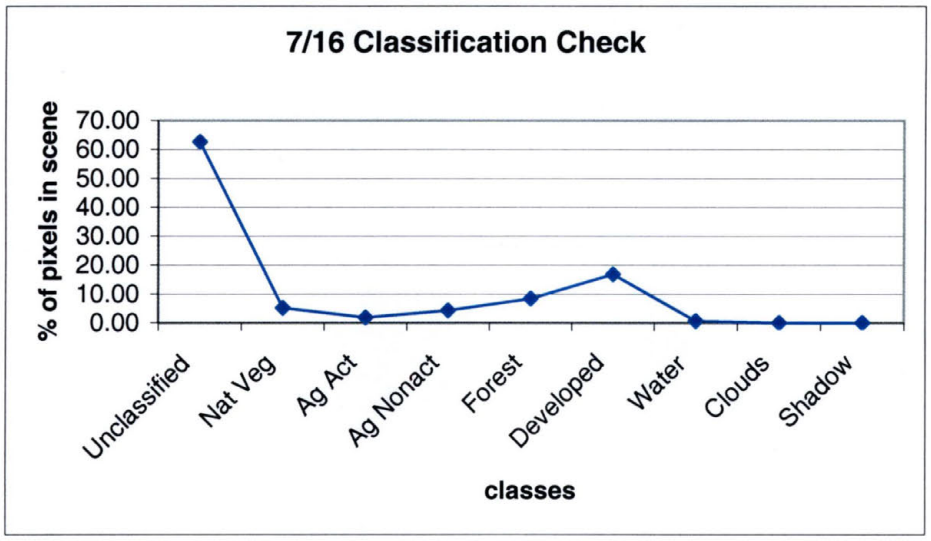
7/16 Classification Check
% of pixels in scene
70.00
60.00
50.00
40.00
30.00
20.00
10.00
0.00
Unclassified
Nat Veg
Ag Act
Ag Nonact
Forest
Developed
Water
Clouds
Shadow
classes

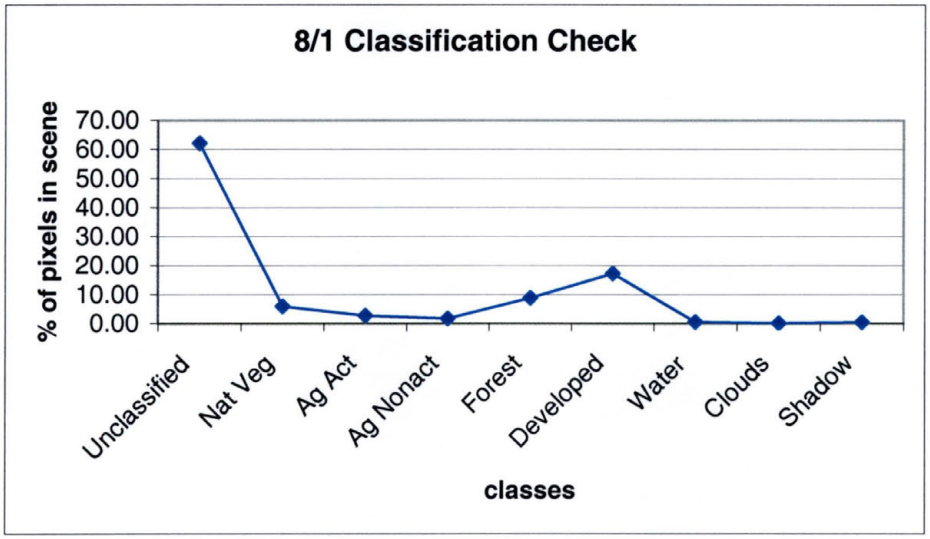
8/1 Classification Check
% of pixels in scene
70.00
60.00
50.00
40.00
30.00
20.00
10.00
0.00
Unclassified
Nat Veg
Ag Act
Ag Nonact
Forest
Developed
Water
Clouds
Shadow
classes

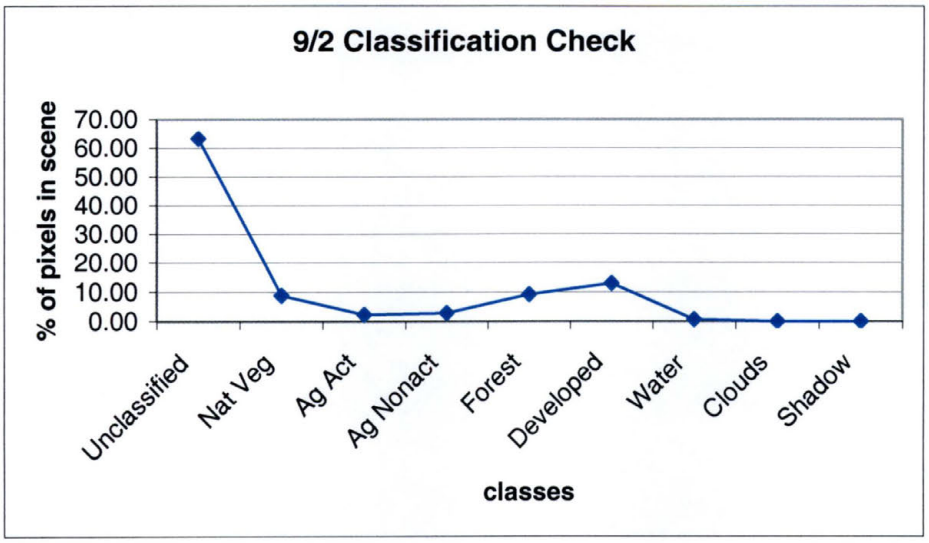
9/2 Classification Check
% of pixels in scene
70.00
60.00
50.00
40.00
30.00
20.00
10.00
0.00
Unclassified
Nat Veg
Ag Act
Ag Nonact
Forest
Developed
Water
Clouds
Shadow
classes

CLASSIFICATION CHECK TABLES WITH RIPARIAN AREA

9/26/99 image		
	# pixels	% total
Unclassified	3121490	61.30
Riparian	68321	1 34
Nat Veg	466880	9 17
Ag Act	45396	0 89
Ag Nonact	162507	3 19
Forest	642362	12 61
Developed	541739	10 64
Water	43873	0 86
Clouds	0	0.00
Shadow	0	0.00
Total	5092568	100 00

10/12 image		
	# pixels	% total
Unclassified	3203710	62.91
Riparian	69887	1 37
Nat Veg	382370	7 51
Ag Act	34982	0.69
Ag Nonact	26351	0.52
Forest	583833	11.46
Developed	760423	14.93
Water	31012	0.61
Clouds	0	0.00
Shadow	0	0 00
Total	5092568	100.00

11/13 image		
	# pixels	% total
Unclassified	3088194	60 64
Riparian	69729	1 37
Nat Veg	420190	8.25
Ag Act	65453	1.29
Ag Nonact	109574	2 15
Forest	700484	13.76
Developed	608802	11.95
Water	30142	0.59
Clouds	0	0.00
Shadow	0	0.00

Total	5092568	100 00
3/4 image		
	# pixels	**% total**
Unclassified	2988979	58 69
Riparian	64435	1 27
Nat Veg	439971	8 64
Ag Act	62618	1.23
Ag Nonact	92655	1.82
Forest	744846	14.63
Developed	660661	12 97
Water	38403	0 75
Clouds	0	0 00
Shadow	0	0 00
Total	5092568	100 00

4/5 image		
	# pixels	**% total**
Unclassified	3055363	60.00
Riparian	58673	1.15
Nat Veg	407770	8 01
Ag Act	49886	0 98
Ag Nonact	118957	2 34
Forest	630275	12 38
Developed	687376	13 50
Water	37445	0.74
Clouds	11368	0 22
Shadow	35455	0 70
Total	5092568	100 00

10/14 image		
	# pixels	**% total**
Unclassified	2847780	55 92
Riparian	60875	1 20
Nat Veg	289924	5 69
Ag Act	217896	4 28
Ag Nonact	82669	1 62
Forest	799962	15 71
Developed	721755	14 17
Water	35433	0 70
Clouds	36274	0 71
Shadow	0	0 00
Total	5092568	100 00

10/30 image		
	# pixels	% total
Unclassified	3039400	59.68
Riparian	68670	1.35
Nat Veg	518872	10.19
Ag Act	58829	1.16
Ag Nonact	154653	3.04
Forest	646849	12 70
Developed	564342	11.08
Water	40953	0.80
Clouds	0	0.00
Shadow	0	0.00
Total	5092568	100.00

3/23 image		
	# pixels	% total
Unclassified	3026124	59.42
Riparian	64026	1.26
Nat Veg	396707	7.79
Ag Act	142915	2.81
Ag Nonact	86133	1.69
Forest	652657	12 82
Developed	682768	13.41
Water	41238	0.81
Clouds	0	0.00
Shadow	0	0.00
Total	5092568	100 00

4/8 image		
	# pixels	% total
Unclassified	3021712	59.34
Riparian	47392	0.93
Nat Veg	220767	4.34
Ag Act	118592	2.33
Ag Nonact	106720	2 10
Forest	603097	11 84
Developed	796278	15 64
Water	27433	0.54
Clouds	37957	0.75
Shadow	112620	2.21
Total	5092568	100 00

8/14 image		
	# pixels	% total
Unclassified	3072206	60.33
Riparian	62628	1.23
Nat Veg	269297	5 29
Ag Act	133162	2.61
Ag Nonact	141742	2.78
Forest	481569	9.46
Developed	824567	16.19
Water	43115	0.85
Clouds	33026	0 65
Shadow	31256	0.61
Total	5092568	100.00

8/30 image		
	# pixels	% total
Unclassified	3171137	62.27
Riparian	65954	1.30
Nat Veg	368441	7 23
Ag Act	185224	3.64
Ag Nonact	159528	3.13
Forest	411417	8.08
Developed	643831	12 64
Water	28634	0.56
Clouds	13535	0.27
Shadow	44867	0.88
Total	5092568	100.00

7/16 image		
	# pixels	% total
Unclassified	3164396	62 14
Riparian	63746	1.25
Nat Veg	264624	5.20
Ag Act	92215	1.81
Ag Nonact	213631	4.19
Forest	398814	7.83
Developed	859575	16.88
Water	35567	0.70
Clouds	0	0.00
Shadow	0	0.00
Total	5092568	100.00

8/1 image		
	# pixels	% total
Unclassified	3147230	61.87
Riparian	63584	1.25
Nat Veg	299068	5.88
Ag Act	135751	2.67
Ag Nonact	91661	1 80
Forest	415665	8.17
Developed	879913	17.30
Water	23960	0 47
Clouds	5266	0 10
Shadow	25070	0.49
Total	5087168	100 00

9/2 image		
	# pixels	% total
Unclassified	3196325	62 76
Riparian	68199	1 34
Nat Veg	444453	8.73
Ag Act	116958	2.30
Ag Nonact	141948	2 79
Forest	435078	8 54
Developed	658376	12.93
Water	31231	0 61
Clouds	0	0.00
Shadow	0	0.00
Total	5092568	100.00

CLASSIFICATON CHECK GRAPHS WITH RIPARIAN AREA

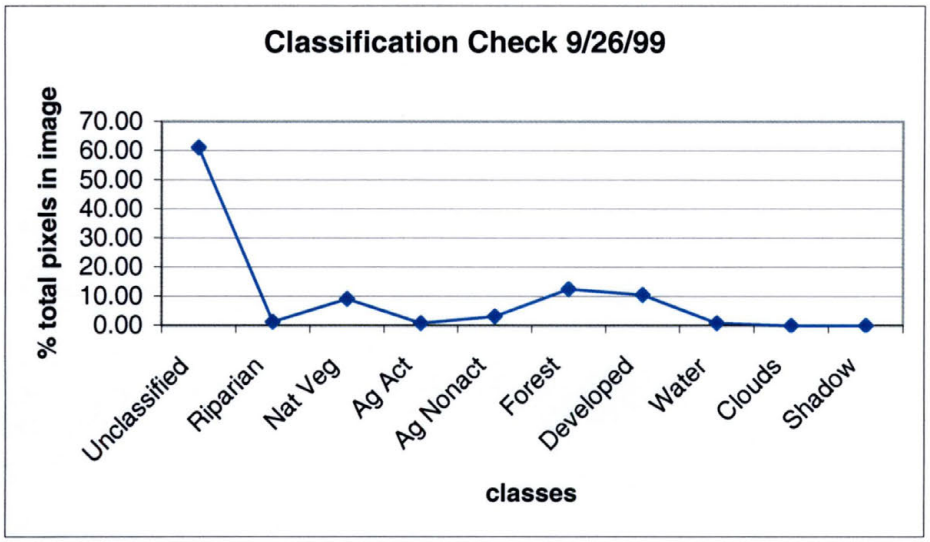

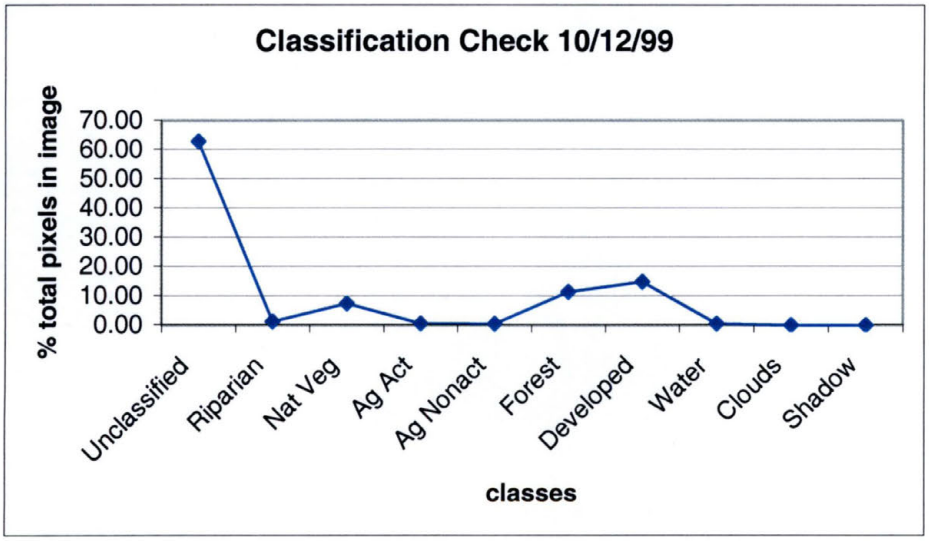

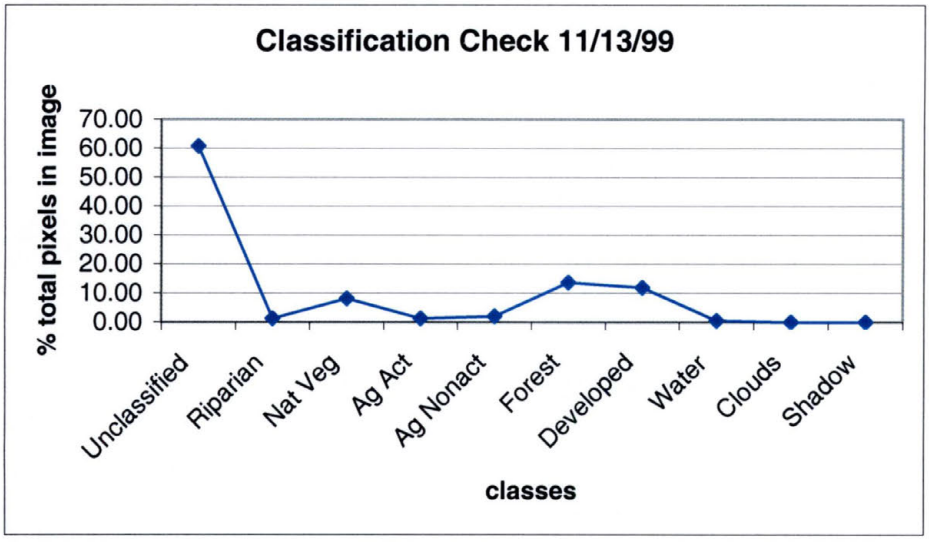
Classification Check 11/13/99
% total pixels in image
70.00
60.00
50.00
40.00
30.00
20.00
10.00
0.00
Unclassified
Riparian
Nat Veg
Ag Act
Ag Nonact
Forest
Developed
Water
Clouds
Shadow
classes

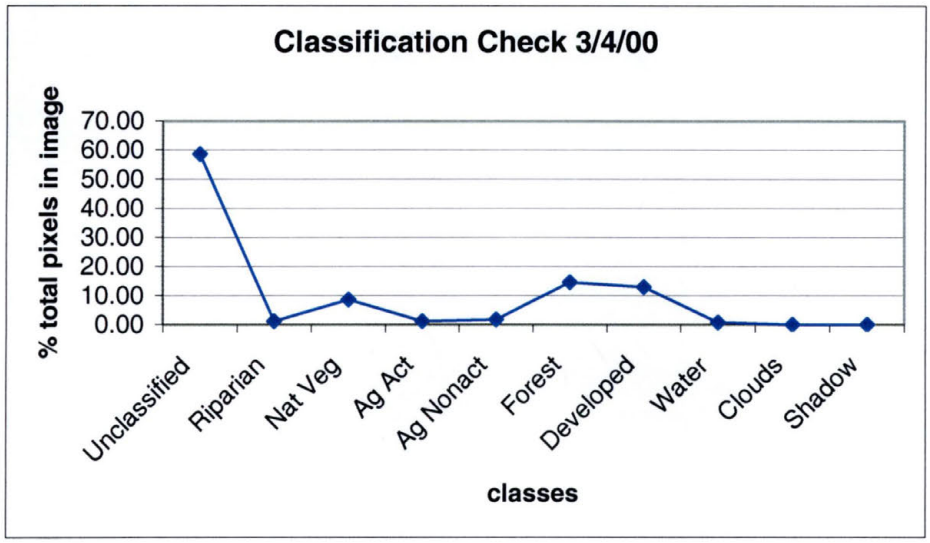
Classification Check 3/4/00
% total pixels in image
70.00
60.00
50.00
40.00
30.00
20.00
10.00
0.00
Unclassified
Riparian
Nat Veg
Ag Act
Ag Nonact
Forest
Developed
Water
Clouds
Shadow
classes

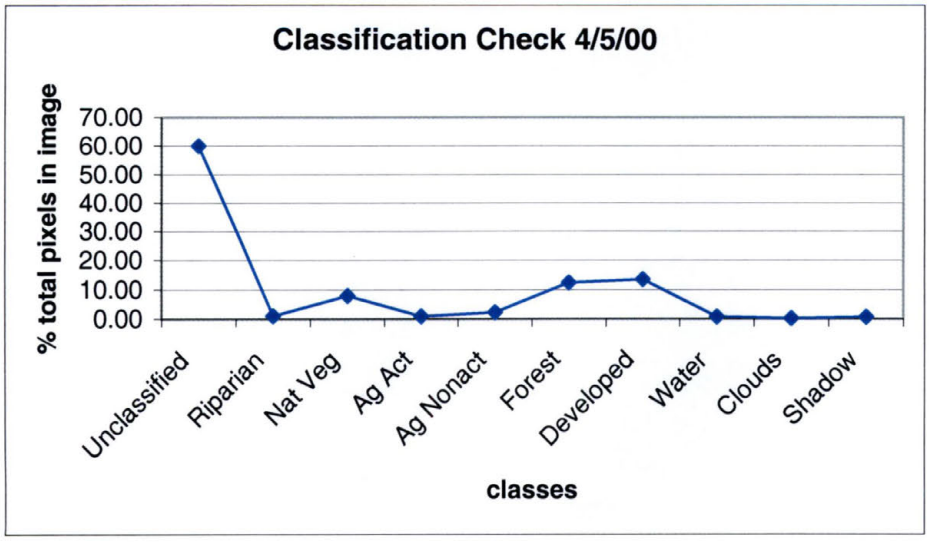
Classification Check 4/5/00
% total pixels in image
70.00
60.00
50.00
40.00
30.00
20.00
10.00
0.00
Unclassified
Riparian
Nat Veg
Ag Act
Ag Nonact
Forest
Developed
Water
Clouds
Shadow
classes

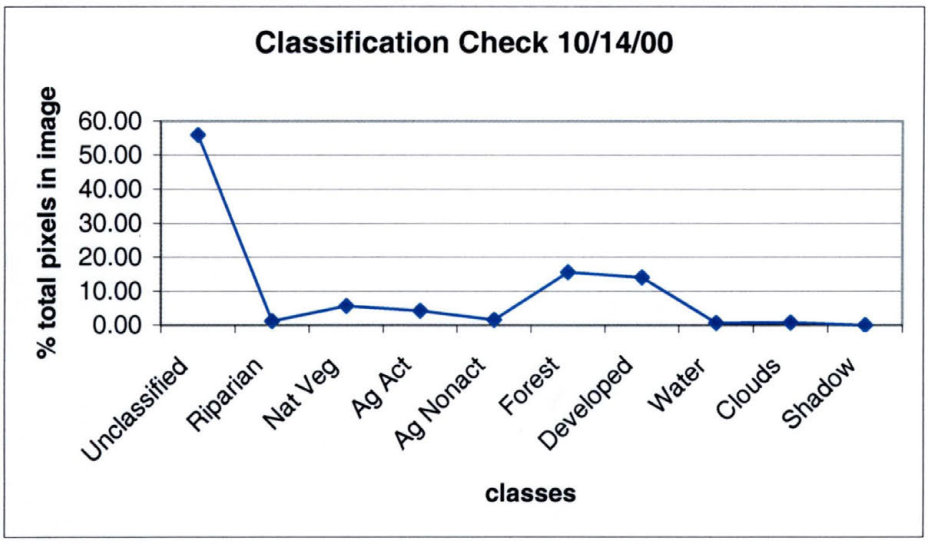
Classification Check 10/14/00
% total pixels in image
60.00
50.00
40.00
30.00
20.00
10.00
0.00
Unclassified
Riparian
Nat Veg
Ag Act
Ag Nonact
Forest
Developed
Water
Clouds
Shadow
classes

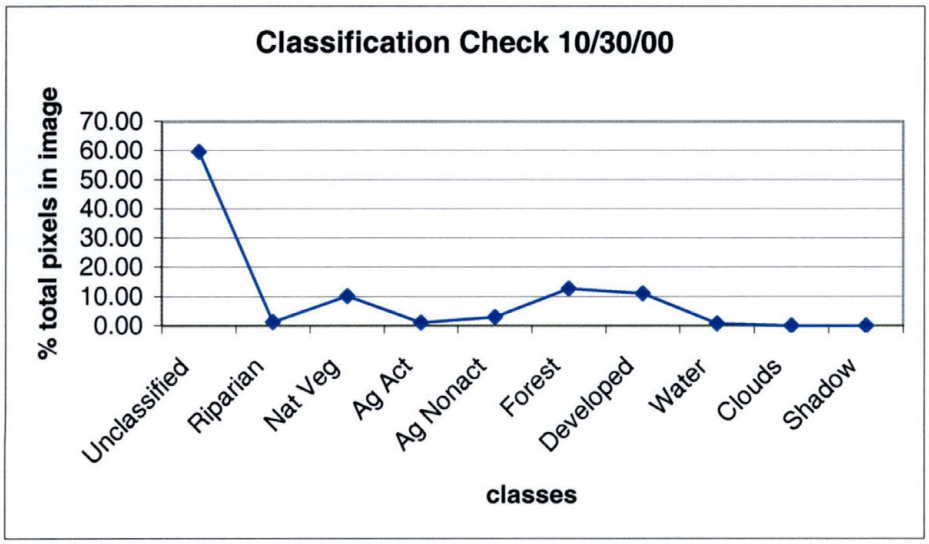
Classification Check 10/30/00
% total pixels in image
70.00
60.00
50.00
40.00
30.00
20.00
10.00
0.00
Unclassified
Riparian
Nat Veg
Ag Act
Ag Nonact
Forest
Developed
Water
Clouds
Shadow
classes

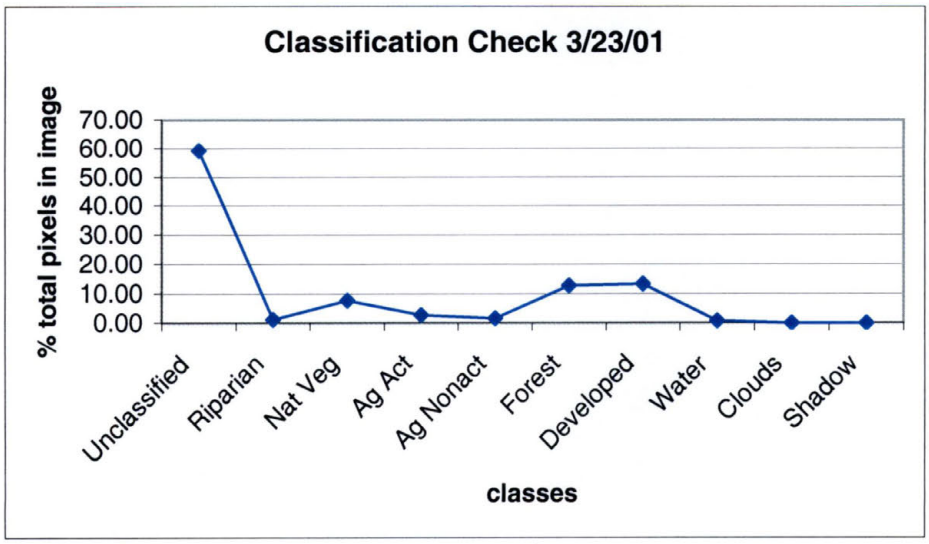
Classification Check 3/23/01
% total pixels in image
70.00
60.00
50.00
40.00
30.00
20.00
10.00
0.00
Unclassified
Riparian
Nat Veg
Ag Act
Ag Nonact
Forest
Developed
Water
Clouds
Shadow
classes

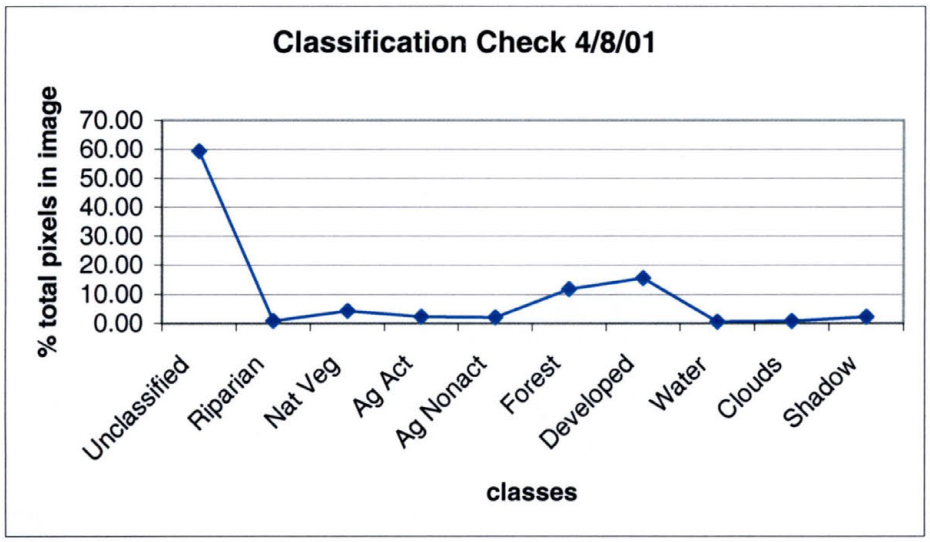
Classification Check 4/8/01
% total pixels in image
70.00
60.00
50.00
40.00
30.00
20.00
10.00
0.00
Unclassified
Riparian
Nat Veg
Ag Act
Ag Nonact
Forest
Developed
Water
Clouds
Shadow
classes

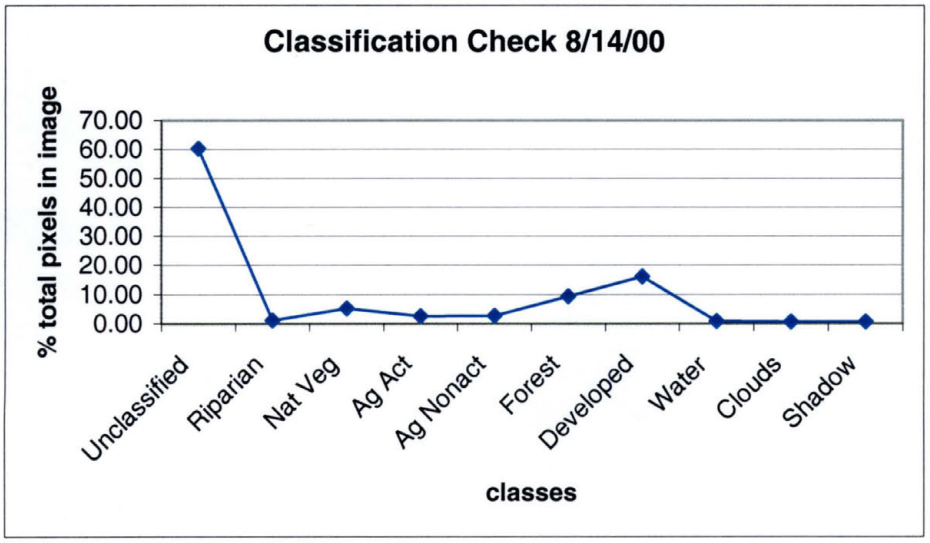
Classification Check 8/14/00
% total pixels in image
70.00
60.00
50.00
40.00
30.00
20.00
10.00
0.00
Unclassified
Riparian
Nat Veg
Ag Act
Ag Nonact
Forest
Developed
Water
Clouds
Shadow
classes

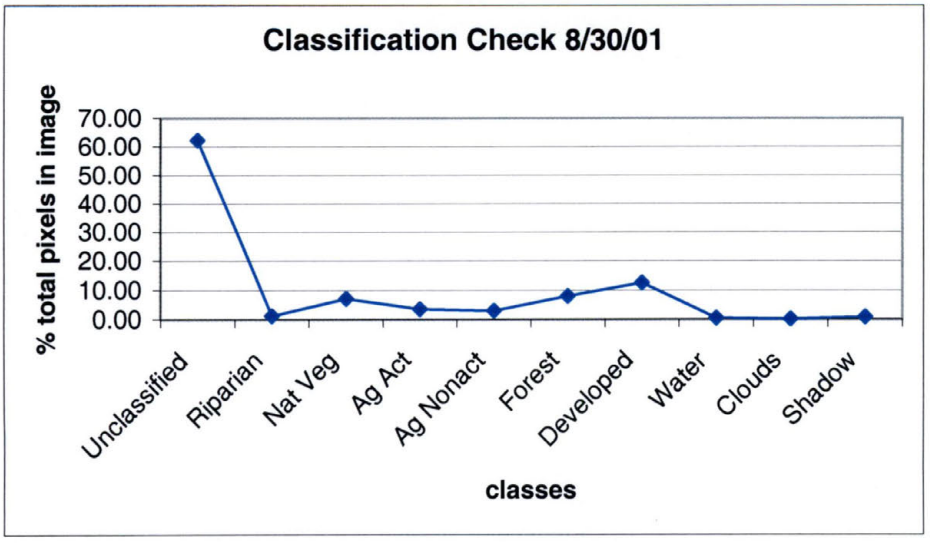
Classification Check 8/30/01
% total pixels in image
70.00
60.00
50.00
40.00
30.00
20.00
10.00
0.00
Unclassified
Riparian
Nat Veg
Ag Act
Ag Nonact
Forest
Developed
Water
Clouds
Shadow
classes

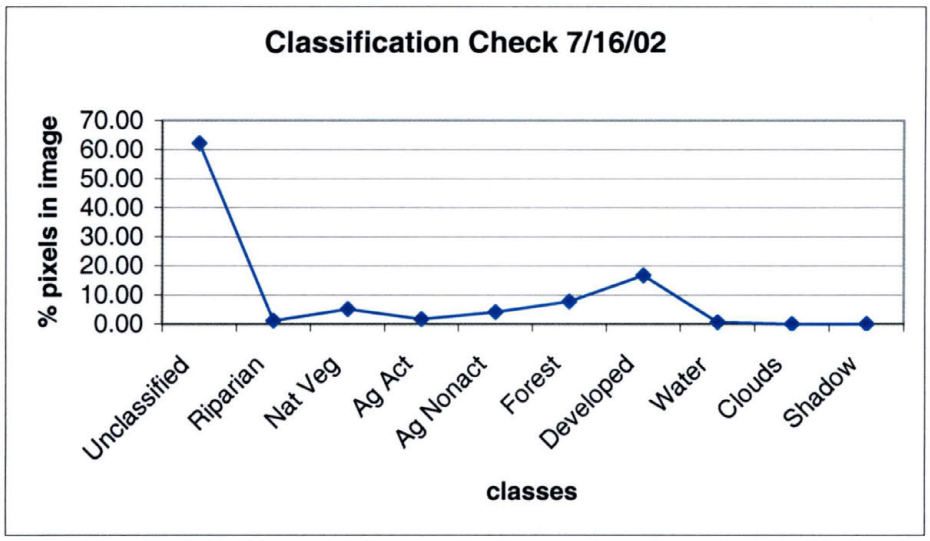
Classification Check 7/16/02
% pixels in image
70.00
60.00
50.00
40.00
30.00
20.00
10.00
0.00
Unclassified
Riparian
Nat Veg
Ag Act
Ag Nonact
Forest
Developed
Water
Clouds
Shadow
classes

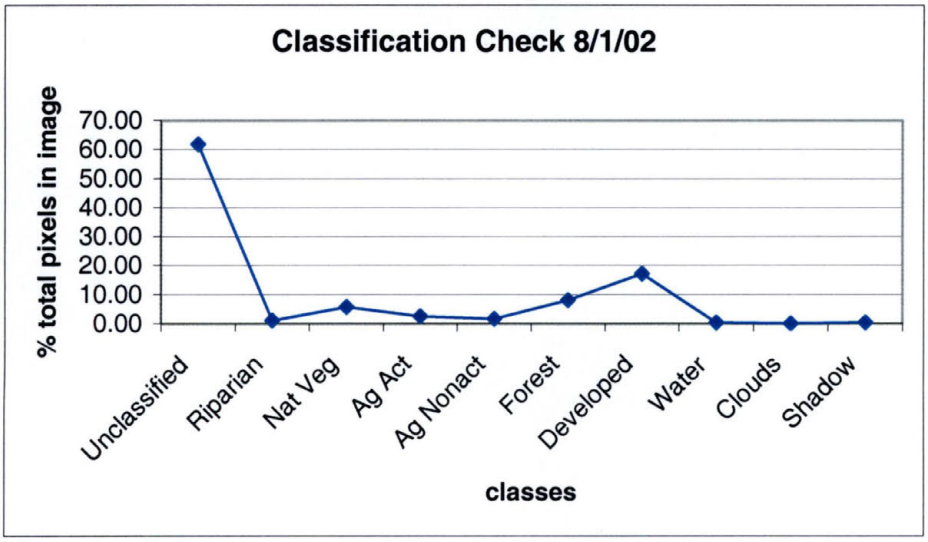
Classification Check 8/1/02
% total pixels in image
70.00
60.00
50.00
40.00
30.00
20.00
10.00
0.00
Unclassified
Riparian
Nat Veg
Ag Act
Ag Nonact
Forest
Developed
Water
Clouds
Shadow
classes

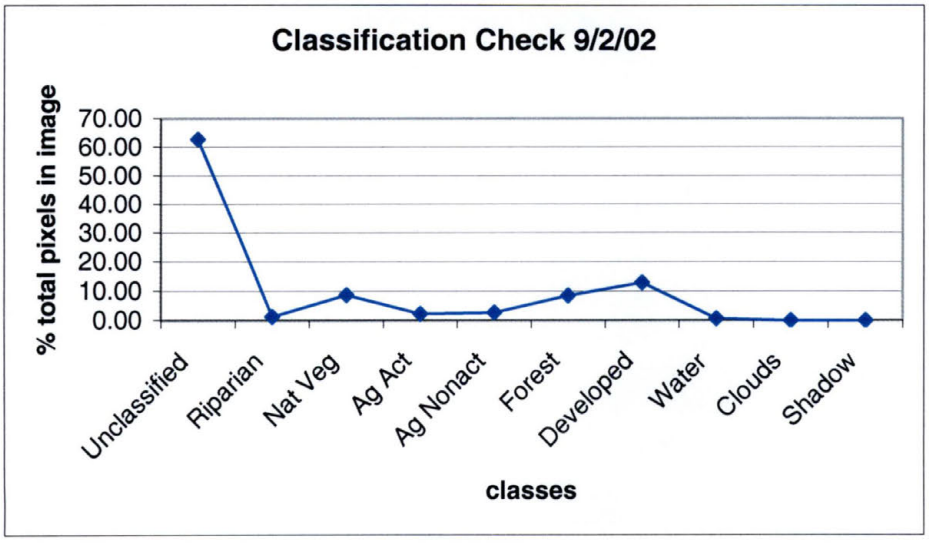
Classification Check 9/2/02
% total pixels in image
70.00
60.00
50.00
40.00
30.00
20.00
10.00
0.00
Unclassified
Riparian
Nat Veg
Ag Act
Ag Nonact
Forest
Developed
Water
Clouds
Shadow
classes

ACCURACY ASSESSMENT REPORT

CLASSIFICATION ACCURACY ASSESSMENT REPORT

Image File : /home/grad/dunhams/rip2/d926.img
User Name : dunhams
Date : Tue May 6 12:13:29 2003

ERROR MATRIX

Classified Data	Reference Data: Undefined	Riparian1	Nonact	ag
Undefined	0	0	0	0
Riparian1	0	4	0	0
Nonact	0	0	4	0
ag	0	0	0	11
forest	0	0	1	1
water	0	1	1	1
developed	0	0	0	6
Natural	0	0	0	3
Column Total	0	5	6	22

Classified Data	Reference Data: forest	water	developed	Natural
Undefined	0	0	0	0
Riparian1	0	0	0	0
Nonact	2	0	2	0
ag	6	0	0	0
forest	23	0	0	0
water	0	16	1	0
developed	3	0	22	0
Natural	5	0	5	9
Column Total	39	16	30	9

ACCURACY TOTALS

Class Name	Reference Totals	Classified Totals	Number Correct	Producers Accuracy	Users Accuracy
Undefined	0	0	0	---	---
Riparian1	5	4	4	80.00%	100.00%
Nonact	6	8	4	66.67%	50.00%
ag	22	17	11	50.00%	64.71%
forest	39	25	23	58.97%	92.00%
water	16	20	16	100.00%	80.00%

developed	30	31	22	73.33%	70.97%
Natural	9	22	9	100.00%	40.91%
Totals	127	127	89		

Overall Classification Accuracy = 70.08%
KAPPA (K^) STATISTICS
Overall Kappa Statistics = 0.6362
Conditional Kappa for each Category.

Class Name	Kappa
Undefined	0.0000
Riparian1	1.0000
Nonact	0.4752
ag	0.5731
forest	0.8845
water	0.7712
developed	0.6199
Natural	0.3640

METADATA

File	Source	Changes	final output
hucs00p020 shp	www nationalatlas.gov Contact organization USGS	originally hydrologic units for entire USA, created a shapefile of just Cuyahoga River hydrologic unit original projection-North American Datum 1983	Cuyahogawatershed.shp transformed data to NAD83 and then to WGS84 using ArcGIS
hydro1020.shp	www nationalatlas gov Contact organization USGS	originally major rivers for the US, created a shapefile of just the Cuyahoga River original projection-North American Datum 1983	Cuyahogar.shp
counties shp	obtained from ESRI data	originally included all 50 states, created a shapefile of just Ohio original projection-assumed geographic	Ohiocounties shp
climate_div shp	National Climate Data Center (NCDC), Contact organization USGS-Water Resources Division	originally included climate divisions for the entire US, created a shapefile for climate regions just in Ohio original projection-albers conical equal area	Ohio shp
hydro1020 shp	www nationalatlas gov Contact organization USGS	adapted from rivers of the US data with 1 2,000,000 scale	river.shp
finalsja shp	on screen digitized by Susan Dunham and merged into one shapefile using Xtools with assistance from Dr.Anderson	projected to NAD83 and then reprojected to WGS84 using ArcGIS	finalsja shp
ussoils_05 e00 gz	USGS http //water usgs.gov/lookup/ getspatial?ussoils	Turned into a shapefile using ArcView extension Import71 original projection Albers Conical Equal Area; reprojected to NAD83 to overlay with watershed boundaries using ArcGIS	NAD83soils shp

ERDAS IMAGINE MODELS

Knowledgebase created for images without clouds for expert classifier

```
PRINTSCALE 100;
VERSION 4;
HYPOTHESIS {
      ID 1;
      TITLE "Riparian1";
      SETBY 1;
      COLOR 0.627451,0.12549,0.941176;
      ENABLED 1;
}
HYPOTHESIS {
      ID 2;
      TITLE "Nonact";
      SETBY 2;
      COLOR 0.647059,0.164706,0.164706;
      ENABLED 1;
}
HYPOTHESIS {
      ID 3;
      TITLE "ag";
      SETBY 3;
      COLOR 1,0,0;
      ENABLED 1;
}
HYPOTHESIS {
      ID 4;
      TITLE "forest";
      SETBY 4;
      COLOR 0,0.392157,0;
      ENABLED 1;
}
HYPOTHESIS {
      ID 5;
      TITLE "water";
      SETBY 5;
      COLOR 0.00555594,0.0527326,0.5;
      ENABLED 1;
}
HYPOTHESIS {
      ID 6;
      TITLE "developed";
      SETBY 6;
      COLOR 0,1,1;
      ENABLED 1;
}
HYPOTHESIS {
      ID 7;
      TITLE "Natural";
      SETBY 7;
      COLOR 1,0.752941,0.796078;
      ENABLED 1;
}
RULE {
```

```
	ID 1;
	TITLE "Riparian ";
	HYPOTHESIS 1;
	ENABLED 1;
	CONDITION {
		VARIABLE 1 <= VALUE 4 CONFIDENCE 1;
		ENABLED 1;
	}
	CONDITION {
		VARIABLE 2 > VALUE 0 CONFIDENCE 1;
		ENABLED 1;
	}
}
RULE {
	ID 2;
	TITLE "nonactag";
	HYPOTHESIS 2;
	ENABLED 1;
	CONDITION {
		VARIABLE 1 == VALUE 3 CONFIDENCE 1;
		ENABLED 1;
	}
}
RULE {
	ID 3;
	TITLE "agact";
	HYPOTHESIS 3;
	ENABLED 1;
	CONDITION {
		VARIABLE 1 == VALUE 2 CONFIDENCE 1;
		ENABLED 1;
	}
}
RULE {
	ID 4;
	TITLE "Forest";
	HYPOTHESIS 4;
	ENABLED 1;
	CONDITION {
		VARIABLE 1 == VALUE 4 CONFIDENCE 1;
		ENABLED 1;
	}
}
RULE {
	ID 5;
	TITLE "water";
	HYPOTHESIS 5;
	ENABLED 1;
	CONDITION {
		VARIABLE 1 == VALUE 6 CONFIDENCE 1;
		ENABLED 1;
	}
}
RULE {
	ID 6;
```

```
      TITLE "developed";
      HYPOTHESIS 6;
      ENABLED 1;
      CONDITION {
            VARIABLE 1 == VALUE 5 CONFIDENCE 1;
            ENABLED 1;
      }
}
RULE {
      ID 7;
      TITLE "natural";
      HYPOTHESIS 7;
      ENABLED 1;
      CONDITION {
            VARIABLE 1 == VALUE 1 CONFIDENCE 1;
            ENABLED 1;
      }
}
VARIABLE {
      ID 1;
      TITLE "LCLU";
      OBJECTTYPE RASTER;
      DATATYPE INTEGER;
      IMAGE "/home/grad/dunhams/recode/recode1012.img"
            LAYER "(:Layer_1)"
            ATTRIBUTE "Cell Value";
}
VARIABLE {
      ID 2;
      TITLE "RipPoly";
      OBJECTTYPE RASTER;
      DATATYPE INTEGER;
      IMAGE "/home/grad/dunhams/recode/vec2rast.img"
            LAYER "(:Layer_1)"
            ATTRIBUTE "Cell Value";
}
```

Knowledgebase created for images with clouds for expert classifier

```
PRINTSCALE 100;
VERSION 2;
HYPOTHESIS {
      ID 1;
      TITLE "Riparian1";
      SETBY 1;
      COLOR 0.627451,0.12549,0.941176;
      ENABLED 1;
}
HYPOTHESIS {
      ID 2;
      TITLE "Nonact";
      SETBY 2;
      COLOR 0.627451,0.321569,0.176471;
      ENABLED 1;
}
HYPOTHESIS {
      ID 3;
      TITLE "ag";
      SETBY 3;
      COLOR 1,0,0;
      ENABLED 1;
}
HYPOTHESIS {
      ID 4;
      TITLE "forest";
      SETBY 4;
      COLOR 0,0.392157,0;
      ENABLED 1;
}
HYPOTHESIS {
      ID 5;
      TITLE "water";
      SETBY 5;
      COLOR 0.054902,0.156863,0.341176;
      ENABLED 1;
}
HYPOTHESIS {
      ID 6;
      TITLE "developed";
      SETBY 6;
      COLOR 0,1,1;
      ENABLED 1;
}
HYPOTHESIS {
      ID 7;
      TITLE "Natural";
      SETBY 7;
      COLOR 0.819608,0.435294,0.47451;
      ENABLED 1;
}
HYPOTHESIS {
      ID 8;
      TITLE "Clouds";
```

```
	SETBY 8;
	ENABLED 1;
}
HYPOTHESIS {
	ID 9;
	TITLE "Shadow";
	SETBY 9;
	COLOR 0.752941,0.752941,0.752941;
	ENABLED 1;
}
RULE {
	ID 1;
	TITLE "Riparian ";
	HYPOTHESIS 1;
	ENABLED 1;
	CONDITION {
		VARIABLE 1 <= VALUE 4 CONFIDENCE 1;
		ENABLED 1;
	}
	CONDITION {
		VARIABLE 2 > VALUE 0 CONFIDENCE 1;
		ENABLED 1;
	}
}
RULE {
	ID 2;
	TITLE "nonactag";
	HYPOTHESIS 2;
	ENABLED 1;
	CONDITION {
		VARIABLE 1 == VALUE 3 CONFIDENCE 1;
		ENABLED 1;
	}
}
RULE {
	ID 3;
	TITLE "agact";
	HYPOTHESIS 3;
	ENABLED 1;
	CONDITION {
		VARIABLE 1 == VALUE 2 CONFIDENCE 1;
		ENABLED 1;
	}
}
RULE {
	ID 4;
	TITLE "Forest";
	HYPOTHESIS 4;
	ENABLED 1;
	CONDITION {
		VARIABLE 1 == VALUE 4 CONFIDENCE 1;
		ENABLED 1;
	}
}
RULE {
```

```
        ID 5;
        TITLE "water";
        HYPOTHESIS 5;
        ENABLED 1;
        CONDITION {
                VARIABLE 1 == VALUE 6 CONFIDENCE 1;
                ENABLED 1;
        }
}
RULE {
        ID 6;
        TITLE "developed";
        HYPOTHESIS 6;
        ENABLED 1;
        CONDITION {
                VARIABLE 1 == VALUE 5 CONFIDENCE 1;
                ENABLED 1;
        }
}
RULE {
        ID 7;
        TITLE "natural";
        HYPOTHESIS 7;
        ENABLED 1;
        CONDITION {
                VARIABLE 1 == VALUE 1 CONFIDENCE 1;
                ENABLED 1;
        }
}
RULE {
        ID 8;
        TITLE "Clouds";
        HYPOTHESIS 8;
        ENABLED 1;
        CONDITION {
                VARIABLE 1 == VALUE 7 CONFIDENCE 1;
                ENABLED 1;
        }
}
RULE {
        ID 9;
        TITLE "Shadow";
        HYPOTHESIS 9;
        ENABLED 1;
        CONDITION {
                VARIABLE 1 == VALUE 8 CONFIDENCE 1;
                ENABLED 1;
        }
}
VARIABLE {
        ID 1;
        TITLE "LCLU1014";
        OBJECTTYPE RASTER;
        DATATYPE INTEGER;
        IMAGE "/home/grad/dunhams/recode/recode1014b.img"
```

```
            LAYER "(:Layer_1)"
            ATTRIBUTE "Cell Value";
}
VARIABLE {
      ID 2;
      TITLE "RipPoly";
      OBJECTTYPE RASTER;
      DATATYPE INTEGER;
      IMAGE "/home/grad/dunhams/recode/vec2rast.img"
            LAYER "(:Layer_1)"
            ATTRIBUTE "Cell Value";
}
```

NDVI model

```
PAGESIZE 6, 9.81461 INCHES;
CELLSIZE MINIMUM;
PRINTERPAGESIZE 8.5, 11;
MARGINS 0.5, 0.5, 0.5, 0.5;
ORIENTATION PORTRAIT;
PRINTSCALE 100;
WINDOW UNION;
PROJECTION DEFAULT;
AOI NONE;
OPTIMIZE NO;
RASTER {
      ID 1;
      TITLE "n1_atcor101400";
      POSITION 2.49438, 0.831461;
      FILENAME "/home/grad/dunhams/atcor/atcor101400.img";
      INTERPOLATION NEAREST;
      ATHEMATIC;
      DATATYPE UNSIGNED8;
      DECLARE "Integer";
      COMPRESSION UNCOMPRESSED;
      COORDINATES MAP;
      AOI NONE;
      RECODE NO;
      CHILD 2, 3;
}
FUNCTION {
      ID 2;
      TITLE "$n1_atcor101400";
      POSITION 0.483146, 2.8427;
      VALUE "($n1_atcor101400(4) - $n1_atcor101400(3))";
      AREA UNION;
      CHILD 5;
}
FUNCTION {
      ID 3;
      TITLE "$n1_atcor101400";
      POSITION 4.44944, 2.85393;
      VALUE "($n1_atcor101400(4) + $n1_atcor101400(3))";
      AREA UNION;
      CHILD 6;
}
FUNCTION {
      ID 4;
      TITLE "EITHER 0 IF ";
      POSITION 2.62921, 6.34831;
      VALUE "EITHER 0 IF ( $n6_memory==0.0) OR $n5_memory / $n6_memory
OTHERWISE ";
      AREA UNION;
      CHILD 7;
}
RASTER {
      ID 5;
      TITLE "n5_memory";
```

```
        POSITION 0.494382, 4.80899;
        TEMPFILE;
        NEWFILE;
        INTERPOLATION NEAREST;
        ATHEMATIC;
        DATATYPE FLOAT;
        DECLARE "Float";
        COMPRESSION UNCOMPRESSED;
        COORDINATES MAP;
        RECODE NO;
        CHILD 4;
}
RASTER {
        ID 6;
        TITLE "n6_memory";
        POSITION 4.32584, 4.64045;
        TEMPFILE;
        NEWFILE;
        INTERPOLATION NEAREST;
        ATHEMATIC;
        DATATYPE FLOAT;
        DECLARE "Float";
        COMPRESSION UNCOMPRESSED;
        COORDINATES MAP;
        RECODE NO;
        CHILD 4;
}
RASTER {
        ID 7;
        TITLE "n7_ndvi2";
        POSITION 0.88764, 8.31461;
        FILENAME "/home/grad/dunhams/ndvi2.img";
        NEWFILE;
        INTERPOLATION NEAREST;
        ATHEMATIC;
        DATATYPE FLOAT;
        DECLARE "Float";
        COMPRESSION UNCOMPRESSED;
        COORDINATES MAP;
        RECODE NO;
}
```

SAVI model

```
PAGESIZE 6, 12.7416 INCHES;
CELLSIZE MINIMUM;
PRINTERPAGESIZE 8.5, 11;
MARGINS 0.5, 0.5, 0.5, 0.5;
ORIENTATION PORTRAIT;
PRINTSCALE 100;
WINDOW UNION;
PROJECTION DEFAULT;
AOI NONE;
OPTIMIZE NO;
RASTER {
      ID 1;
      TITLE "n1_atcor9202";
      POSITION 2.25843, 0.516854;
      FILENAME "/home/grad/dunhams/atcor/atcor9202.img";
      INTERPOLATION NEAREST;
      ATHEMATIC;
      DATATYPE UNSIGNED8;
      DECLARE "Float";
      COMPRESSION UNCOMPRESSED;
      COORDINATES MAP;
      AOI NONE;
      RECODE NO;
      CHILD 3, 4;
}
RASTER {
      ID 2;
      TITLE "n2_memory";
      POSITION 0.58427, 4.95506;
      TEMPFILE;
      NEWFILE;
      INTERPOLATION NEAREST;
      ATHEMATIC;
      DATATYPE FLOAT;
      DECLARE "Float";
      COMPRESSION UNCOMPRESSED;
      COORDINATES MAP;
      RECODE NO;
      CHILD 6;
}
FUNCTION {
      ID 3;
      TITLE "$n1_atcor9202";
      POSITION 0.584265, 2.83146;
      VALUE "($n1_atcor9202(4) - $n1_atcor9202(3))";
      AREA UNION;
      CHILD 2;
}
FUNCTION {
      ID 4;
      TITLE "$n1_atcor9202";
      POSITION 3.83146, 2.5618;
      VALUE "($n1_atcor9202(4) + $n1_atcor9202(3) + 0.5)";
      AREA UNION;
```

```
        CHILD 5;
}
RASTER {
        ID 5;
        TITLE "n5_memory";
        POSITION 4.13483, 4.85393;
        TEMPFILE;
        NEWFILE;
        INTERPOLATION NEAREST;
        ATHEMATIC;
        DATATYPE FLOAT;
        DECLARE "Float";
        COMPRESSION UNCOMPRESSED;
        COORDINATES MAP;
        RECODE NO;
        CHILD 6;
}
FUNCTION {
        ID 6;
        TITLE "$n2_memory";
        POSITION 2.44944, 6.64045;
        VALUE "$n2_memory / $n5_memory";
        AREA UNION;
        CHILD 7;
}
RASTER {
        ID 7;
        TITLE "n7_memory";
        POSITION 2.50562, 8.20225;
        TEMPFILE;
        NEWFILE;
        INTERPOLATION NEAREST;
        ATHEMATIC;
        DATATYPE FLOAT;
        DECLARE "Float";
        COMPRESSION UNCOMPRESSED;
        COORDINATES MAP;
        RECODE NO;
        CHILD 8;
}
FUNCTION {
        ID 8;
        TITLE "$n7_memory";
        POSITION 2.47191, 9.94382;
        VALUE "$n7_memory * 1.5";
        AREA UNION;
        CHILD 9;
}
RASTER {
        ID 9;
        TITLE "n9_savi92";
        POSITION 2.57303, 11.7416;
        FILENAME "/home/grad/dunhams/savi/savi92.img";
        NEWFILE;
        INTERPOLATION NEAREST;
```

```
        ATHEMATIC;
        DATATYPE FLOAT;
        DECLARE "Float";
        COMPRESSION UNCOMPRESSED;
        COORDINATES MAP;
        RECODE NO;
}
```

Tasseled Cap Greenness model

```
PAGESIZE 6, 8 INCHES;
CELLSIZE MINIMUM;
PRINTERPAGESIZE 8.5, 11;
MARGINS 0.5, 0.5, 0.5, 0.5;
ORIENTATION PORTRAIT;
PRINTSCALE 100;
WINDOW UNION;
PROJECTION DEFAULT;
AOI NONE;
OPTIMIZE NO;
RASTER {
      ID 1;
      TITLE "n1_atcor9202";
      POSITION 2, 0.617978;
      FILENAME "/home/grad/dunhams/atcor/atcor9202.img";
      INTERPOLATION NEAREST;
      ATHEMATIC;
      DATATYPE UNSIGNED8;
      DECLARE "Float";
      COMPRESSION UNCOMPRESSED;
      COORDINATES MAP;
      AOI NONE;
      RECODE NO;
      CHILD 2;
}
FUNCTION {
      ID 2;
      TITLE "-0.3344 * $n1_atcor9202";
      POSITION 1.96629, 2.83146;
      VALUE "((-0.3344 * $n1_atcor9202(1)) + (-0.3544 *
$n1_atcor9202(2)) + (-0.4556 * $n1_atcor9202(3)) + (0.6966 *
$n1_atcor9202(4)) + (-0.0242 * $n1_atcor9202(5)) + (-0.2630 *
$n1_atcor9202(7)))";
      AREA UNION;
      CHILD 3;
}
RASTER {
      ID 3;
      TITLE "n3_tc92";
      POSITION 2.21348, 4.98876;
      FILENAME "/home/grad/dunhams/tc-greenness/tc92.img";
      NEWFILE;
      INTERPOLATION NEAREST;
      ATHEMATIC;
      DATATYPE FLOAT;
      DECLARE "Float";
      COMPRESSION UNCOMPRESSED;
      COORDINATES MAP;
      RECODE NO;
}
```

Tasseled Cap Wetness model

```
PAGESIZE 6, 8 INCHES;
CELLSIZE MINIMUM;
PRINTERPAGESIZE 8.5, 11;
MARGINS 0.5, 0.5, 0.5, 0.5;
ORIENTATION PORTRAIT;
PRINTSCALE 100;
WINDOW UNION;
PROJECTION DEFAULT;
AOI NONE;
OPTIMIZE NO;
RASTER {
      ID 1;
      TITLE "n1_atcor92699";
      POSITION 1.88764, 0.348315;
      FILENAME "/home/grad/dunhams/atcor/atcor92699.img";
      INTERPOLATION NEAREST;
      ATHEMATIC;
      DATATYPE UNSIGNED8;
      DECLARE "Float";
      COMPRESSION UNCOMPRESSED;
      COORDINATES MAP;
      AOI NONE;
      RECODE NO;
      CHILD 2;
}
FUNCTION {
      ID 2;
      TITLE "0.2626 *$n1_atcor92699";
      POSITION 1.97753, 2.73034;
      VALUE "(0.2626 *$n1_atcor92699(1)) + (0.2141 * $n1_atcor92699(2))
+ (0.0926 * $n1_atcor92699(3)) + (0.0656 * $n1_atcor92699(4)) + (-
0.7629*$n1_atcor92699(5)) + (-0.5388 * $n1_atcor92699(7))";
      AREA UNION;
      CHILD 3;
}
RASTER {
      ID 3;
      TITLE "n3_tcw926";
      POSITION 2, 4.53932;
      FILENAME "/home/grad/dunhams/tc-wetness/tcw926.img";
      NEWFILE;
      INTERPOLATION NEAREST;
      ATHEMATIC;
      DATATYPE FLOAT;
      DECLARE "Float";
      COMPRESSION UNCOMPRESSED;
      COORDINATES MAP;
      RECODE NO;
}
```

Zonal Function model (to calculate mean index value for each vegetation type)

```
PAGESIZE 6.91573, 8 INCHES;
CELLSIZE MINIMUM;
PRINTERPAGESIZE 8.5, 11;
MARGINS 0.5, 0.5, 0.5, 0.5;
ORIENTATION PORTRAIT;
PRINTSCALE 100;
WINDOW UNION;
PROJECTION DEFAULT;
AOI NONE;
OPTIMIZE NO;
RASTER {
      ID 1;
      TITLE "n1_PROMPT_USER";
      POSITION 1.01124, 0.898876;
      PROMPT;
      INTERPOLATION NEAREST;
      THEMATIC;
      DATATYPE UNSIGNED8;
      DECLARE "Integer";
      COMPRESSION UNCOMPRESSED;
      COORDINATES MAP;
      AOI NONE;
      RECODE NO;
      CHILD 3;
}
FUNCTION {
      ID 3;
      TITLE "ZONAL MEAN ";
      POSITION 3.04494, 2.93258;
      VALUE "ZONAL MEAN ( $n1_PROMPT_USER , $n7_memory ) ";
      AREA UNION;
      CHILD 4;
}
TABLE {
      ID 4;
      TITLE "n4_PROMPT_USER";
      POSITION 3.03371, 4.49438;
      SIZE 0;
      DATATYPE SIGNED32;
      OUTPUT;
      WRITE;
      PROMPT;
}
RASTER {
      ID 5;
      TITLE "n5_PROMPT_USER";
      POSITION 4.20225, 0.662921;
      PROMPT;
      INTERPOLATION NEAREST;
      ATHEMATIC;
      DATATYPE UNSIGNED8;
      DECLARE "Integer";
      COMPRESSION UNCOMPRESSED;
      COORDINATES MAP;
```

```
        AOI NONE;
        RECODE NO;
        CHILD 6;
}
FUNCTION {
        ID 6;
        TITLE "integer";
        POSITION 5.41573, 1.41573;
        VALUE "integer($n5_PROMPT_USER * 1000)";
        AREA UNION;
        CHILD 7;
}
RASTER {
        ID 7;
        TITLE "n7_memory";
        POSITION 4.78652, 2.68539;
        TEMPFILE;
        NEWFILE;
        INTERPOLATION NEAREST;
        ATHEMATIC;
        DATATYPE FLOAT;
        DECLARE "Integer";
        COMPRESSION UNCOMPRESSED;
        COORDINATES MAP;
        RECODE NO;
        CHILD 3;
}
```

APPENDIX II

PALMER DROUGHT SEVERITY INDEX MAPS

PDSI Maps-1999 (for images available)

PDSI Maps-2000 (for available images)

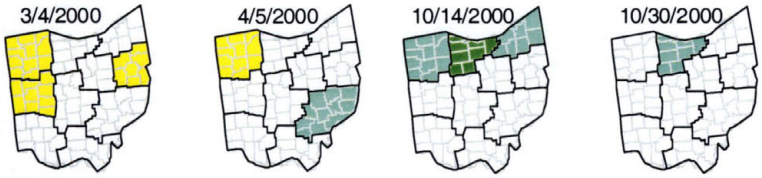

PDSI Maps-2001 (for available images)

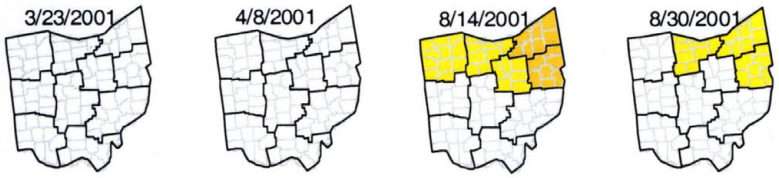

PDSI Maps-2002 (for images available)

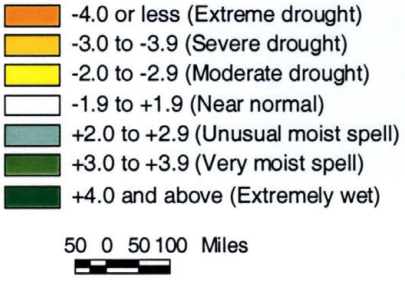

SATELLITE IMAGES

Landsat 7 ETM+ image 9/26/1999 (4-3-2 composite)

Landsat 7 ETM+ image 9/26/1999 after ATCOR (4-3-2 composite)

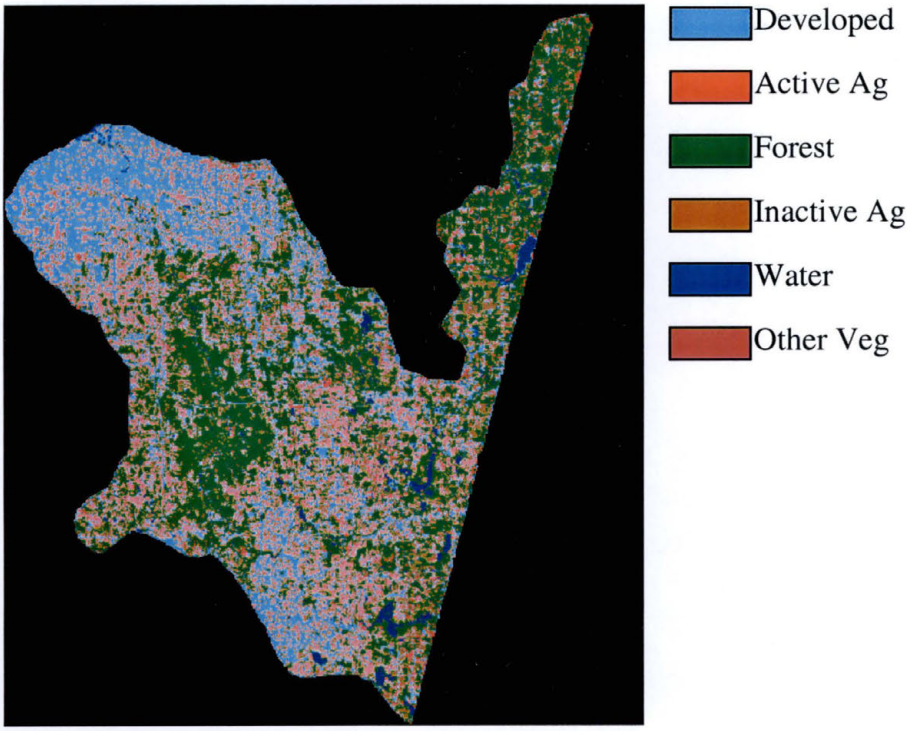

Classified 9/26/1999 image

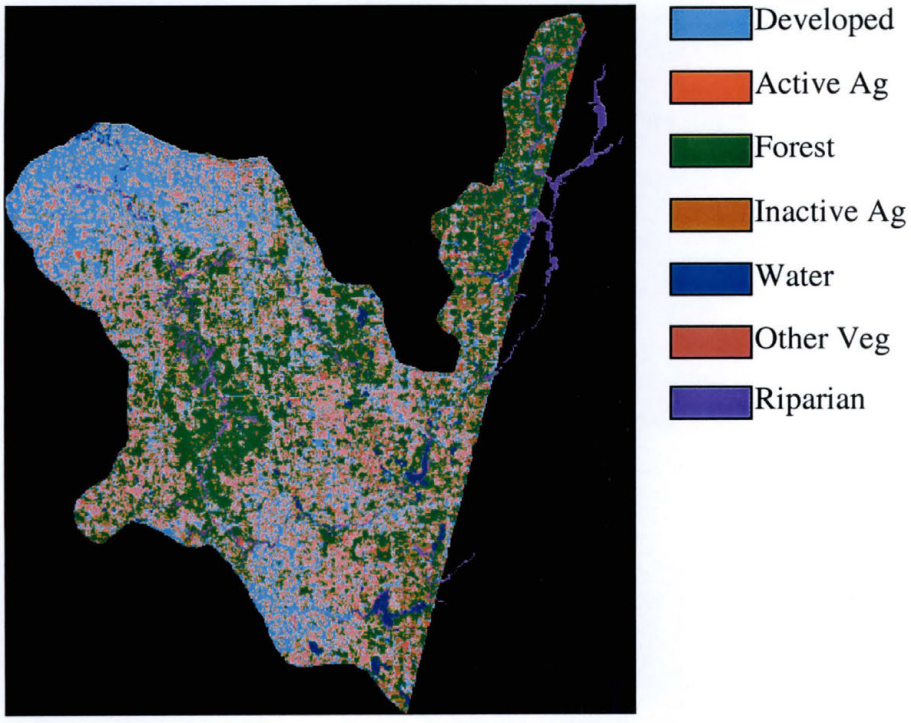

Classified 9/26/1999 image using expert classifier

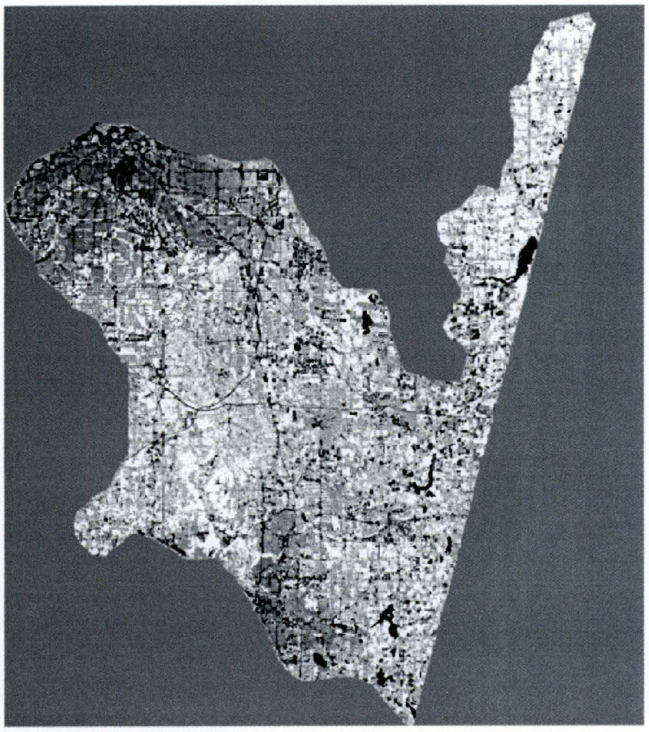

NDVI image 9/26/1999

SAVI image 9/26/1999

Tasseled cap greenness image 9/26/1999

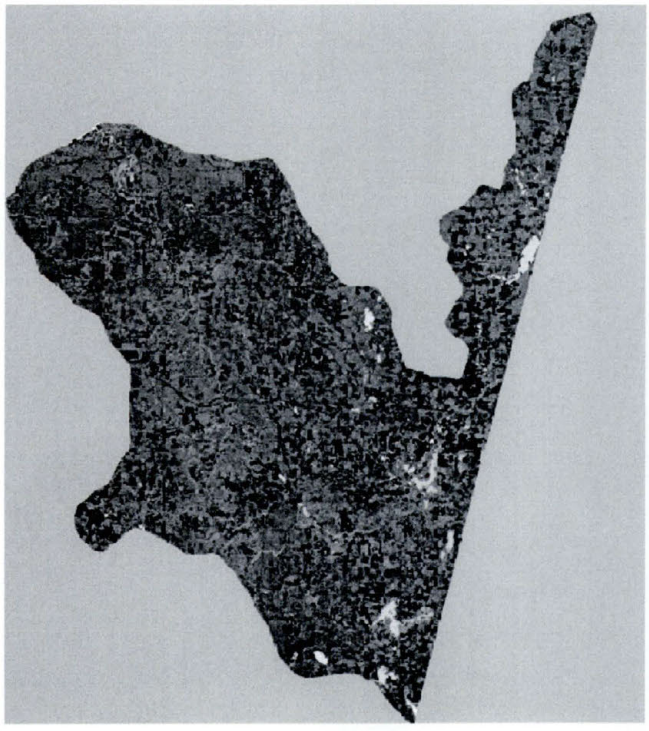

Tasseled cap wetness image 9/26/1999

Landsat 7 ETM+ image 10/12/1999 (4-3-2 composite)

Landsat 7 ETM+ image 10/12/1999 after ATCOR (4-3-2 composite)

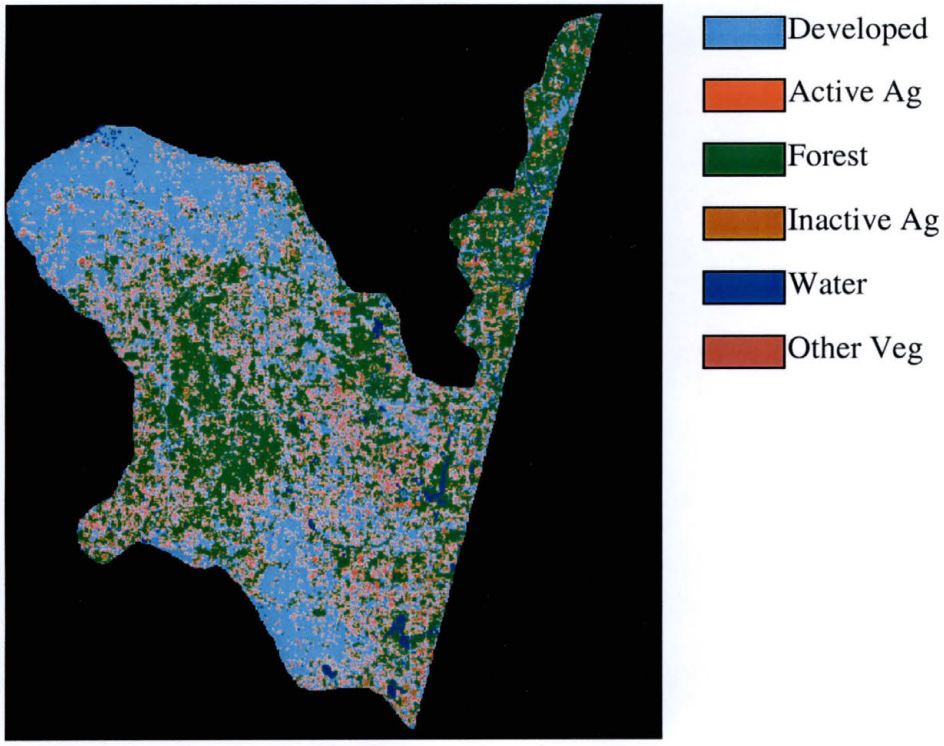

Classified 10/12/1999 image

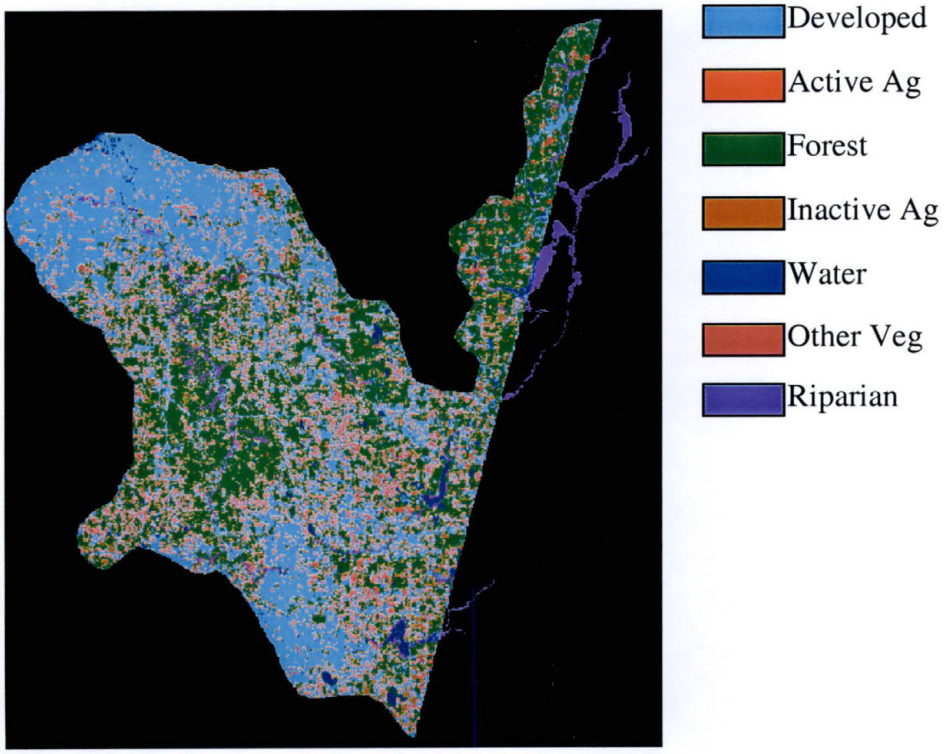

Classified 10/12/1999 image using expert classifier

NDVI image 10/12/1999

SAVI image 10/12/1999

Tasseled Cap Greenness image 10/12/1999

Tasseled Cap Wetness image 10/12/1999

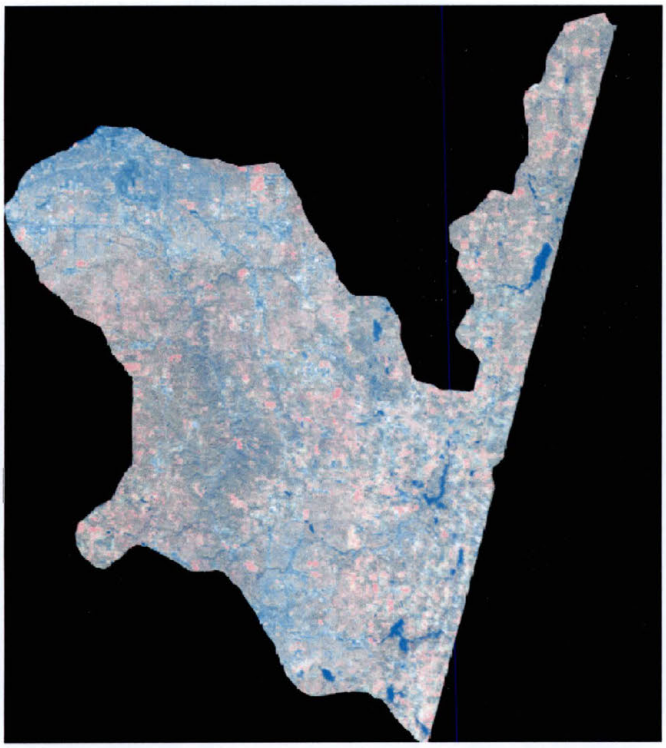

Landsat 7 ETM+ image 11/13/1999 (4-3-2 composite)

Landsat 7 ETM+ image 11/13/1999 after ATCOR (4-3-2 composite)

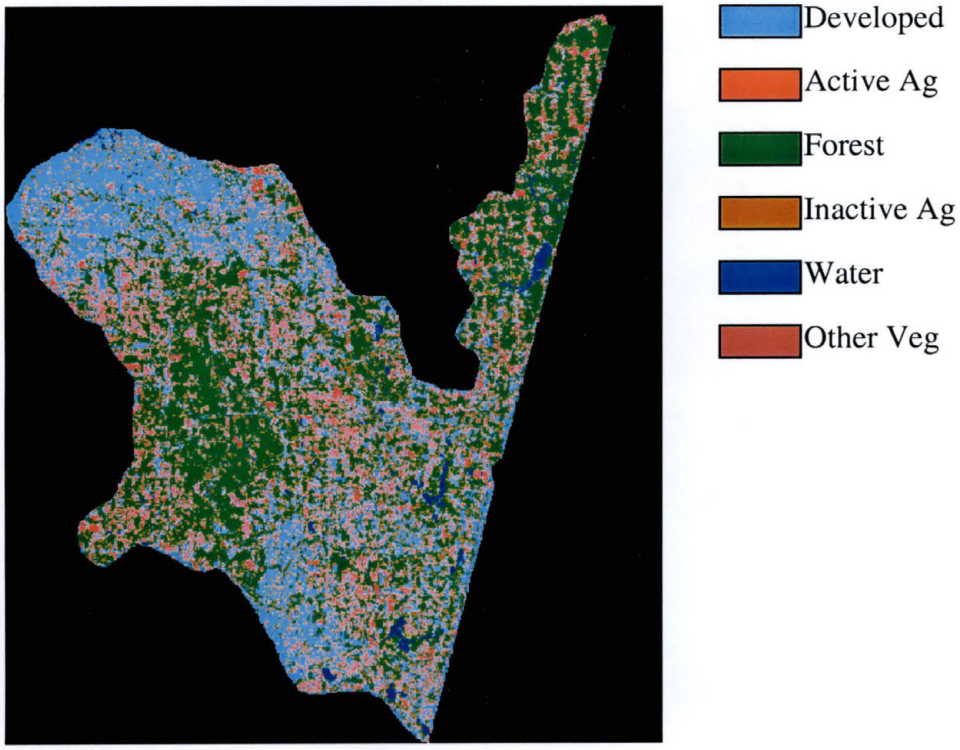

Classified 11/13/1999 image

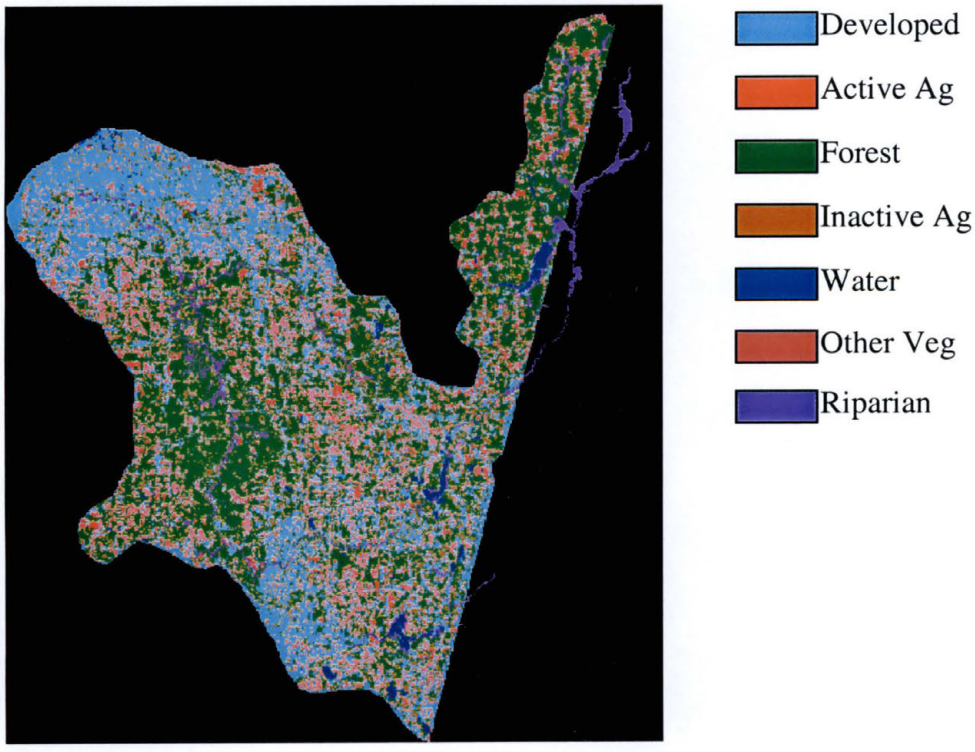

Classified 11/13/1999 image using expert classifier

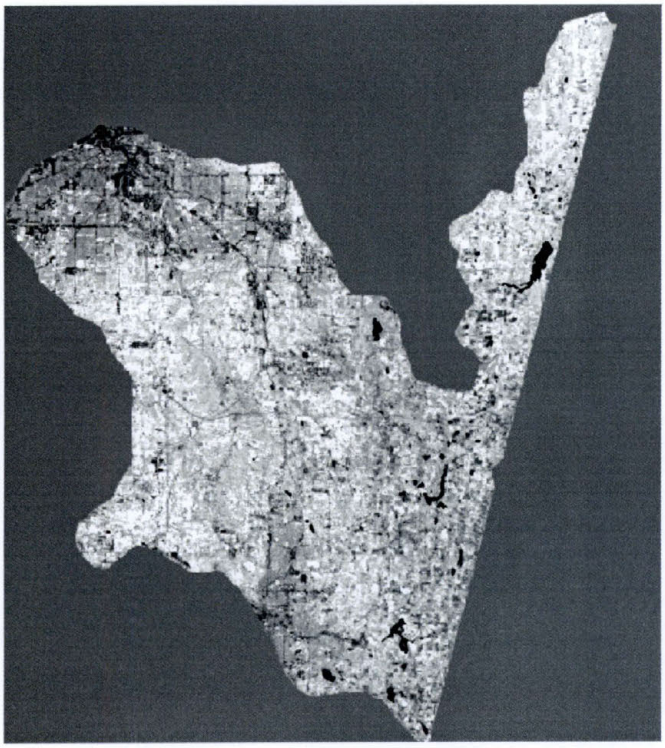

NDVI image 11/13/1999

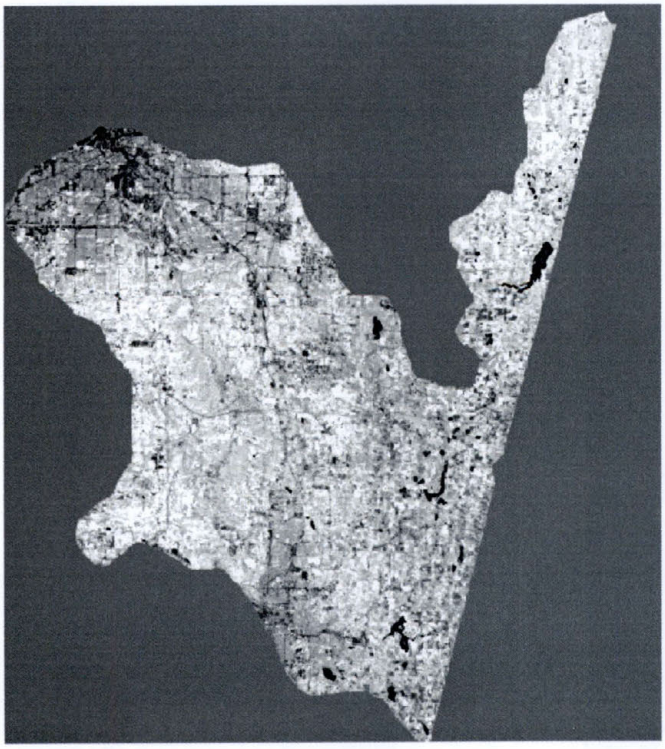

SAVI image 11/13/1999

Tasseled Cap Grenness image 11/13/1999

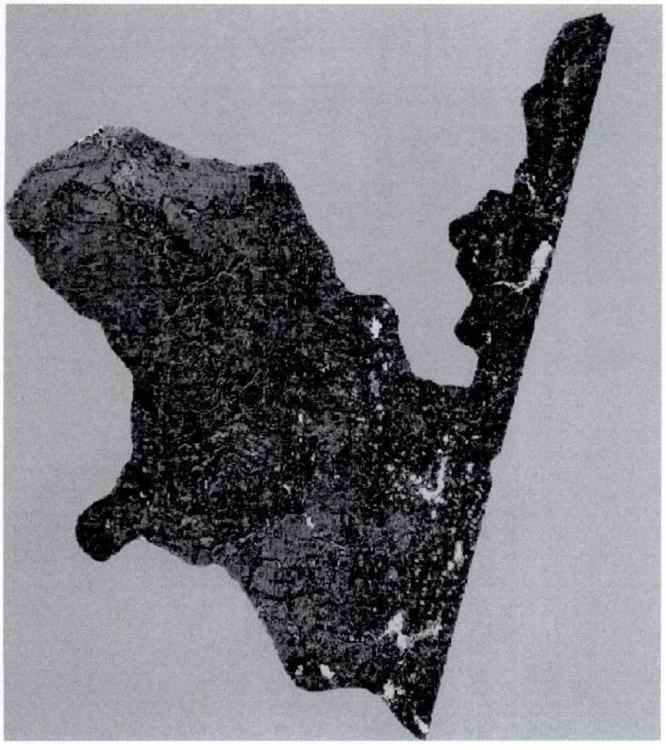

Tasseled Cap Wetness image 11/13/1999

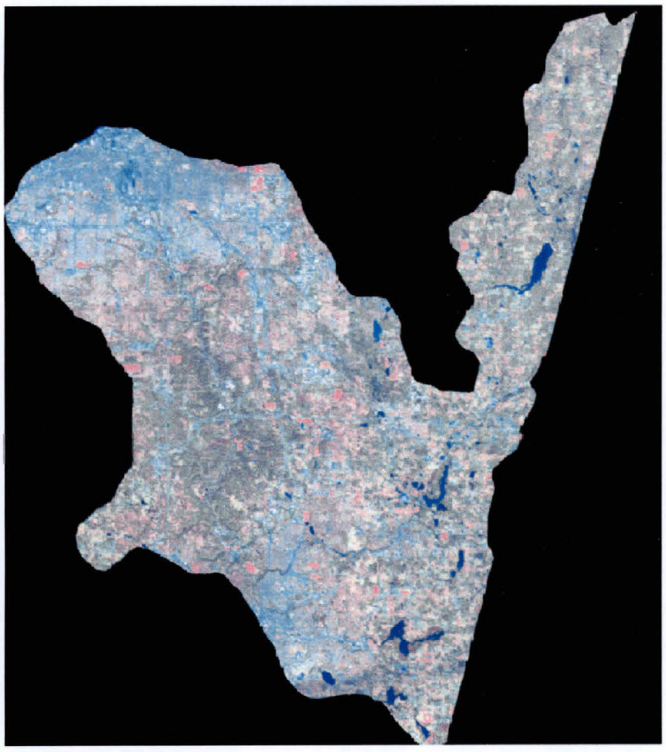

Landsat 7 ETM+ image 3/4/2000 (4-3-2 composite)

Landsat 7 ETM+ image 3/4/2000 after ATCOR (4-3-2 composite)

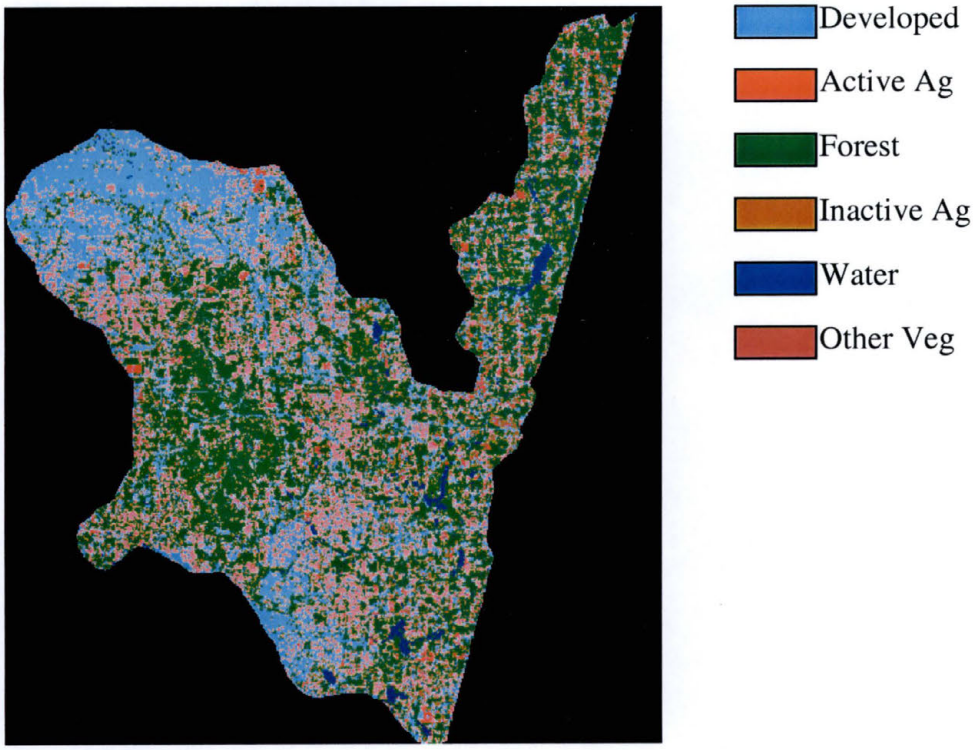

Classified 3/4/2000 image

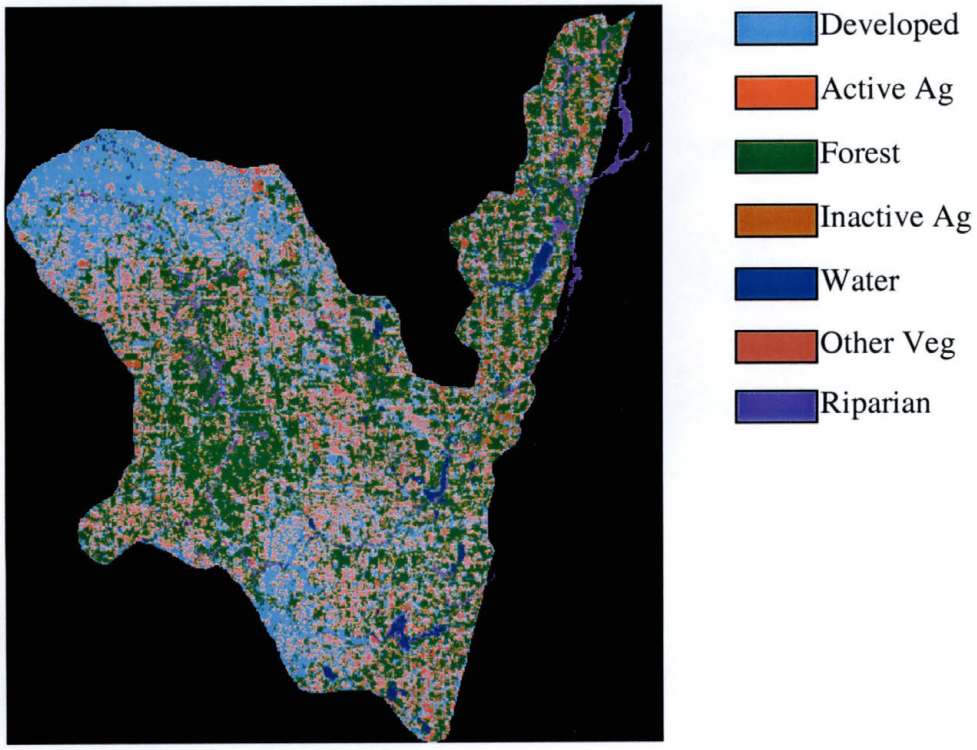

Classified 3/4/2000 image using expert classifier

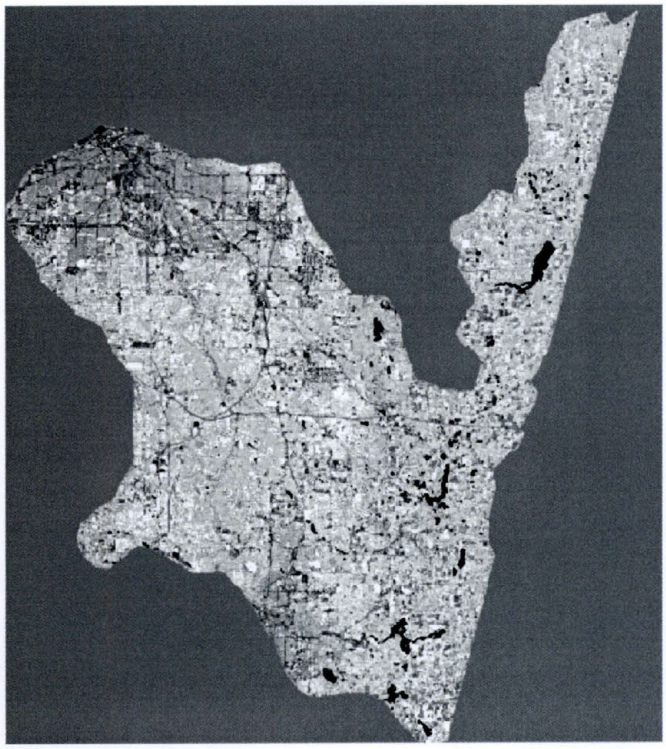

NDVI image 3/4/2000

SAVI image 3/4/2000

Tasseled Cap Greenness image 3/4/2000

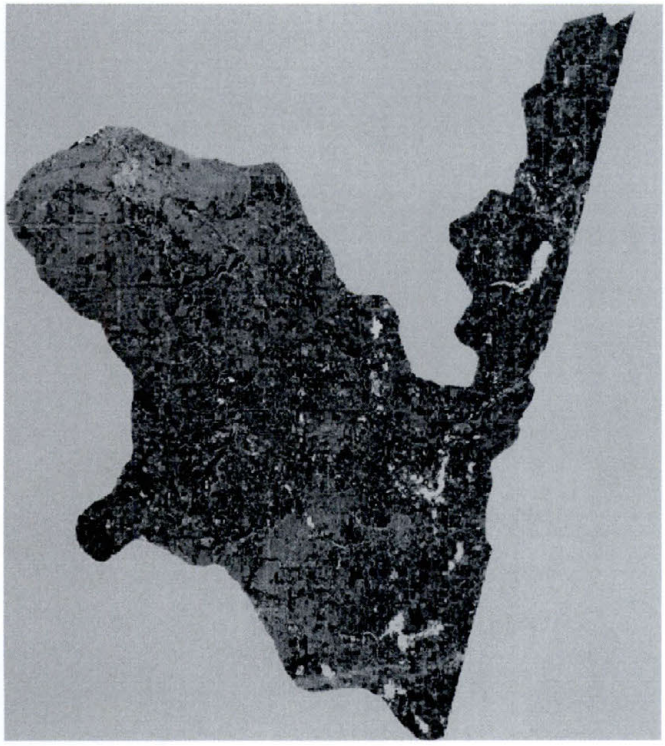

Tasseled Cap Wetness image 3/4/2000

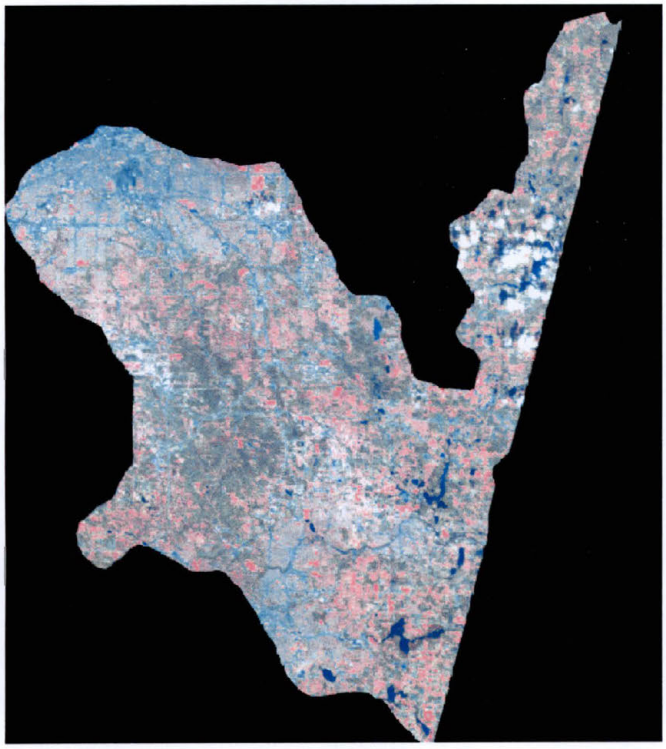

Landsat 7 ETM+ image 4/5/2000 (4-3-2 composite)

Landsat 7 ETM+ image 4/5/2000 after ATCOR (4-3-2 composite)

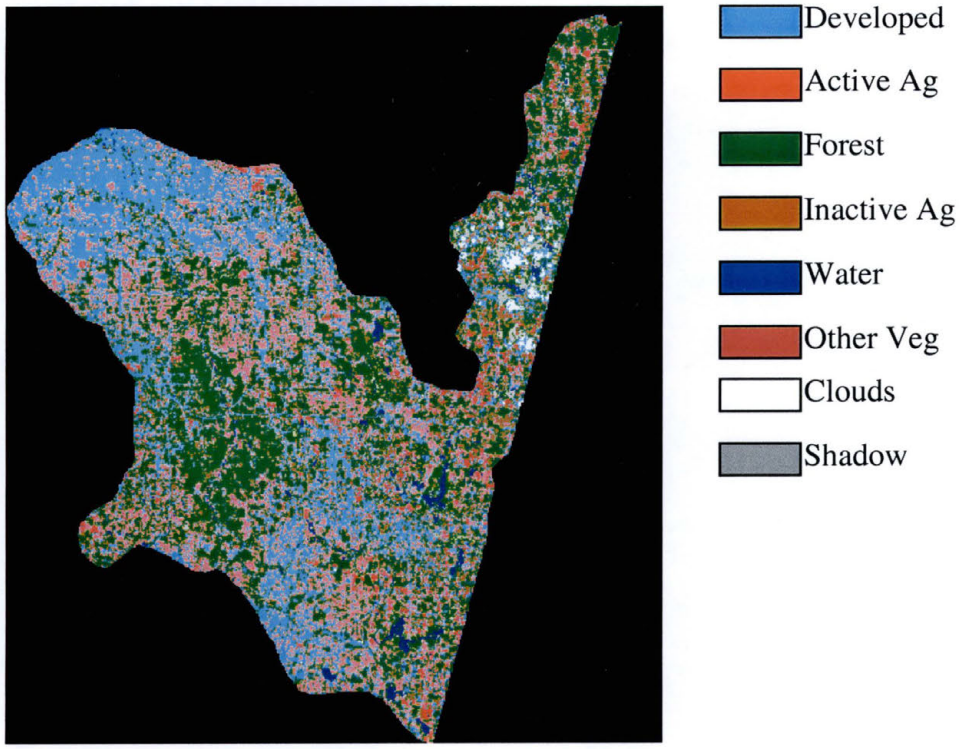

Classified 4/5/2000 image

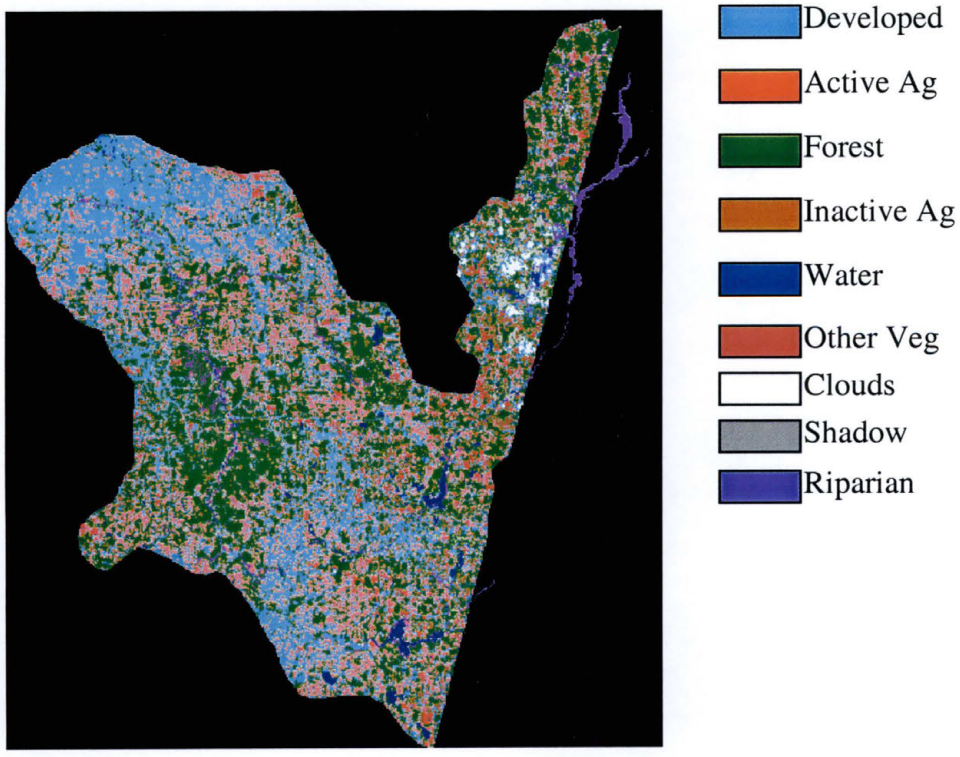

Classified 4/5/2000 image using expert classifier

NDVI image 4/5/2000

SAVI image 4/5/2000

Tasseled Cap Greenness image 4/5/2000

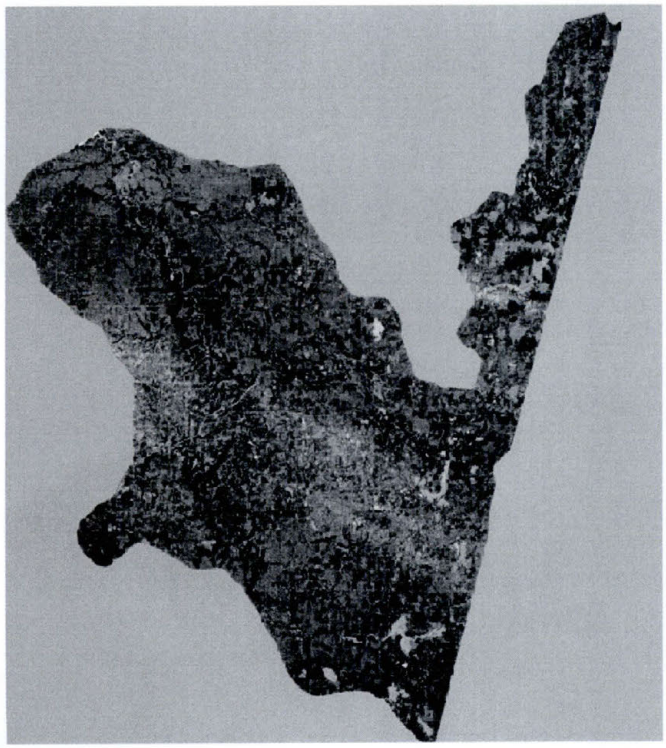

Tasseled Cap Wetness iamge 4/5/2000

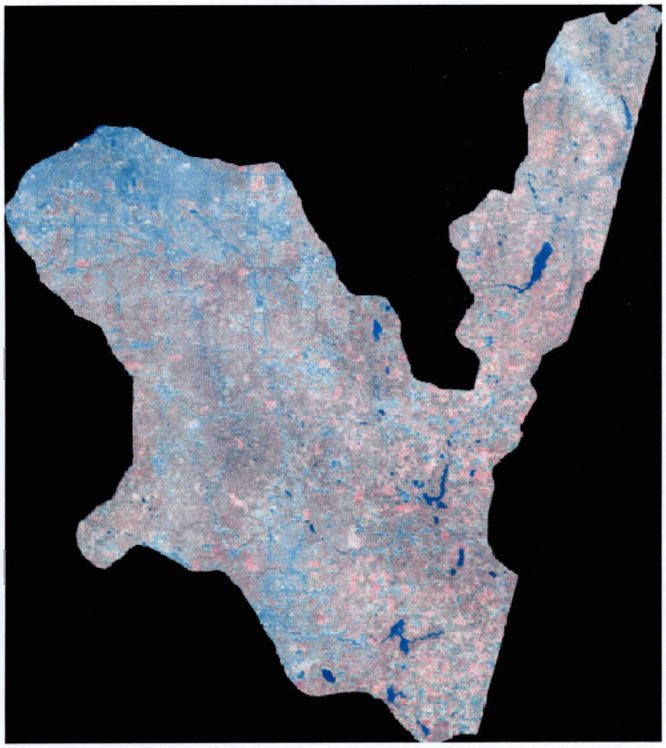

Landsat 7 ETM+ image 10/14/2000 (4-3-2 composite)

Landsat 7 ETM+ image 10/14/2000 after ATCOR (4-3-2 composite)

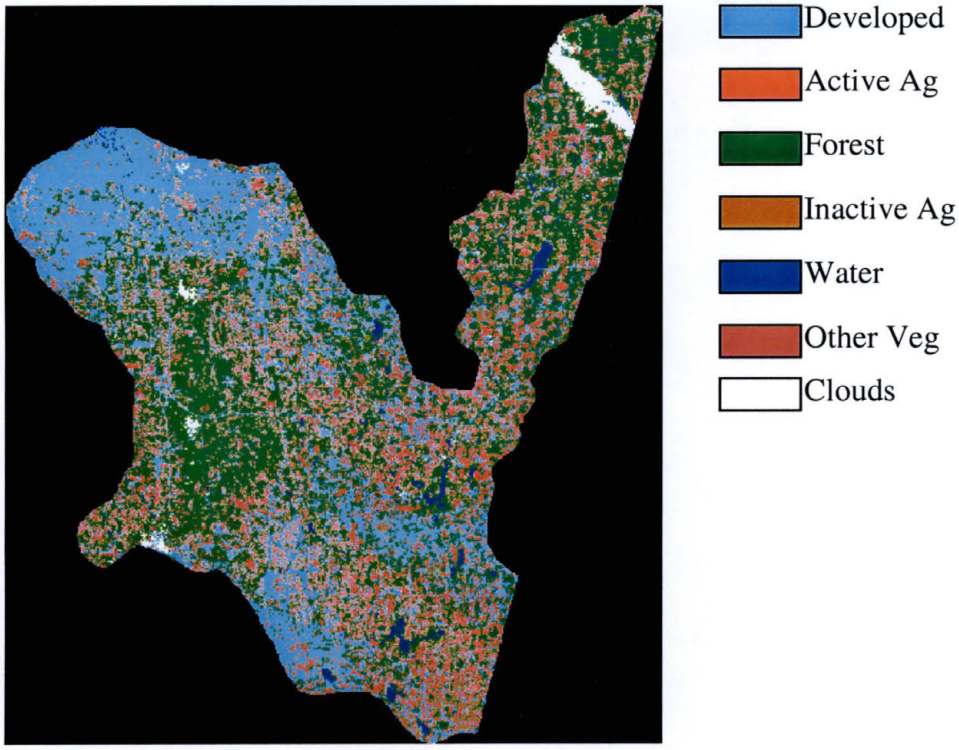

Classified 10/14/2000 image

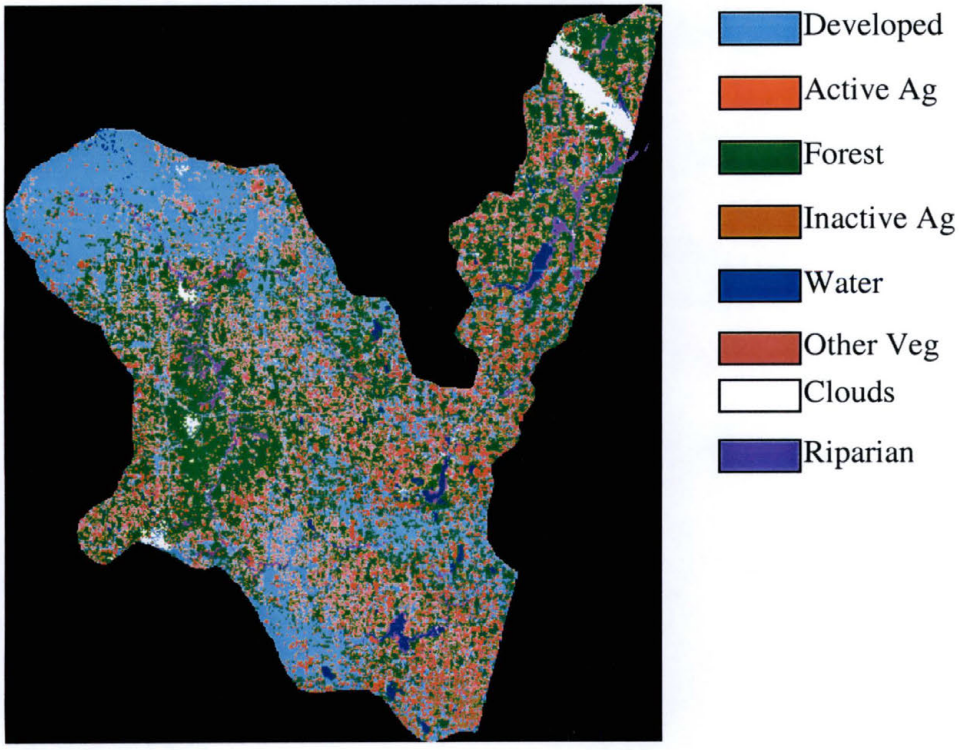

Classified 10/14/2000 image using expert classifier

NDVI image 10/14/2000

SAVI image 10/14/2000

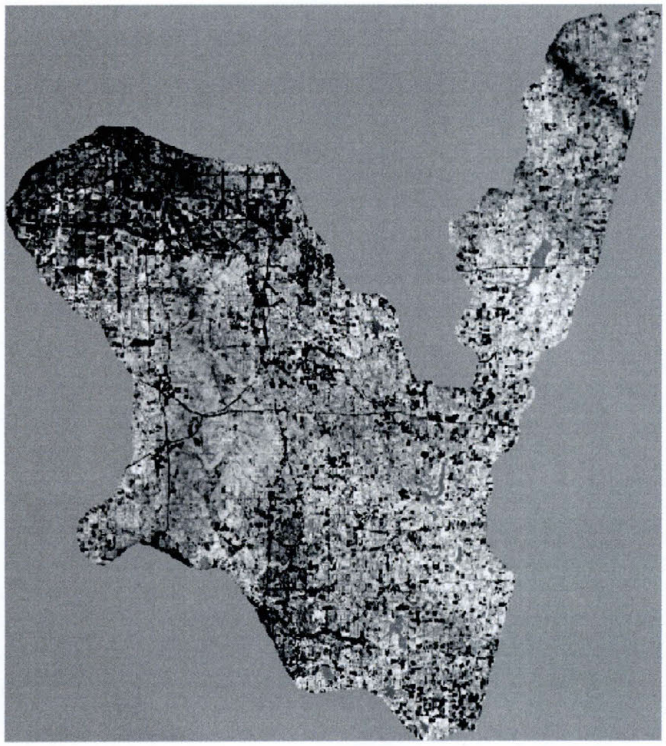

Tasseled Cap Greenness image 10/14/2000

Tasseled Cap Wetness image 10/14/2000

Landsat 7 ETM+ image 10/30/2000 (4-3-2 composite)

Landsat 7 ETM+ image 10/30/2000 after ATCOR (4-3-2 composite)

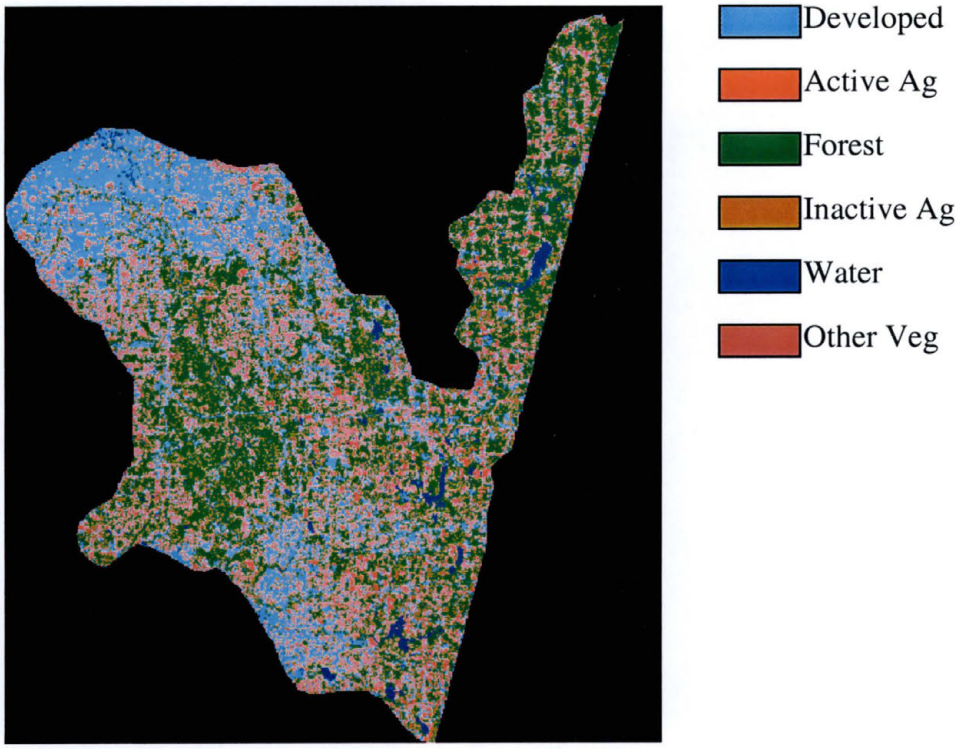

Classified image 10/30/2000

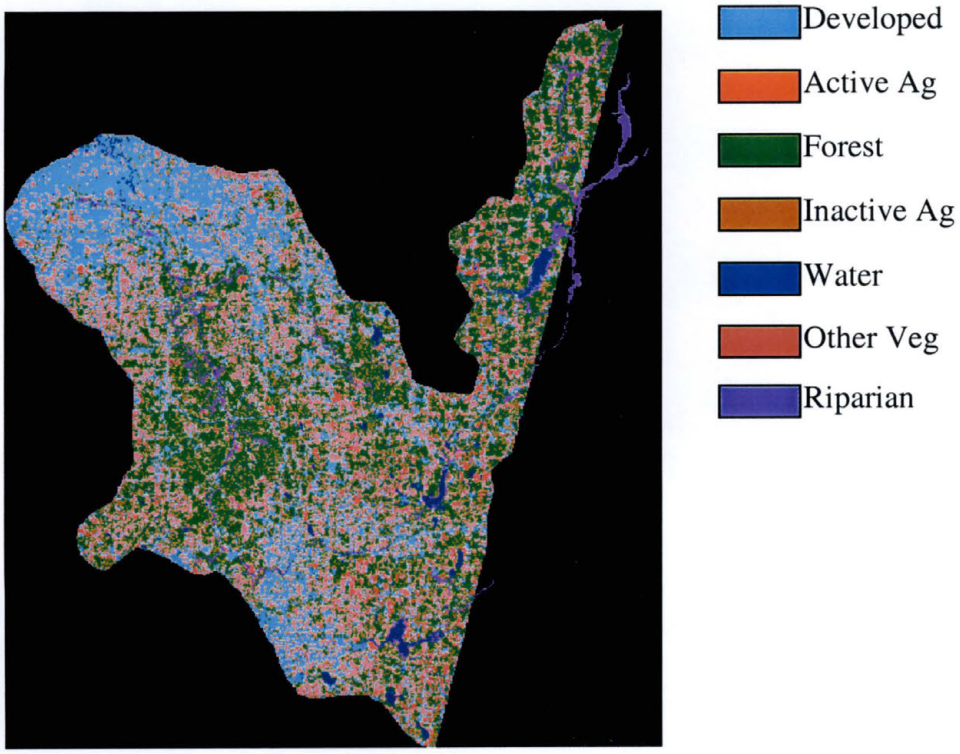

Classified image 10/30/2000 using expert classifier

NDVI image 10/30/2000

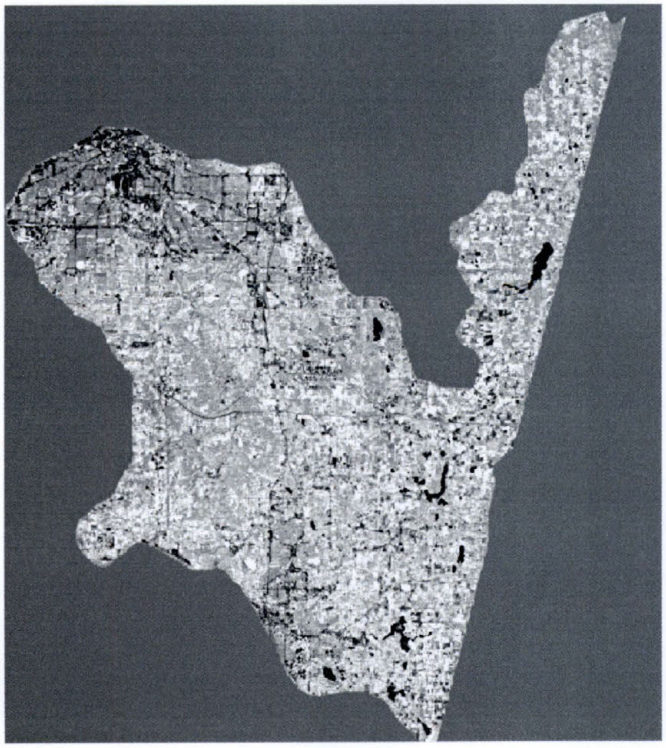

SAVI image 10/30/2000

Tasseled Cap Greenness image 10/30/2000

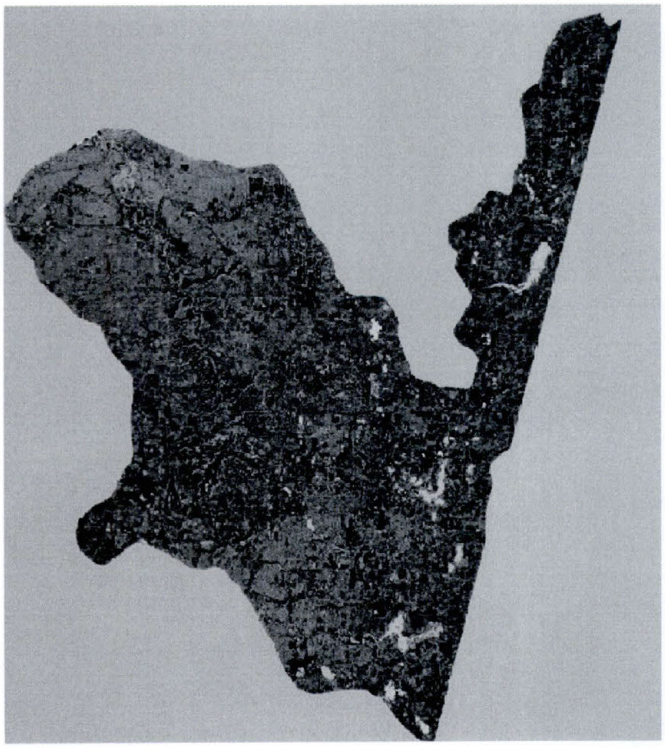

Tasseled Cap Wetness 10/30/2000

Landsat 7 ETM+ image 3/23/2001 (4-3-2 composite)

Landsat 7 ETM+ image 3/23/2001 after ATCOR (4-3-2 composite)

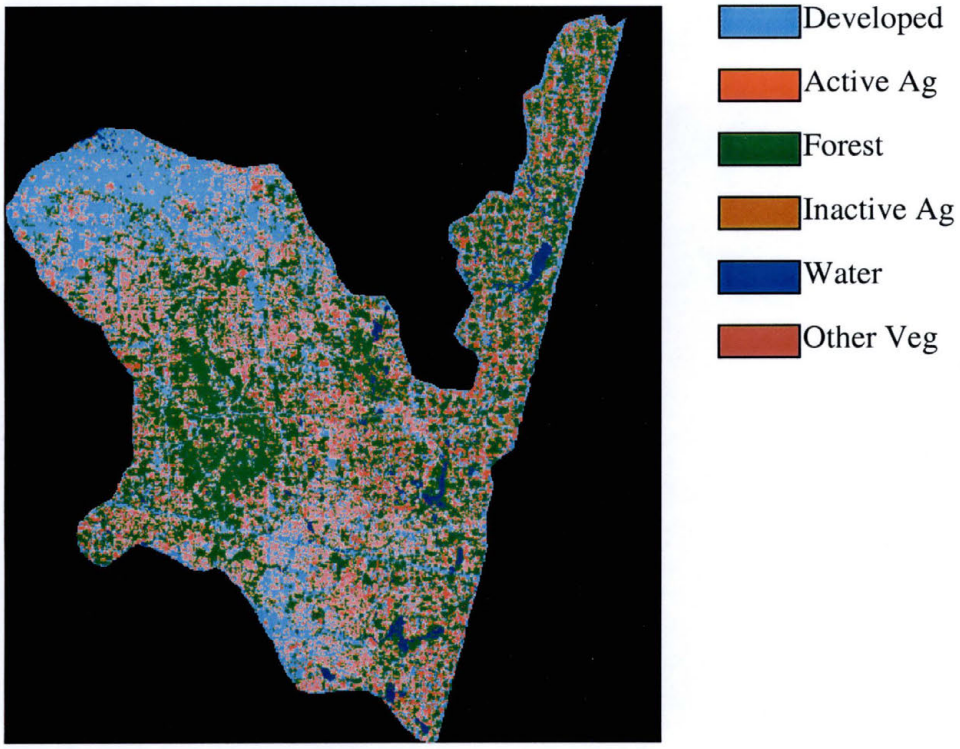

Classified image 3/23/2001

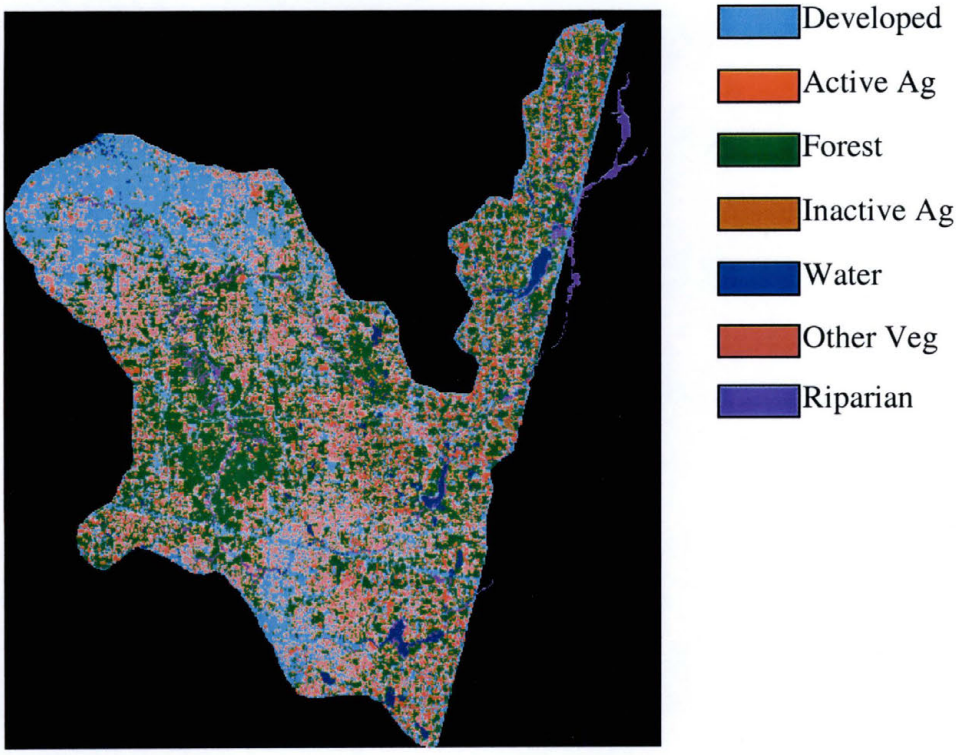

Classified image 3/23/2001 using expert classifier

NDVI image 3/23/2001

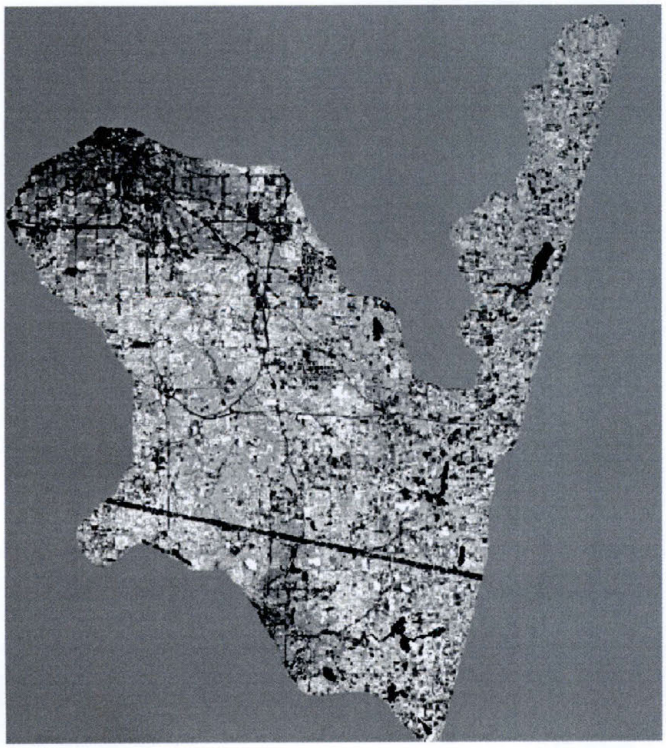

SAVI image 3/23/2001

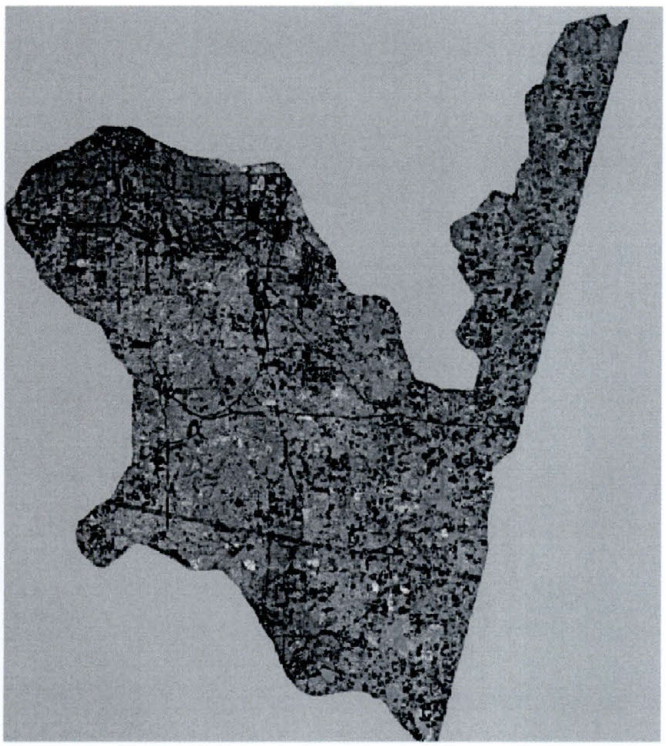

Tasseled Cap Greenness image 3/23/2001

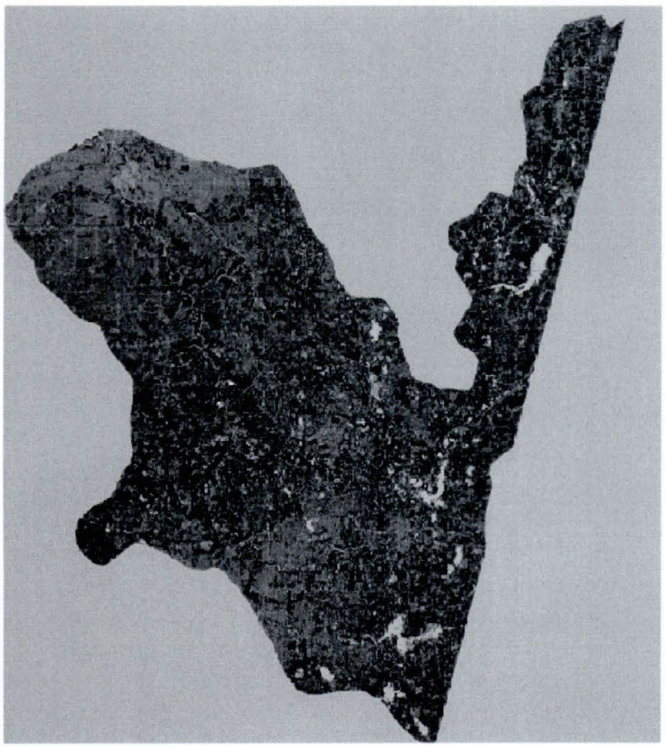

Tasseled Cap Wetness image 3/23/2001

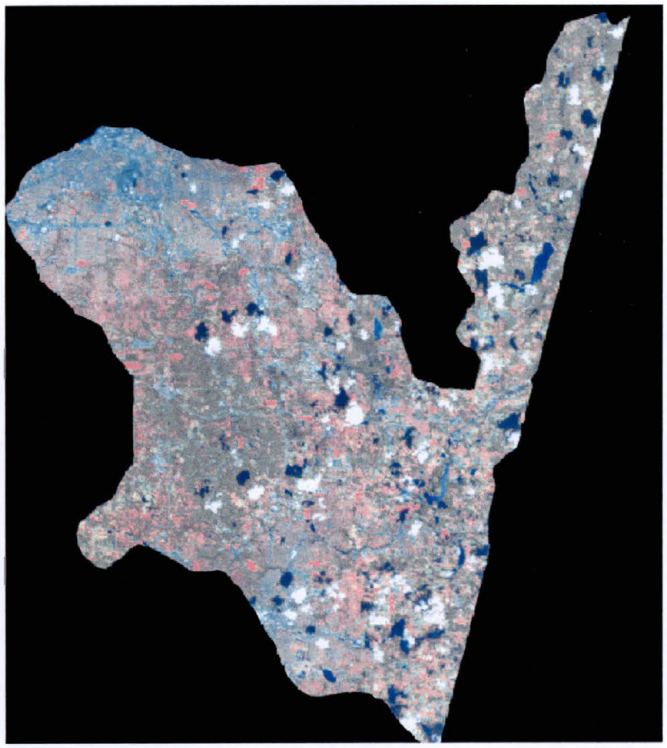

Landsat 7 ETM+ image 4/8/2001 (4-3-2 composite)

Landsat 7 ETM+ image 4/8/2001 after ATCOR (4-3-2 composite)

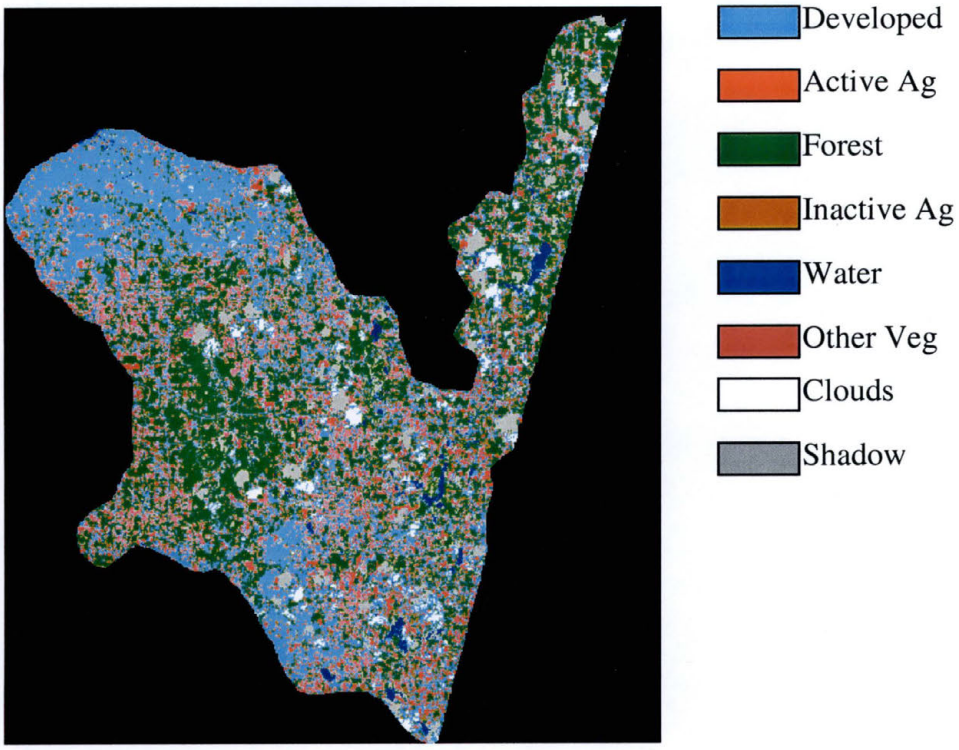

Classified 4/8/2001 image

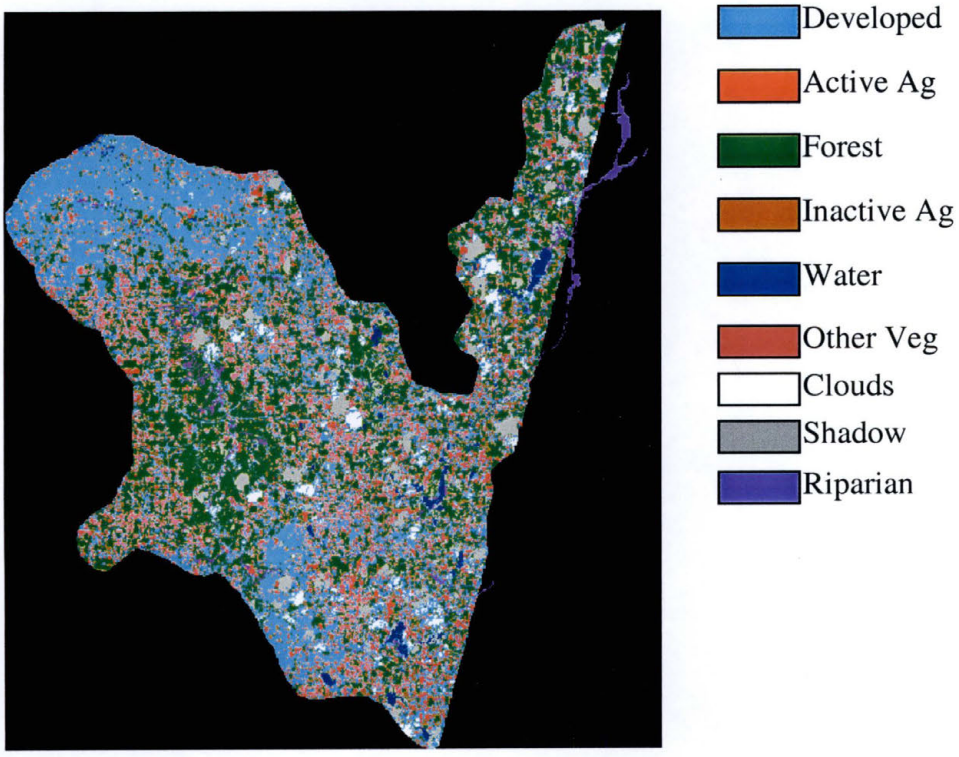

Classified 4/8/2001 image using expert classifier

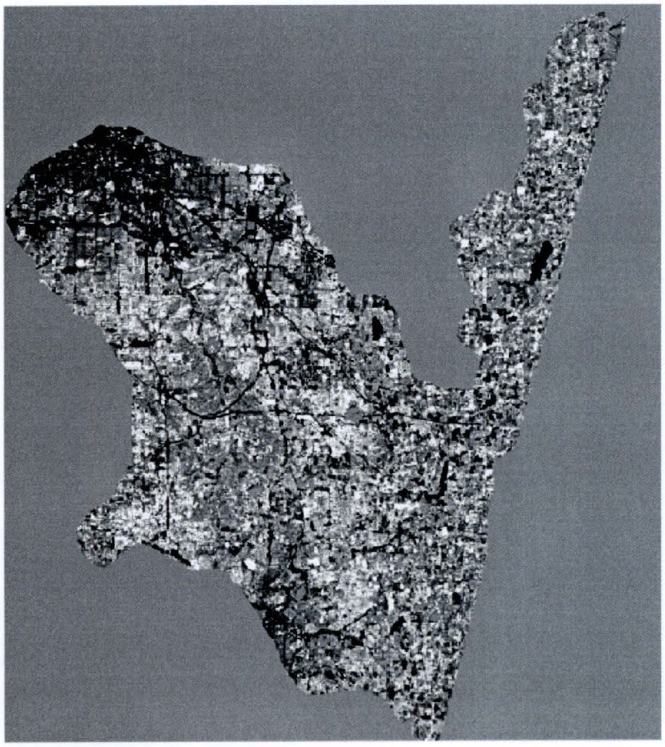

NDVI image 4/8/2001

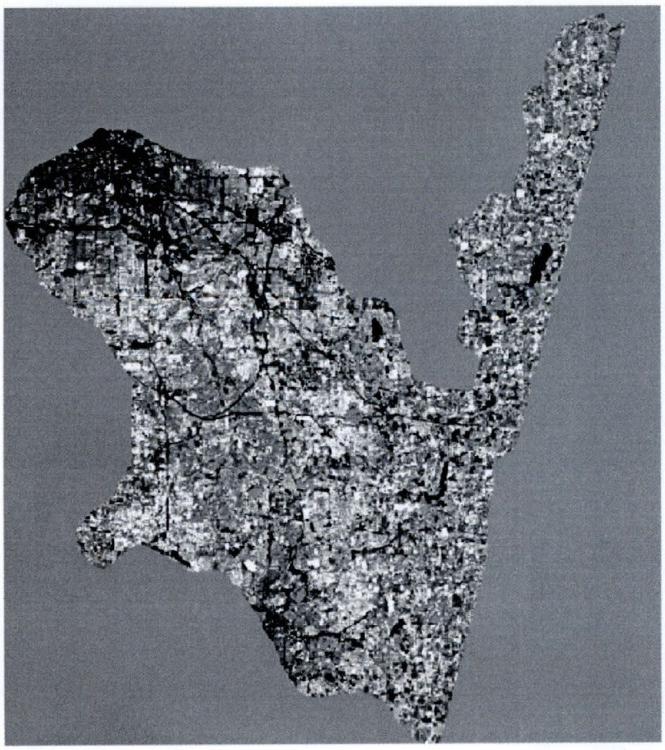

SAVI image 4/8/2001

Tasseled Cap Greenness image 4/8/2001

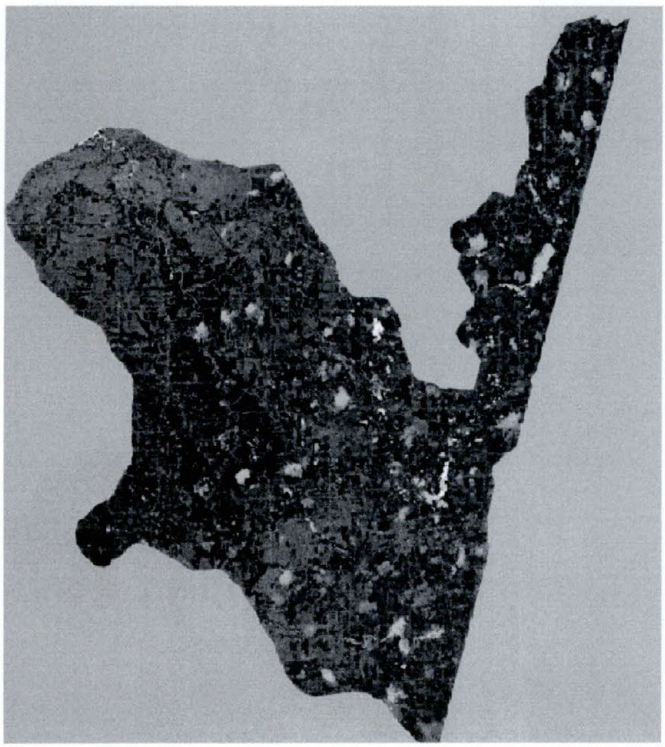

Tasseled Cap Wetness image 4/8/2001

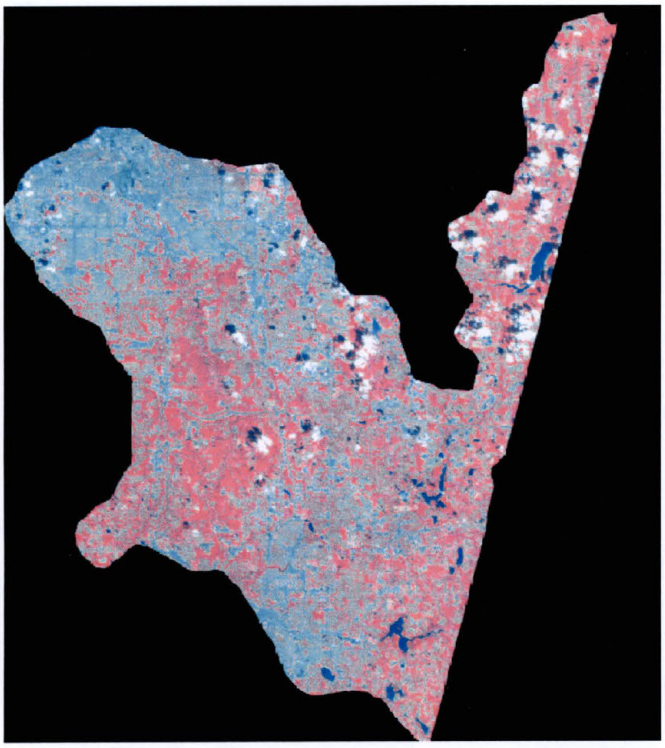

Landsat 7 ETM+ 8/14/2001 image (4-3-2 composite)

Landsat 7 ETM+ 8/14/2001 image after ATCOR (4-3-2 composite)

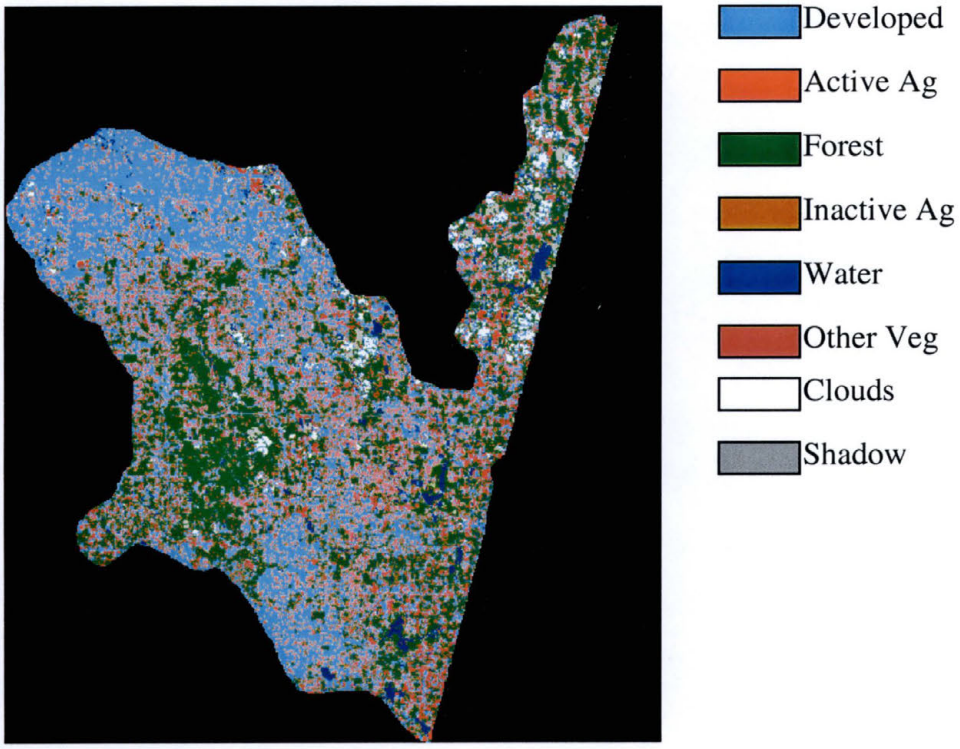

Classified image 8/14/2001

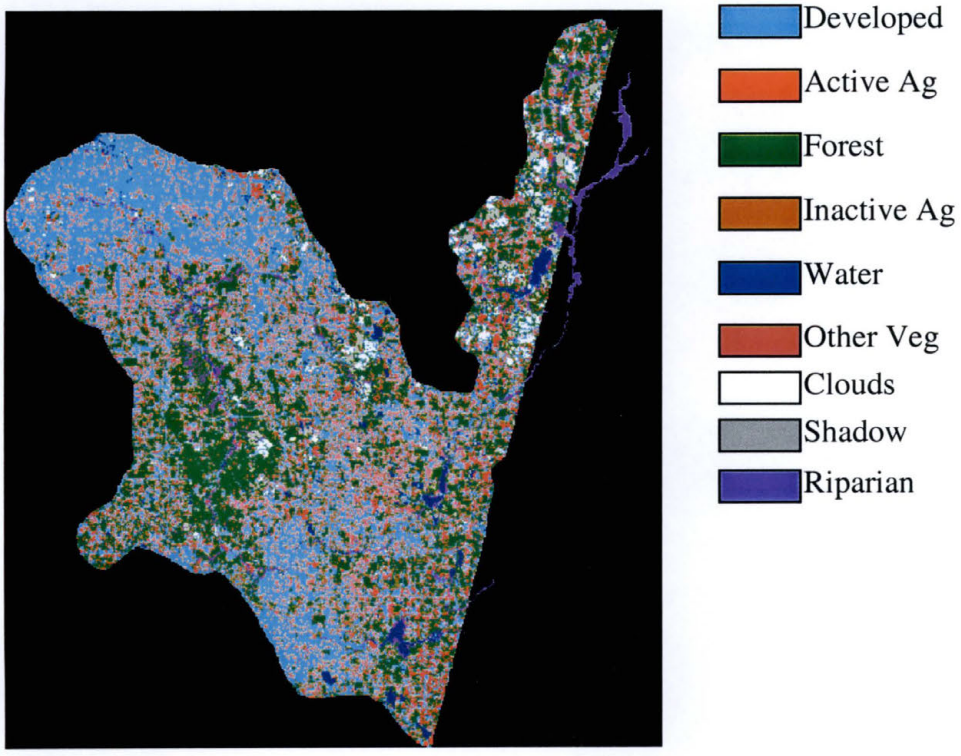

Classified image 8/14/2001 using expert classifier

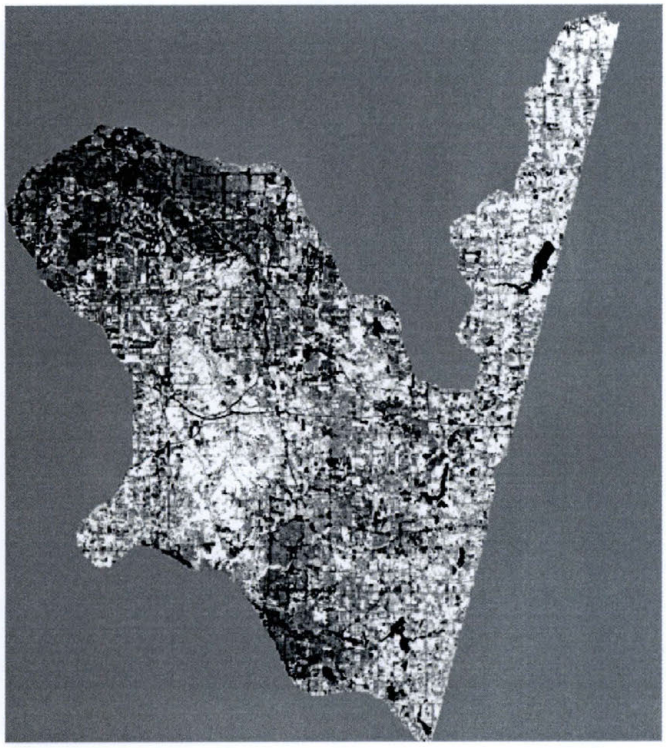

NDVI image 8/14/2001

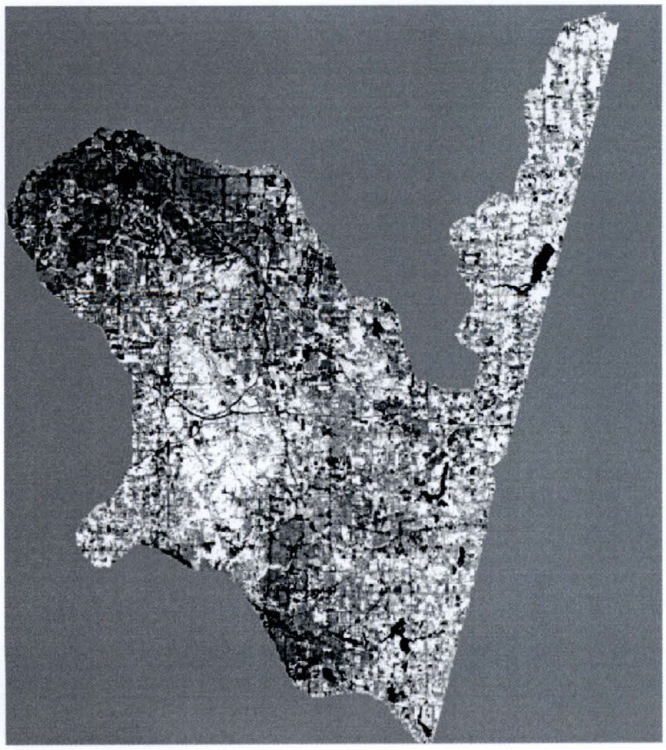

SAVI image 8/14/2001

Tasseled Cap Greenness image 8/14/2001

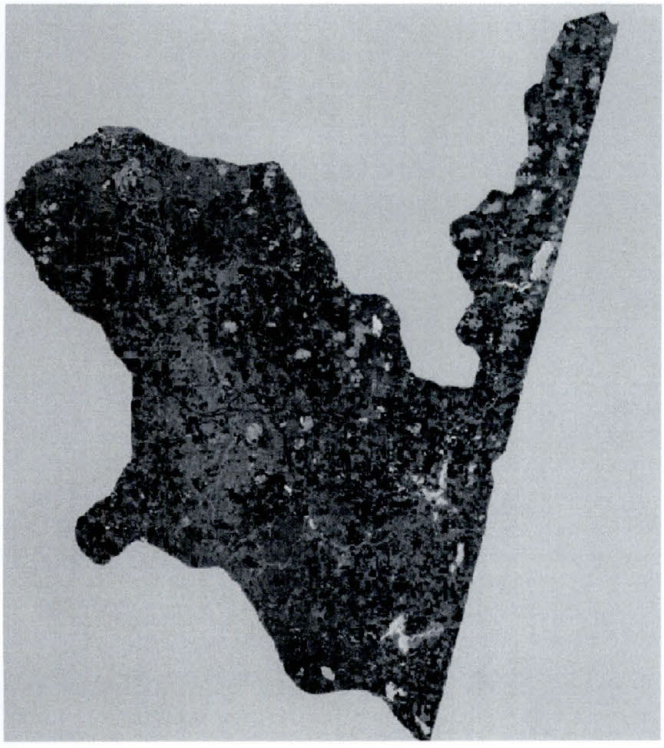

Tasseled Cap Wetness image 8/14/2001

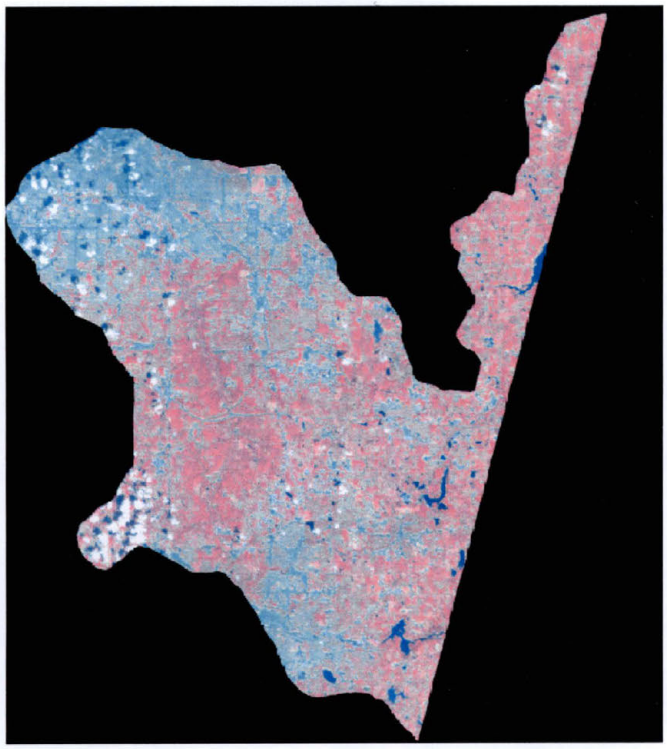

Landsat 7 ETM+ 8/30/2001 image (4-3-2 composite)

Landsat 7 ETM+ 8/30/2001 image after ATCOR (4-3-2 composite)

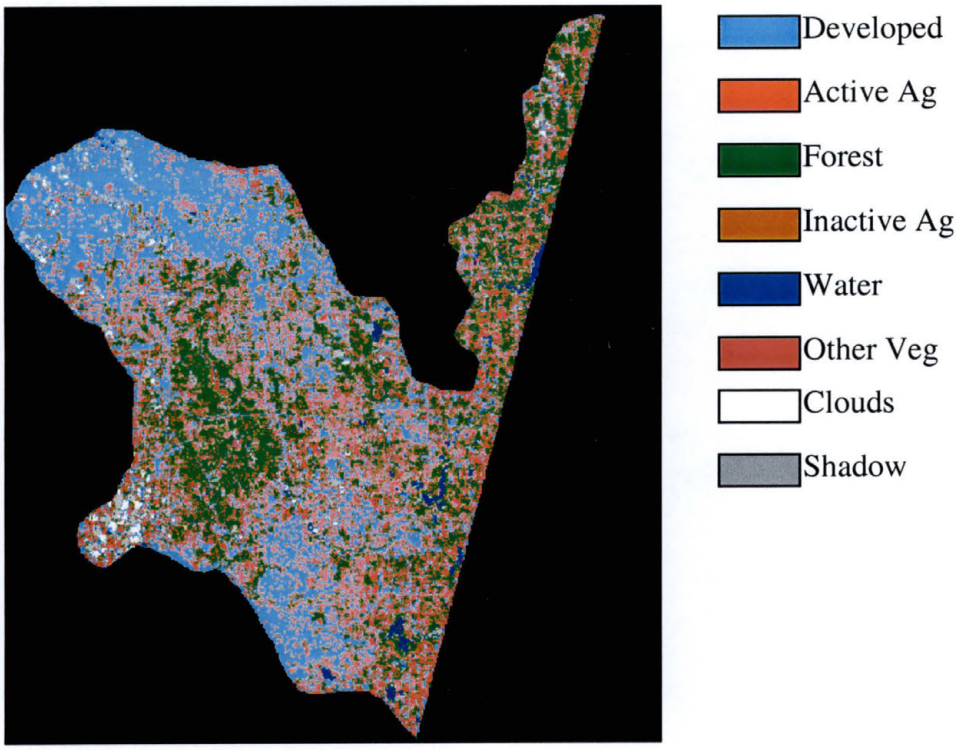

Classified 8/30/2001 image

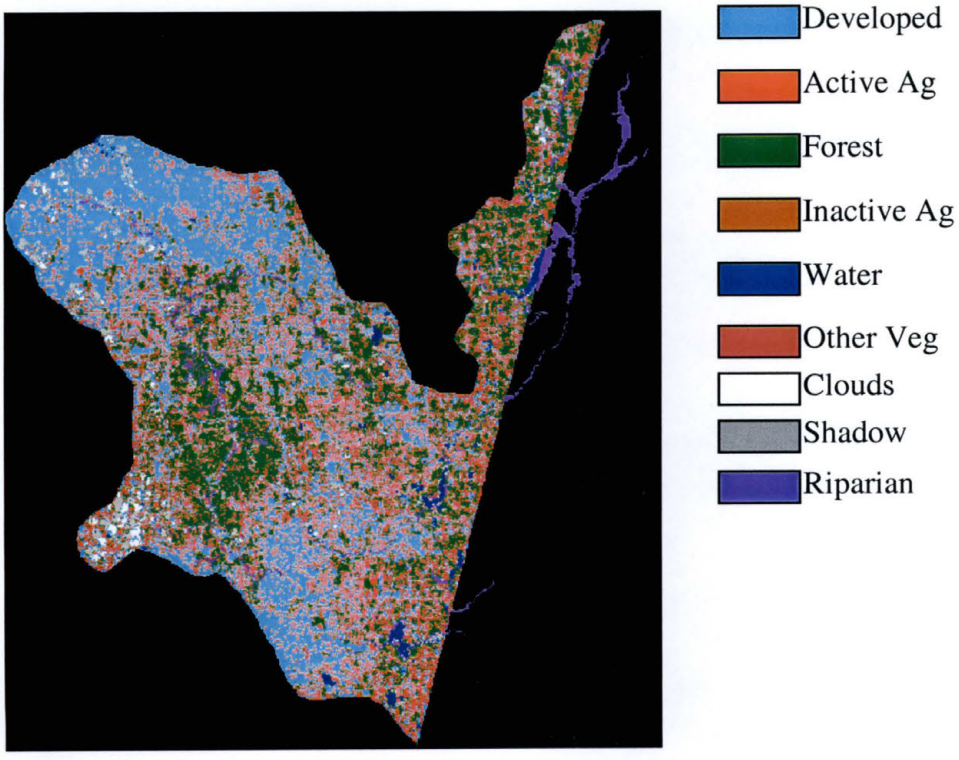

Classified 8/30/2001 image using expert classifier

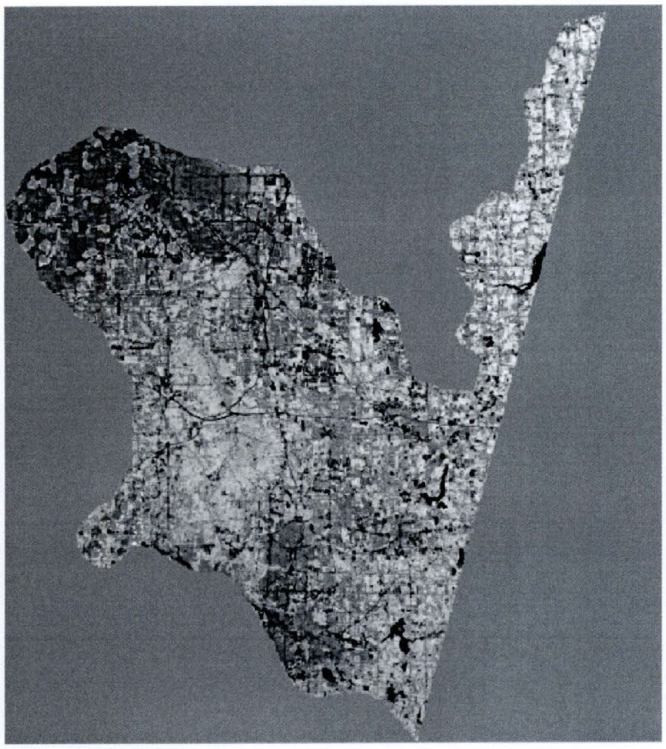

NDVI image 8/30/2001

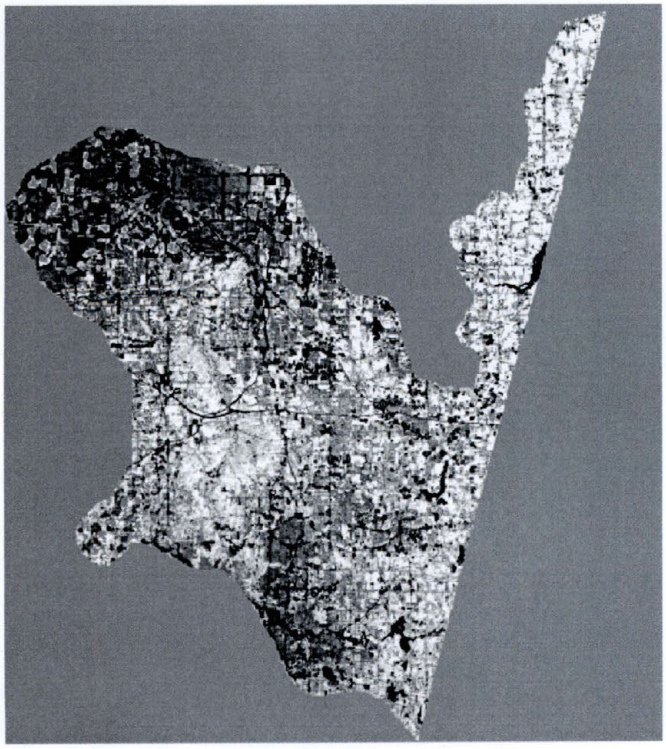

SAVI image 8/30/2001

Tasseled Cap Greenness image 8/30/2001

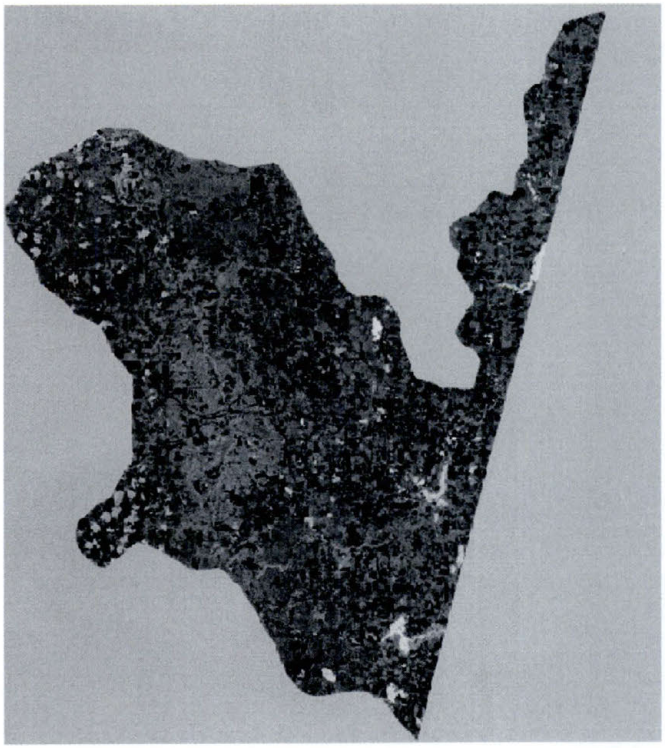

Tasseled Cap Wetness image 8/30/2001

Landsat 7 ETM+ 7/16/2002 image (4-3-2 composite)

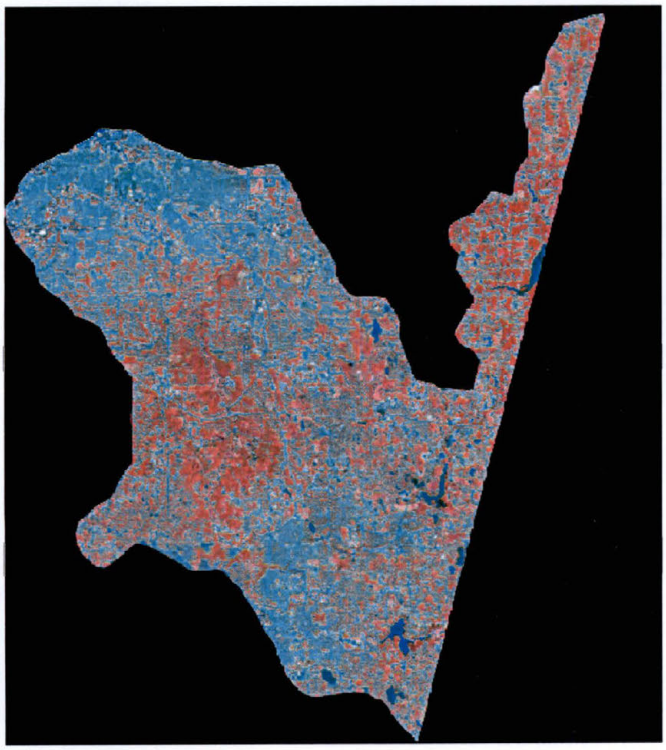

Landsat 7 ETM+ 7/16/2002 image after ATCOR (4-3-2 composite)

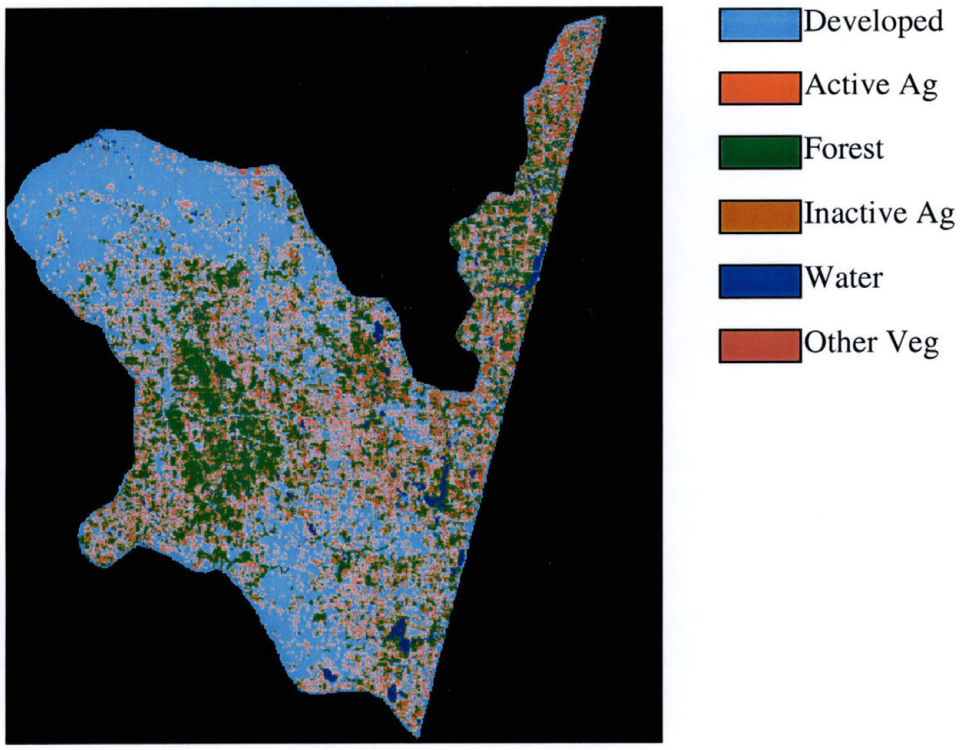

Classified 7/16/2002 image

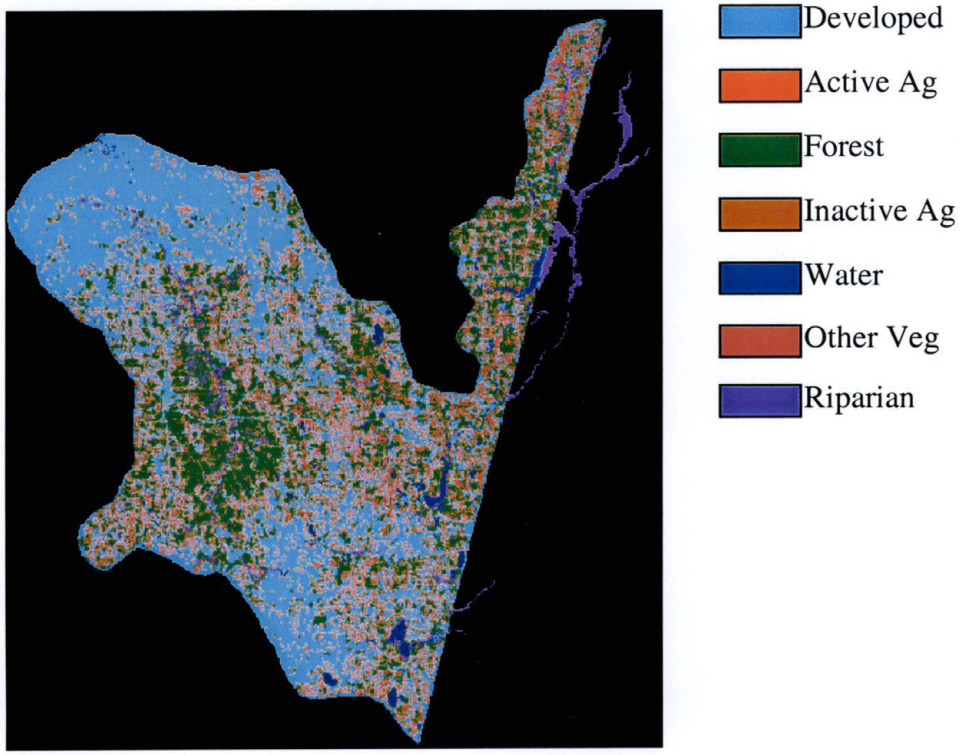

Classified 7/16/2002 image using expert classifier

NDVI image 7/16/2002

SAVI image 7/16/2002

Tasseled Cap Greenness image 7/16/2002

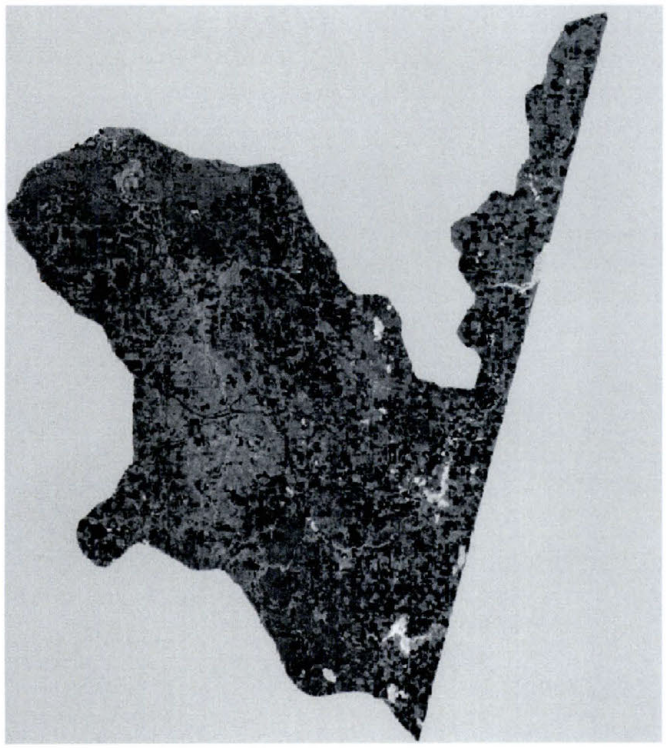

Tasseled Cap Wetness image 7/16/2002

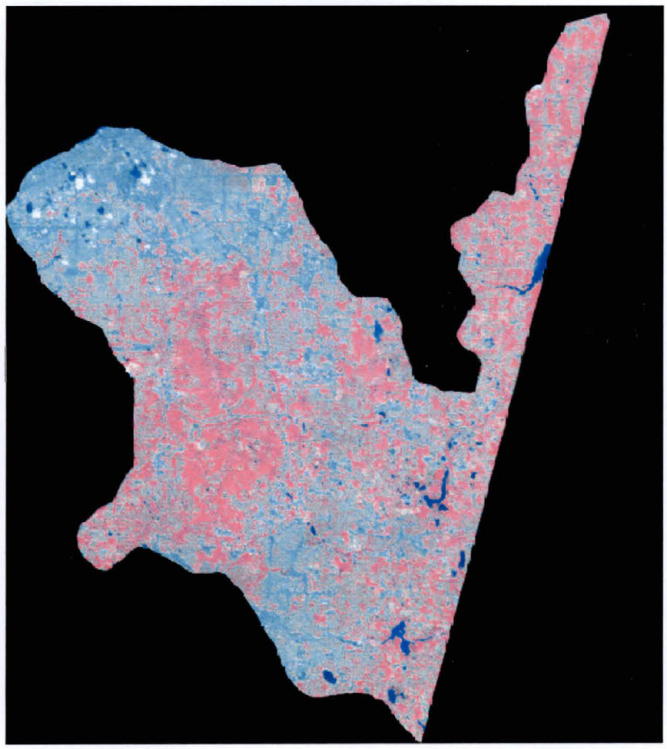

Landsat 7 ETM+ 8/1/2002 image (4-3-2 composite)

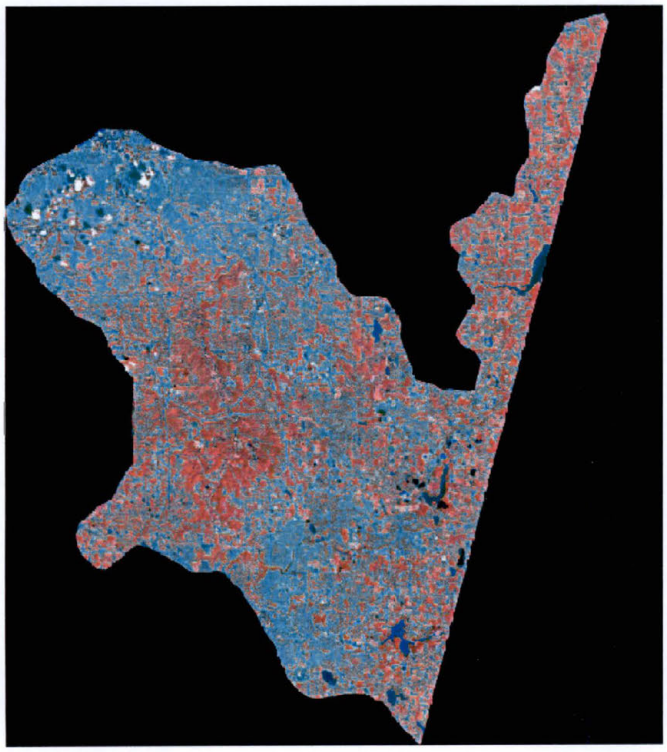

Landsat 7 ETM+ 8/1/2002 image after ATCOR (4-3-2 composite)

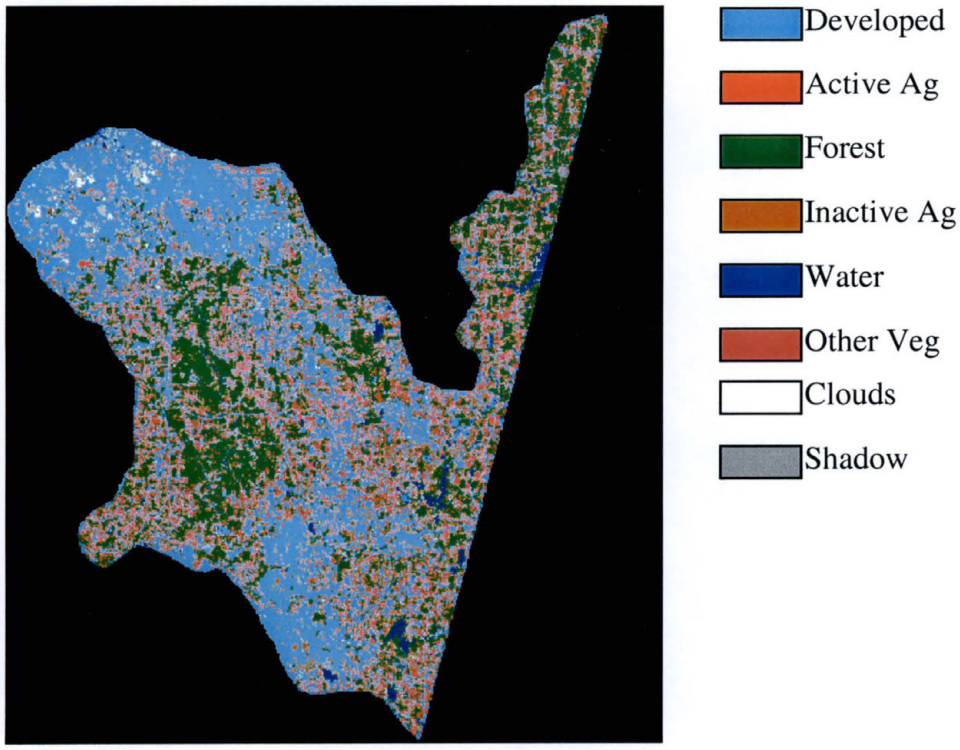

Classified 8/1/2002 image

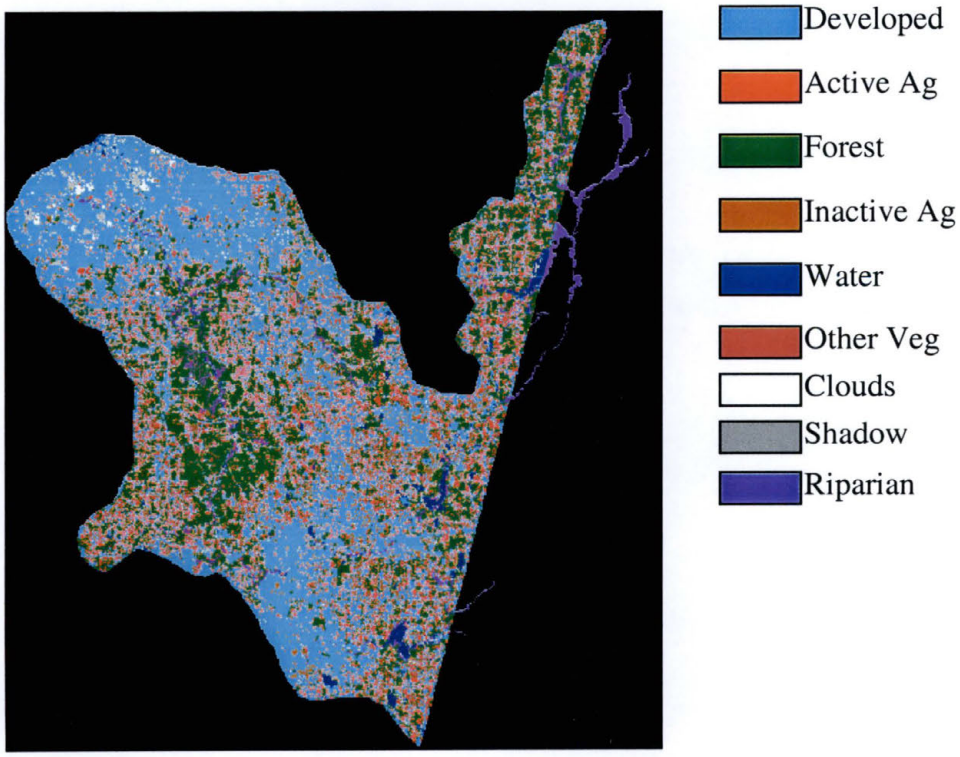

Classified 8/1/2002 image using expert classifier

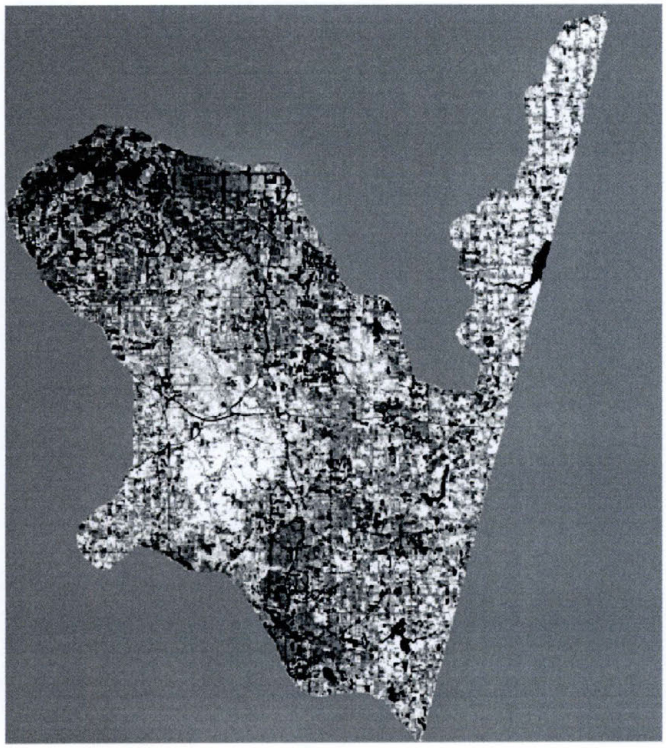

NDVI image 8/1/2002

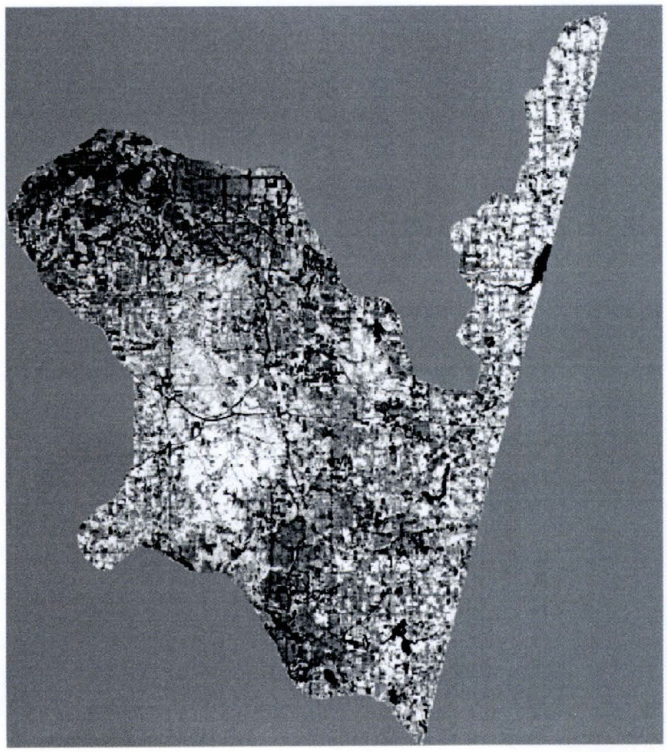

SAVI image 8/1/2002

Tasseled Cap Greenness image 8/1/2002

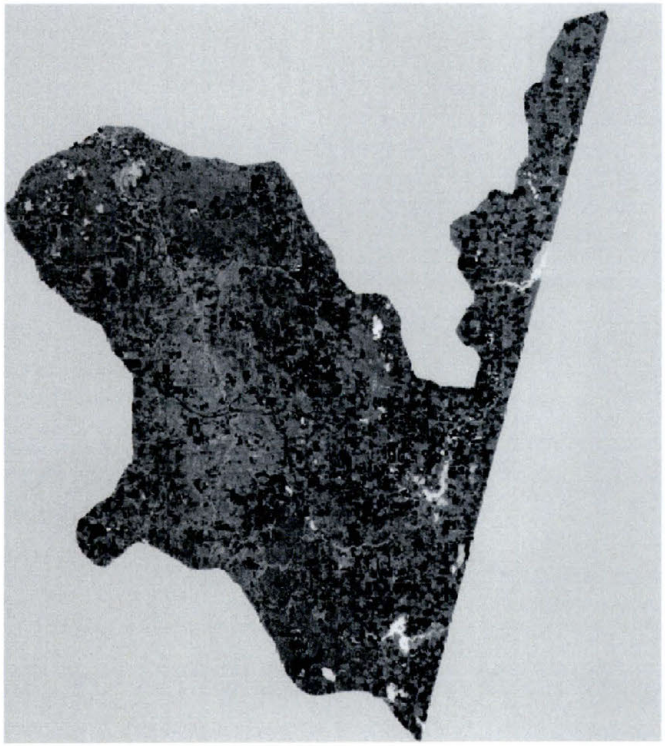

Tasseled Cap Wetness image 8/1/2002

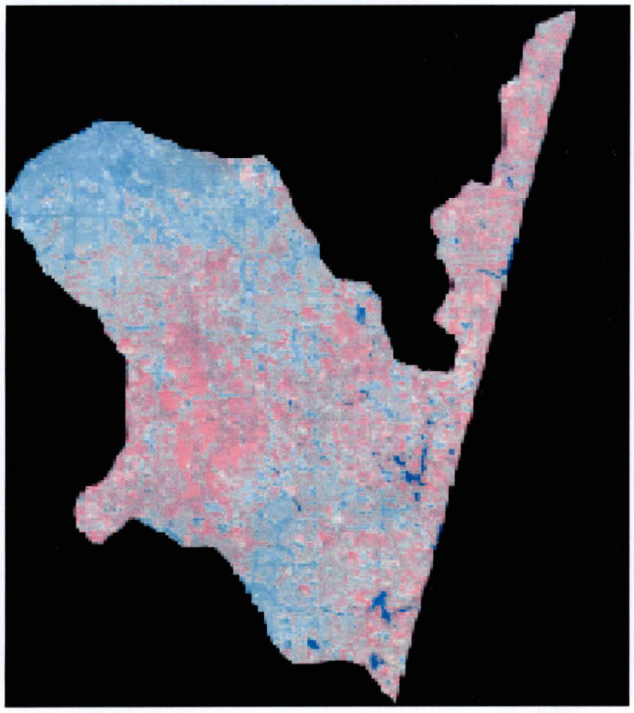

Landsat 7 ETM+ image 9/2/2002 (4-3-2 composite)

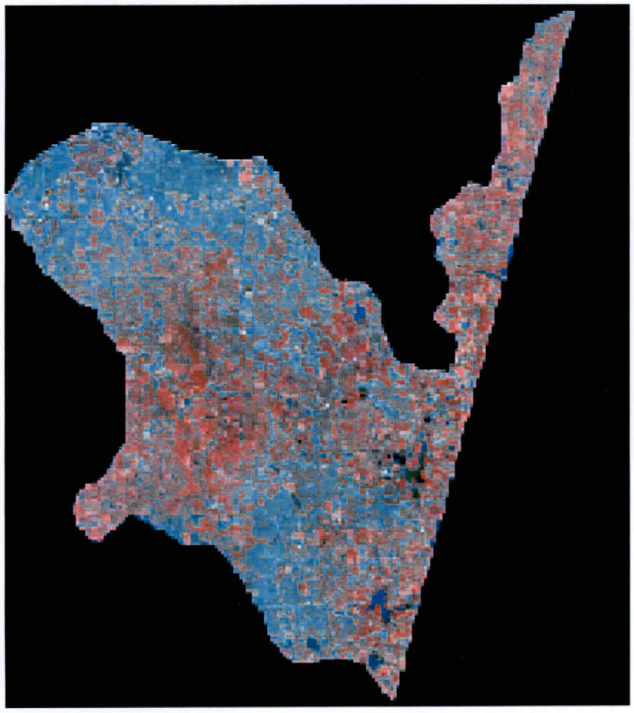

Landsat 7 ETM+ image 9/2/2002 after ATCOR (4-3-2 composite)

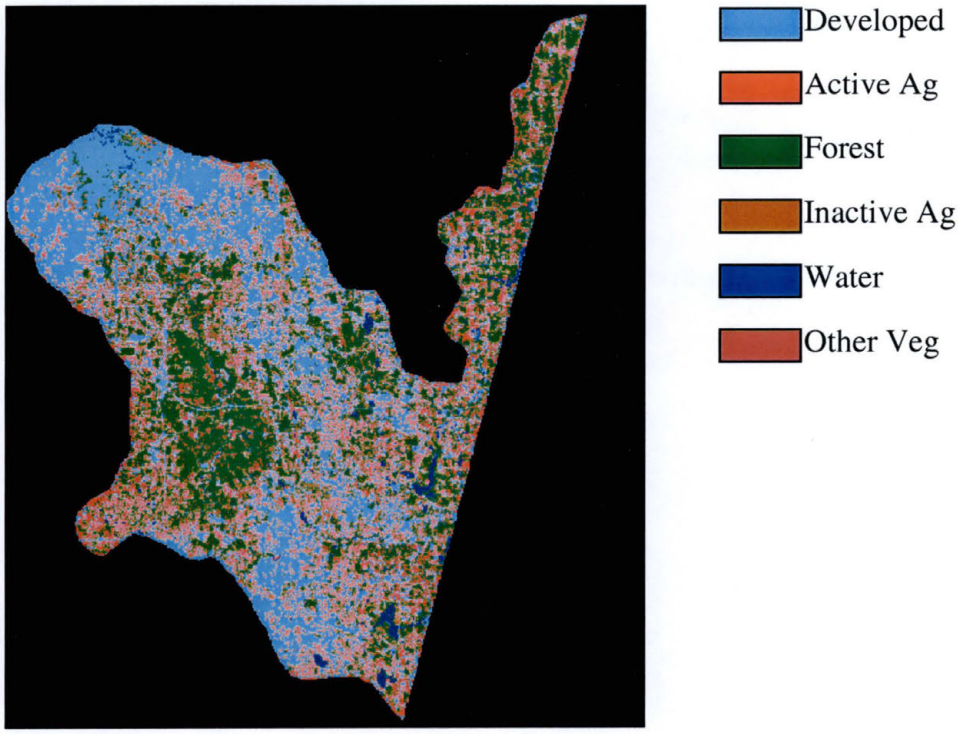

Classified 9/2/2002 image

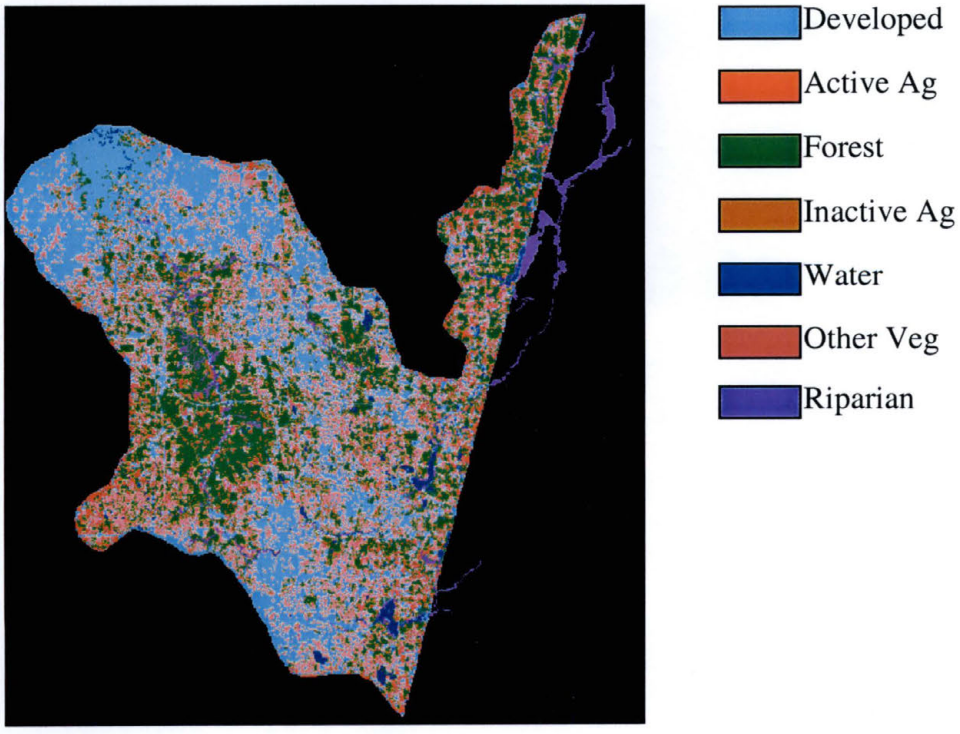

Classified image 9/2/2002 using expert classifier

NDVI image 9/2/2002

SAVI image 9/2/2002

Tasseled cap greenness image 9/2/2002

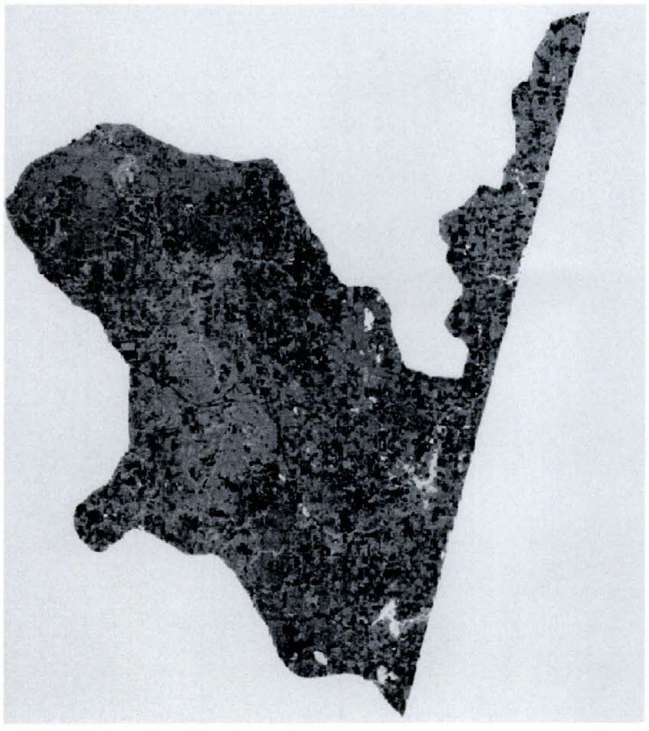

Tasseled cap wetness image 9/2/2002

APPENDIX III
DATA TABLES

For Entire Watershed

Date	NDVI	SAVI	TCG	TCW	palmer	PDSI 2	PDSI 4
9/26/1999	0.133	0 278	-32.392	-87 928	-0.85	-1 96	-2.42
10/12/1999	0 198	0 327	-19 165	-92 368	0 05	-2.08	-0.83
11/13/1999	0.109	0.241	-40.527	-101.475	1.56	-0.83	1 49
3/4/2000	0.062	0 250	-18 097	-109 948	0.4	-3 38	-2.97
4/5/2000	0 121	0.172	-59 089	-89 918	1.24	-2.97	-3.34
10/14/2000	0 168	0 330	-18 871	-113.641	2.34	-0.81	0.00
10/30/2000	0 206	0 337	-12 366	-98 590	1.52	-0.39	1.28
3/23/2001	-0 058	-0 038	-57.154	-130 241	-0.27	1.90	2.11
4/8/2001	0 002	0.027	-98.087	-118.403	-1 06	1 74	0 96
8/14/2001	0 141	0 226	-46 400	-109 014	-3.38	-0.52	-0.35
8/30/2001	0 002	0 050	-64 422	-88 555	-2 61	1.59	1.14
7/16/2002	0.012	0 072	-43.795	-94.735	-2 08	0 44	0 05
8/1/2002	0 006	0 026	-61 418	-92.081	-2.21	-0 85	-2 51
9/2/2002	0 019	0.033	-50 936	-69.180	-2.82	-2.51	-2 50

NDVI	undef	riparian	nonact_ag	act_ag	forest	water	dev	other_veg	clouds	shadow	PDSI	PDSI 2	PDSI 4
9/26/1999(N)	0.000	0.248	0.000	0.455	0.472	-0.172	0.012	0.052			-0.85	-1.96	-2.42
10/12/1999(N)	0.000	0.211	0.000	0.783	0.353	-0.064	0.039	0.264			0.05	-2.08	-0.83
11/13/1999(N)	0.000	0.013	0.000	0.695	0.012	-0.002	0.001	0.153			1.56	-0.83	1.49
3/4/2000(N)	0.000	0.065	0.000	0.509	0.076	-0.516	0.024	0.340			0.4	-3.38	-2.97
4/5/2000(N)	0.000	0.027	0.000	0.738	0.025	-0.078	-0.008	0.287	0.000	0.215	1.24	-2.97	-3.34
10/14/2000(W)	0.000	0.376	0.000	0.436	0.483	-0.017	0.087	0.137	0.006		2.34	-0.81	0.00
10/30/2000(N)	0.000	0.118	0.199	0.986	0.072	-0.113	0.005	0.378			1.52	-0.39	1.28
3/23/2001(N)	0.000	0.004	0.000	0.004	0.006	-0.521	0.006	0.039			-0.27	1.90	2.11
4/8/2001(N)	0.000	0.005	0.000	0.113	0.002	-0.271	0.005	0.145	0.000	0.017	-1.06	1.74	0.96
8/14/2001(D)	0.000	0.289	0.012	0.234	0.568	-0.452	-0.037	0.037	0.000	0.756	-3.38	-0.52	-0.35
8/30/2001(D)	0.000	0.107	0.042	0.140	0.332	-0.568	-0.097	0.003	0.000	0.058	-2.61	1.59	1.14
7/16/2002(D)	0.000	0.091	0.000	0.118	0.232	-0.325	-0.017	0.000			-2.08	0.44	0.05
8/1/2002(D)	0.000	0.109	-0.001	0.168	0.238	-0.399	-0.042	0.000	0.000	-0.011	-2.21	-0.85	-2.51
9/2/2002(D)	0.000	0.033	0.000	0.024	0.087	0.008	-0.002	0.000			-2.82	-2.51	-2.50

SAVI	undef	riparian	nonact_ag	act_ag	forest	water	dev	other_veg	clouds	shadow	PDSI	PDSI 2	PDSI 4
9/26/1999(N)	0.000	0.471	-0.006	0.991	0.788	-0.337	-0.070	0.385			-0.85	-1.96	-2.42
10/12/1999(N)	0.000	0.391	-0.033	0.998	0.671	-0.145	0.058	0.673			0.05	-2.08	-0.83
11/13/1999(N)	0.000	0.169	0.000	0.998	0.310	-0.057	0.013	0.493			1.56	-0.83	1.49
3/4/2000(N)	0.000	0.431	0.001	0.830	0.535	-0.611	0.067	0.750			0.4	-3.38	-2.97
4/5/2000(N)	0.000	0.065	-0.045	0.922	0.078	-0.192	-0.098	0.529	0.000	0.463	1.24	-2.97	-3.34
10/14/2000(W)	0.000	0.665	0.003	0.795	0.749	0.074	0.175	0.417	0.094		2.34	-0.81	0.00
10/30/2000(N)	0.000	0.348	0.472	0.999	0.271	-0.143	0.019	0.726			1.52	-0.39	1.28
3/23/2001(N)	0.000	0.028	-0.003	0.056	0.040	-0.617	-0.012	0.203			-0.27	1.90	2.11
4/8/2001(N)	0.000	0.018	-0.010	0.273	0.016	-0.458	-0.066	0.402	0.000	0.093	-1.06	1.74	0.96
8/14/2001(D)	0.000	0.493	0.109	0.805	0.835	-0.671	-0.229	0.110	0.000	0.804	-3.38	-0.52	-0.35
8/30/2001(D)	0.000	0.282	0.068	0.614	0.659	-0.792	-0.330	0.065	0.000	-0.062	-2.61	1.59	1.14
7/16/2002(D)	0.000	0.282	0.023	0.472	0.648	-0.696	-0.153	0.001			-2.08	0.44	0.05
8/1/2002(D)	0.000	0.297	-0.064	0.614	0.603	-0.665	-0.192	0.000	0.000	-0.337	-2.21	-0.85	-2.51
9/2/2002(D)	0.000	0.104	0.000	0.219	0.303	-0.240	-0.135	0.015			-2.82	-2.51	-2.50

TCG	undef	riparian	nonact_ag	act_ag	forest	water	dev	other_veg	clouds	shadow	PDSI	PDSI 2	PDSI 4
9/26/1999(N)	0.000	-1.050	-81.526	28.057	18.020	-65.786	-129.340	-27.507			-0.85	-1.96	-2.42
10/12/1999(N)	0.000	3.489	-101.637	49.784	14.788	-40.830	-83.447	4.537			0.05	-2.08	-0.83
11/13/1999(N)	0.000	-30.886	-99.937	20.736	-35.037	-66.930	-99.506	-12.656			1.56	-0.83	1.49
3/4/2000(N)	0.000	-10.891	-59.236	38.571	-12.654	-25.334	-92.276	17.046			0.4	-3.38	-2.97
4/5/2000(N)	0.000	-42.746	-119.068	51.537	-57.650	-41.995	-166.251	-18.238	-191.994	-4.483	1.24	-2.97	-3.34
10/14/2000(W)	0.000	11.667	-73.217	24.313	30.102	-25.042	-76.556	-8.525	-52.581		2.34	-0.81	0.00
10/30/2000(N)	0.000	-11.477	-28.700	72.282	-22.676	-23.623	-100.515	15.778			1.52	-0.39	1.28
3/23/2001(N)	0.000	-39.991	-94.754	-66.875	-52.306	-39.498	-122.835	-40.971			-0.27	1.90	2.11
4/8/2001(N)	0.000	-64.571	-238.934	-70.666	-93.359	-83.552	-178.204	-35.523	-194.200	-21.863	-1.06	1.74	0.96
8/14/2001(D)	0.000	7.279	-43.017	15.527	32.566	-91.032	-149.928	-68.116	-174.721	7.440	-3.38	-0.52	-0.35
8/30/2001(D)	0.000	-11.098	-77.863	-3.068	2.552	-94.646	-162.277	-58.417	-183.846	-57.554	-2.61	1.59	1.14
7/16/2002(D)	0.000	-8.615	-67.338	-11.725	-0.019	-86.696	-116.118	-59.846			-2.08	0.44	0.05
8/1/2002(D)	0.000	-7.958	-107.383	-0.091	-1.980	-72.304	-116.468	-56.946	-180.311	-70.735	-2.21	-0.85	-2.51
9/2/2002(D)	0.000	-20.457	-67.020	-40.160	-20.613	-76.738	-115.437	-67.059			-2.82	-2.51	-2.50

TCW	undef	riparian	nonact_ag	act_ag	forest	water	dev	other_veg	clouds	shadow	PDSI	PDSI 2	PDSI 4
9/26/1999(N)	0.000	-62.040	-142.473	-150.749	-93.136	22.199	-145.763	-131.458			-0.85	-1.96	-2.42
10/12/1999(N)	0.000	-56.735	-173.801	-163.116	-103.782	6.102	-124.201	-123.414			0.05	-2.08	-0.83
11/13/1999(N)	0.000	-92.719	-165.652	-162.813	-150.402	22.992	-128.306	-134.900			1.56	-0.83	1.49
3/4/2000(N)	0.000	-110.400	-183.016	-157.174	-164.913	6.114	-128.150	-142.042			0.4	-3.38	-2.97
4/5/2000(N)	0.000	-102.535	-148.436	-13.117	-154.311	-14.334	-110.260	-124.351	-168.210	-63.622	1.24	-2.97	-3.34
10/14/2000(W)	0.000	-103.593	-204.394	-188.078	-106.027	-8.393	-137.728	-143.674	-130.885		2.34	-0.81	0.00
10/30/2000(N)	0.000	-97.462	-147.502	-148.037	-146.798	-2.465	-120.540	-125.915			1.52	-0.39	1.28
3/23/2001(N)	0.000	-123.998	-202.222	-208.122	-187.666	-0.768	-155.956	-163.197			-0.27	1.90	2.11
4/8/2001(N)	0.000	-138.870	-176.737	-153.128	-205.044	21.518	-132.547	-150.398	-167.454	-81.365	-1.06	1.74	0.96
8/14/2001(D)	0.000	-85.675	-135.218	-162.122	-122.831	-20.649	-158.795	-181.098	-165.923	-57.833	-3.38	-0.52	-0.35
8/30/2001(D)	0.000	-59.915	-145.734	-133.898	-96.413	8.549	-133.121	-133.777	-162.328	-28.915	-2.61	1.59	1.14
7/16/2002(D)	0.000	-61.164	-157.158	-135.299	-101.325	-5.657	-151.557	-145.717			-2.08	0.44	0.05
8/1/2002(D)	0.000	-59.198	-201.548	-120.116	-96.176	0.338	-134.516	-125.245	-144.371	-39.974	-2.21	-0.85	-2.51
9/2/2002(D)	0.000	-4.811	-106.532	-111.736	-83.087	-13.555	-119.269	-114.446			-2.82	-2.51	-2.50

WORKS CITED

Alley, William M. 1984. The Palmer drought severity index: Limitations and assumptions. *Journal of Climate and Applied Meteorology*. 23:1100-09.

American Meteorological Society. 1997. Meteorological drought-Policy statement. *Bulletin of the American Meteorological Society*. 78: 847-49.

Beuerlein, Jim, Don Eckert, Dan Jeffers, Jay Johnson, Patrick Lipps, Mark Loux, Ed McCoy, Walter Schmidt, Mark Sulc, Paul Sutton, Peter Thomison, John Understood, Maurice Watson, and Hal Willson. 1995. *Ohio agronomy guide: Bulletin 472*. Columbus, OH: The Ohio State University.

Blair, Bill. 1999. *Using light to learn about the universe-the electromagnetic spectrum* [online]. Baltimore, MD: Johns Hopkins University. Available at http://fuse.pha.jhu.edu/~wpb/spectroscopy/em_spec.html. Accessed on January 14, 2003.

Chavez, Pat S., Jr. 1988. An improved dark-object subtraction technique for atmospheric scattering correction of multispectral data. *Remote Sensing of Environment* 24: 459-79.

_____ and David J. MacKinnon. 1994. Automatic detection of vegetation changes in the southwestern United States using remotely sensed images. *Photogrammetric Engineering & Remote Sensing* 60, no. 5: 571-83.

Cleanwater Action Plan Partners (CWAP). 2000. *The Cuyahoga River Watershed-Restoring an American heritage river* [online]. Available from http://www.cleanwater.gov/success/cuyahoga.html. Accessed on October 8, 2002.

Climate Prediction Center. 2002. *Drought monitoring* [online]. Camp Springs, MD: National Oceanic and Atmospheric Administration/National Weather Service. Available at: http://www.cpc.ncep.noaa.gov/products/monitoring_and_data/drought.html. Accessed on May 21, 2002.

Coppin, P. R. and M. E. Bauer. 1994. Processing of multitemporal Landsat TM imagery to optimize extraction of forest cover change features. *IEEE Transactions on Geoscience and Remote Sensing* 32: 918-27.

Crist, Eric P. and Richard C. Cicone. 1984a. A physically-based transformation of Thematic Mapper data-the TM tasseled cap. *IEEE Transactions on Geoscience and Remote Sensing* GE-22, no. 3: 256-63.

_____ and Richard C. Cicone. 1984b. Application of the tasseled cap concept to simulated Thematic Mapper data. *Photogrammetric Engineering and Remote Sensing* 50, no. 3: 343-52.

DeMers, Michael N. 2002. *GIS modeling in raster*. New York, NY: John Wiley & Sons, Inc.

Federal Geographic Data Committee. 1996. *FGDC vegetation subcommittee draft vegetation standards* [online]. Reston, VA: University of Michigan. Available at http://www.eecs.umich.edu/~josefk/TESTSITES/FGDC-NVCS/vegclass.html. Accessed on November 12, 2002.

GEOSystems. 2000. *ATCOR2 for Imagine, version 1.7 white paper*. Riesstrae, Germany: GEOSystems.

Gosh, T. K. 1997. Investigation of drought through digital analysis of satellite data and geographical information systems. *Theoretical and Applied Climatology* 58:105-12.

Griffith, Daniel A., and Carol G. Amrhein. 1991. *Statistical analysis for geographers*. Englewood Cliffs, NJ: Prentice Hall.

Harrington, John A., Jr. and David H. Greegor, Jr. 1988. Weather and climate effects on the normalized difference vegetation index. *1988 ACSM-ASPRS Fall Convention ASPRS Technical Papers*. 207-13.

Hayes, Michael J. 1999. *Drought indices* [online]. Lincoln, NE: University of Nebraska. Available at http://enso.unl.edu/udmc/enigma/indices.htm. Accessed on May 21, 2002.

Heddinghaus, Thomas R., and Paul Sabol. 1991. A review of the Palmer drought severity index and where do we go from here. *Proceedings of the Seventh Conference on Applied Climatology*. 242-46.

Heim, Richard R., Jr. 2002. A review of twentieth-century drought indices used in the United States. *Bulletin of the American Meteorological Society* 83, no. 8: 1149-65.

Hounam, C. E., J. J. Burgos, M. S. Kalik, W. C. Palmer and J. Rodda, eds. 1975. *World meteorological organization technical note no. 138: Drought and agriculture*. Geneva, Switzerland: World Meteorological Association.

Huang, Chengquan, Bruce Wylie, Limin Yang, Collin Homer, and Gregory Zylstra. 2002. *Derivation of a tasseled cap transformation based on Landsat 7 at-satellite reflectance* [online]. Sioux Falls, SD: USGS EROS Data Center. Available at http://landcover.usgs.gov/pdf/tasseled.pdf. Accessed on October 10, 2002.

Huete, A. R. 1988. A soil-adjusted vegetation index. *Remote Sensing of Environment* 25: 295-309.

____ H. Q. Liu, K. Batchily, and W. van Leeuwen. 1997. A comparison of vegetation indices over a global set of TM images for EOS-MODIS. *Remote Sensing Environment* 59: 440-51.

Jensen, John R. 1996. *Introductory digital image processing: A remote sensing perspective.*Upper Saddle River, NJ: Prentice Hall.

____. 2000. *Remote sensing of the environment: An earth response perspective.* Upper Saddle River, New Jersey: Prentice Hall.

Kachigan, Sam Kash. 1991. *Multivariate statistical analysis: A conceptual introduction-second edition.* New York: Radius Press.

Kauth, R. J. and G. S. Thomas. 1976. The tasseled cap-a graphic description of the spectral-temporal development of agricultural crops as seen by Landsat. *Proceedings, Machine Processing of Remotely Sensed Data.* West Lafayette, IN: Laboratory for the Applications of Remote Sensing: 41-51.

Keyantash, John and John A. Dracup. 2002. The quantification of drought: an evaluation of drought indices. *Bulletin of the American Meteorological Society* 83, no. 8: 1167-80.

Kogan, F. N. 1990. Remote sensing of weather impacts on vegetation in non-homogeneous areas. *International Journal of Remote Sensing* 11, no. 8: 1405-19.

____. 1995a. How drought looks from space. *Geocarto International* 10, no. 1: 51-56.

____. 1995b. Droughts of the Late 1980s in the Unites States as derived from NOAA Polar-Orbiting satellite data. *Bulletin of the American Meteorological Society* 76, no. 5: 655-68.

____. 1997. Global drought watch from space. *Bulletin of the American Meteorological Society* 78, no. 4: 621-36.

Malanson, George P. 1993. *Riparian landscapes*. New York: Cambridge University Press.

Mather, Paul. 1999. *Computer processing of remotely sensed images: An introduction-second edition*. Chichester, NY: John Wiley & Sons.

Muller, Etienne. 1997. Mapping riparian vegetation along rivers: old concepts and new methods. *Aquatic Botany* 58: 411-37.

Nagler, Pamela L., Edward P. Glenn, Alfredo R. Huete. 2001. Assessment of spectral variation indices for riparian vegetation in the Colorado River delta, Mexico. *Journal of Arid Environments*. 49: 91-110.

Ohio Public Library Information Network. 2003. Ohio's county almanac [online]. Available at http://www.oplin.lib.oh.us/products/OCA/index.cfm. Accessed on May 20, 2003.

OhioView. 2002. *About OhioView: purpose and mission* [online]. Available at http:// www.ohioview.org/about/purpose/html. Accessed on October 7, 2002.

Palmer, W. C. 1965. *Meteorological drought*. U.S. Weather Bureau Research Paper 45, 58 pp.Washington, DC.

Peters, A. J., D. C. Rundquist, and D. A. Wilhite. 1991. Satellite detection of the geographic core of the 1988 Nebraska drought. *Agricultural and Forest Meteorology* 57, no. 1-3: 35-47.

____ Bradley C. Reed, Marlen D. Eve, and Kris M. Havstad. 1993. Satellite assessment of drought impacts on native plant communities in southeastern New Mexico, U.S.A. *Journal of Arid Environments* 24: 305-19.

____ E. A. Walter-Shea, L. Ji, A. Vina, M. Hayes, and M. D. Svoboda. 2002. Drought monitoring with NDVI-based standardized vegetation index. *Photogrammetric Engineering and Remote Sensing* 68, no. 1: 71-75.

Pinder, John E. III and Kenneth W. McLeod. 1999. Indications of relative drought stress in longleaf pine from Thematic Mapper data. *Photogrammetric Engineering & RemoteSensing* 65, no. 4: 495-501.

Ray, Terrill W. 1994. *A FAQ on vegetation in remote sensing* [online]. Pasadena, CA: California Institute of Technology. Available at http://www.yale.edu/ceo/ Documentations/rsvegfaq.html. Accessed on February 27, 2002.

Rouse, J. W., R. H. Haas, J. A. Schell, and D. W. Deering. 1974. Monitoring vegetation systems in the Great Plains with ERTS. *Proceedings Third Earth Resources Technology Satellite-1 Symposium*. Greenbelt: NASA SP-351, 3010-17.

Rundquist, Bradley C. 1997. Spatial and temporal variation in NDVI response to climatic variables in Kansas. *Papers and Proceedings of the Applied Geography Conferences* 20: 304-09.

____ J. A. Harrington Jr., and D. G. Goodin. 2000. Mesoscale satellite bioclimatology. *Professional Geographer* 52, no. 2: 331-44.

Schultz, Bill. 2003. Ohio's trees [online]. Ohio Department of Natural Resources. Available at http://www.dnr.state.oh.us/forestry/Education/ohiotrees/ ohiotreesintro.html. Accessed on May 23, 2003.

Tao, Yongyi, Chi Zhenhuan, John Harrington Jr., and Brad Rundquist. 1997. Analysis of the relationship between NDVI and rainfall in subhumid agricultural areas and the influence of environmental factors. *Papers and Proceedings of the Applied Geography Conferences* 20: 310-17.

University of Arizona. 2002. *Geospatial tools for natural resource management-normalized difference vegetation index* [online]. Tuscan, AZ: The University of Arizona. Available at http://rangeview.arizona.edu/ glossary/ndvi.html. Accessed on November 13, 2002.

U.S. Geological Survey. 2003. *Digital orthophoto program* [online]. Reston, VA: U.S. Department of the Interior. Available at http://mapping.usgs.gov/www/ndop/.

Washington-Allen, R. A., R. D. Ramsey, B. E. Norton, and N. E. West. 1998. Change detection of the effect of severe drought on subsistence agropastoral communities on the Bolivian altiplano. *International Journal of Remote Sensing* 19, no. 7: 1319-33.

Wells, Nathan. 2002. *Palmer Drought Severity Index* [online]. Lincoln, NE: University of Nebraska. Available at http://nadss.unl.edu/pdsi/doc/index.html. Accessed on May 23, 2003.

Wilhite, Donald A. 1983. Government response to drought in the U.S: with particular reference to the Great Plains. *Journal of Climate and Applied Meteorology* 22: 40-50.

____ William E. Easterling, and Deborah A. Wood, eds. 1987. *Planning for drought: Toward a reduction of societal vulnerability*. Boulder, CO: Westview Press.

Williams, Darrel. 2003. *Landsat 7 science data users handbook* [online]. Greenbelt, MD: Goddard Space Flight Center. Available at http://ltpwww.gsfc.nasa.gov/IAS/ handbook/handbook_toc.html. Accessed on August 7, 2002.

Woolf, Henry Bosley and others, eds. 1977. *Webster's new collegiate dictionary*. Springfield, MA: C. & G. Merriam Company.

World Meteorological Organization. 1992. *International Meteorological Vocabulary-second edition*. World Meteorological Organization Paper No. 184, 784 pp. World Meteorological Organization.

VITA

Susan Dunham was born in Southampton, New York, on December 29, 1978, the daughter of Patricia H. and John A. Dunham. After graduating from Westhampton Beach High School in Westhampton Beach, New York, in 1997, she entered the State University of New York College at Geneseo in Geneseo, New York. She declared her major as Geography at the end of her sophomore year and proceeded to receive a Bachelor of Arts degree in Geography with a minor in Environmental Studies in May, 2001. In August 2001, she entered the master's program in Geography with a Resource and Environmental Studies concentration at Southwest Texas State University in San Marcos, Texas.

Permanent Address: 5 Oakland Lane
East Quogue, NY 11942

This thesis was typed by Susan Dunham.